UNIVERSIDAD AUTÓNOMA DE MADRID

FACULTAD DE CIENCIAS

DEPARTAMENTO DE BIOLOGÍA MOLECULAR

Doctoral Thesis

A novel role for p21 in regulation of late activation events in effector/memory T cells and its effect on autoimmunity

Kathrin Weber

Madrid,

January 2015

TO MY PARENTS

The research described in this thesis was performed in the Department of Immunology and Oncology, National Centre for Biotechnology (CSIC), Madrid, Spain.

Director: Dr. Dimitrios Balomenos

Co-director: Dr. Carlos Martínez-A.

TABLE OF CONTENTS

ABBREVIATIONS

A96I	altered peptide ligand differing from PCC (88–104) by isoleucine substitution for alanine at position 96 (KAERADLIIYLKQATAK); low TCR affinity
ACID	activation-induced cell death
Ag	antigen
Akt	protein kinase B
ALPS	autoimmune lymphoproliferative syndrome
AML	acute myeloid leukemia
AP-1	activation protein 1
APC	antigen-presenting cell
$BAY_{11\text{-}7082}$	(E)-3-(4-methylphenylsulfonyl)-2-propenenitrile; specific inhibitor of IκB kinase (IKK)
BFA	brefeldin A
BrdU	5-bromo-2'-deoxyuridine
BSA	bovine serum albumin
CARMA1	CARD and MAGUK domain-containing protein-1
CBM	complex composed of CARMA1, Bcl10, MALT1
CDK	cyclin-dependent kinase
CFSE	carboxyfluorescein diacetate succinimidyl ester
ConA	concanavalin A
CVT-313	2(bis-(hydroxyethyl)amino)-6-(4-methoxybenzylamino)-9-isopropyl-purine; specific inhibitor for CDK2
DAG	diacylglycerol
DAPI	4'6-diamidino-2-phenylindole
DC	dendritic cell
DMSO	dimethyl sulfoxide
DN	double negative
DNA	deoxyribonucleic acid
DTT	dithiothreitol
EDTA	ethylenediaminetetraacetic acid
ERK1/2	extracellular signal-regulated kinase 1/2
FACS	fluorescence-activated cell sorting
FasL	Fas ligand

FCS	fetal calf serum
FITC	fluorescein isothiocyanate
GEF	guanine nucleotide exchange factor
GM-CSF	granulocyte-macrophage colony-stimulating factor
HEPES	4-(2-hydroxyethyl)-1-piperazineethanesulfonic acid
hrIL-2	human recombinant interleukin-2
IFN	interferon
Ig	immunoglobulin
IκBα	nuclear factor of kappa light polypeptide gene enhancer in B-cells inhibitor, alpha
IKKα	IκB kinase alpha
IKKβ	IκB kinase beta
IL	interleukin
IP_3	inositol 1,4,5-trisphosphate
ITAM	immunoreceptor tyrosine-based activation motif
LAT	linker for activation of T cells
Lck	lymphocyte-specific protein tyrosine kinase
lpr	lymphoproliferation
MALT1	mucosa-associated lymphoid tissue 1
MAPK	mitogen-activated protein kinase
MHC	major histocompatibility complex
MS	multiple sclerosis
NEMO	NF-κB essential modulator
NFAT	nuclear factor of activated T cells
NF-κB	nuclear factor –kappa B
NLS	nuclear localization sequence
PBS	phosphate buffered saline
PCC	pigeon cytochrome C (KAERADLIAYLKQATAK); dominant agonist peptide
PE	phycoerythrin
PI	propidium iodide
PI_3K	phosphatidylinositol 3 kinase
PIP_2	phosphatidylinositol 4,5-bisphosphate
PKCθ	protein kinase C-theta
PMA	phorbol myristate acetate
poly(dI-dC)	polydeoxy(Inosinate-Cytidylate Acid), sodium salt
Rb	retinoblastoma
RT	room temperature

SD	standard deviation
SDS-PAGE	sodium dodecyl sulfate polyacrylamide gel electrophoresis
SLE	systemic lupus erythematosus
Src	sarcoma tyrosine kinase
TCR	T cell receptor
TCRtg	transgenic TCR
tg	transgenic
T_H	helper T cell
TNFα	tumor necrosis factor alpha
T_{reg}	regulatory T cell
U0126	1,4-diamino-2,3-dicyano-1,4-bis(2-aminophenylthio)butadiene; specific inhibitor for MEK
ZAP70	zeta-chain-assicoated protein kinase 70 kDa
zVAD	benzyloxycarbonyl-Val-Ala-Asp (Ome) fluoromethylketone; apoptosis inibitor

PRESENTACIÓN

El delicado equilibrio entre activación, proliferación y muerte de las células T es crucial para el desarrollo y el mantenimiento de la tolerancia, una característica importante del sistema inmune. Estos procesos deben estar muy controlados, ya que una mínima desregulación puede dar lugar a graves defectos en el sistema inmune. En un trabajo previamente publicado por nuestro equipo, mostramos que la ausencia de p21 – una molécula conocida como inhibidor del ciclo celular – provoca la hiperproliferación de las células T de memoria conduciendo al desarrollo de una patología autoinmune tipo lupus[56]. Sin embargo, un elevado porcentaje de células T de memoria se identificó en los ratones deficientes en p21. Por lo tanto, estaba por determinar el modo de actuación de p21 y su influencia en la activación de las células T. En ésta tesis usamos diferentes sistemas de cultivos *in vitro* y modelos de ratón *in vivo* para examinar el possible papel de p21 en la activación de las células T y para determinar la función de p21 en este proceso.

Definición de los objetivos de ésta tesis:

1. Estudiar el efecto de p21 en la activación y la proliferación de las células T en distintos sistemas *in vitro* e identificar las rutas de activación controladas por p21.
2. Examinar si p21 regula la activación de las células T de forma independiente de su papel como inhibidor del ciclo celular.
3. Definir la influencia de p21 en la activación de las células T en respuesta a antígenos de afinidad baja, un evento que se considera crítico para el desarrollo de autoinmunidad.
4. Analizar el efecto de la ausencia de p21 en conjunto con el defecto en Fas (*lpr*) en la actvación de las células T.
5. Determinar el efecto terapéutico de la sobre-expresión de p21 restringida a las células T en ratones B6/*lpr* .

En esta tesis se ha confirmado que p21 controla la activación de las células T de memoria/efectoras vía CDK2 después de una estimulación repetida. Se comprobó que p21 no controla eventos de activación proximales al TCR pero podría actuar a nivel de la PKCθ o en las vías de

activación reguladas por PKCθ ya que está localizado en el citoplasma de las células T de memoria/efectoras.

p21 controla la respuesta proliferativa de las células T de memoria/efectoras regulando de forma negativa las vías de activación de ERK1/2 y NF-κB. En ausencia de p21, se observó la sobreactivatión de ERK1/2 y NF-κB en éstas células, lo cual lleva a una hiperproliferación y una mayor producción de citoquinas pro-inflammatorias (IFNγ, IL-2).

Analizando la respuesta de células T presentando un TCR transgénico, se detectó una elevada respuesta de las células T p21$^{-/-}$ re-estimuladas *in vitro* con un antígeno específico de baja afinidad. Este resultado apunta a un menor umbral de activación en las células T de memoria deficientes en p21 y relaciona la hiperactivación detectada en éstas células con una respuesta frente a antígenos propios.

El estudio de ratones B6/*lpr* deficientes en p21 (B6/*lpr*-p21$^{-/-}$) ha confirmado la relevancia biológica de nuestros resultados. En ausencia de p21, las manifestaciones de la enfermedad autoinmune empeoran considerablemente causando finalmente la muerte. La hiperactivación y los elevados niveles de IFNγ detectados en las células T CD4^{+} de memoria B6/*lpr*-p21$^{-/-}$podrían ser responsables del desarrollo de una enfermedad autoinmune severa en estos ratones.

Finalmente, estudios con ratones expresando un p21 transgénico humano específicamente en las células T revelaron una notable reducción en la activación de las células T CD4^{+} de memoria B6/*lpr*-p21tg, asi como en la producción de IFNγ. Este fenotipo conlleva una considerable mejoría de las manifestaciones autoinmunes en los ratones B6/*lpr*-p21tg respecto a las manifestaciones observadas en los ratones B6/*lpr*.

En general, los datos presentados en esta tesis demuestran un importante papel de p21 como regulador negativo de la activación de las células T de memoria, en concreto de la población de células T potencialmente auto-reactivas y de su producción de IFNγ. Por lo tanto, p21 puede ser considerado como supresor de la autoinmunidad y podría servir para el desarrollo de nuevas estrategias terapéuticas en ciertas enfermedades autoinmunes.

ABSTRACT

The maintenance of T cell tolerance, which is established by the fine balance between Tcell activation, proliferation and apoptosis, is crucial to avoid of autoimmunity development. Lack of p21, a cell cycle inhibitor also implicated in effector/memory T cell activation, is linked to SLE in human patients; in accordance, C57BL/6 p21-deficient mice lose tolerance and develop mild autoimmune disease with age. Here we study the effect of p21 on T cell activation. Whereas p21 regulated activation of effector/memory T cells in a CDK2-independent manner, it had no effect on naïve T cells. We also found that cytoplasmic p21 is unrelated to TCR proximate events, but controls memory T cell activation via downstream MAPK and NF-κB pathways. Lack of p21 caused hyperactivation of ERK1/2 and NF-κB in memory-phenotype T cells, leading to increased proliferation and pro-inflammatory cytokine production (IFNγ, IL-2). Stimulation of TCR-transgenic (tg) T cells with specific antigens *in vivo* confirmed our finding that p21 is involved in effector/memory T cell activation. In response to *in vitro* stimulation with low affinity antigens that mimic auto-antigens, p21 influenced the activation threshold of effector/memory T cells, a critical factor for tolerance maintenance and autoimmunity suppression. In lupus-prone B6/*lpr* mice, lack of p21 in hyperactivated memory T cells caused increased production of pro-inflammatory cytokines such as IFNγ, as well as marked aggravation of lupus-like disease manifestations, leading to death. These effects were reversed by T cell-specific overexpression of p21. B6/*lpr*-p21tg mice showed reduced memory T cell activation and lower IFNγ levels, which efficiently restrained autoimmunity development. By inhibiting T cell activation and reducing pro-inflammatory cytokine production in auto-reactive, but not in normal T cells after repeated antigen encounter, p21 might thus have a therapeutic effect as a suppressor of autoimmunity.

1. INTRODUCTION

1. INTRODUCTION

1.1 The Immune System

In the course of evolution, vertebrates developed complex mechanisms to protect themselves against potential pathogens to which they are constantly exposed. The basic challenge of the immune system is to distinguish between self (originating from the same organism) and non-self particles (such as bacteria, viruses or parasites). This process is tightly regulated; in consequence, any dysregulation is likely to cause severe damage to the organism.

Once a pathogen manages to penetrate physical and chemical surface barriers and invades the body, the **innate immune system** is activated[1]. This immediate and nonspecific cellular defense mechanism is provided primarily by phagocytes (macrophages, neutrophils, eosinophils, basophils and dendritic cells; DC), which recognize foreign molecular patterns and subsequently engulf and destroy the pathogen. Small particles of engulfed pathogens are presented on the surface of so-called antigen-presenting cells (APC; mainly macrophages and DC), where they can be recognized by cells of the adaptive immune system. APC also release pro-inflammatory cytokines to amplify the inflammatory response. In addition, natural killer (NK) cells recognize infected or malignant tumor cells and free cytolytic chemicals to promote cell lysis.

Although this first-line defense is effective in controlling and clearing infectious agents, many pathogens developed strategies to escape the nonspecific mechanisms of the innate immune system. Therefore, the **acquired immune system** provides adaptive protection towards antigens (Ag) and, in contrast to the innate immune system, is able to develop an immunological memory[2]. This kind of immune response is mediated by B and T lymphocytes, which circulate constantly through secondary lymphatic organs and present an immense repertoire of specific surface receptors (BCR/TCR) generated from rearranged gene segments. Upon contact of a B cell with a foreign substance, the specific BCR (B cell receptor) mediates endocytosis of the antigen, which is subsequently processed and presented embedded in MHC class II molecules on the B cell surface. Interaction with a primed T helper cell of the appropriate specificity then leads to B cell activation, Ig class switch recombination and differentiation into plasma cells that secrete antibodies (Ab) to the target antigen (**humoral immunity**). Finally, immune complexes (Ab-Ag) are neutralized by phagocytosis.

Recognition of a specific Ag bound to MHC II molecules on the APC surface by the corresponding TCR (T cell receptor) leads to activation and proliferation of T helper cells ($CD4^+$) (*for details see 1.3*). This type of effector T cell acts indirectly by releasing chemical mediators (cytokines and chemokines) to enhance the inflammatory response, and directly by activating B cells through cell-cell-interaction. Cytotoxic T cells ($CD8^+$), in contrast, effect **cell-mediated immunity**; they recognize Ag presented on MHC I molecules and release cytotoxins (perforin, granzymes) to directly lyse foreign, virus-infected or cancer cells.

After the first exposure to a specific antigen, an immunological memory is generated to protect the organism from subsequent infections. Both B and T cells are able to develop resting, long-lived memory cells, able to mediate a rapid, effective immune response after secondary challenge with the same pathogen (*for details see 1.4*).

1.2 Establishment of self-tolerance during T cell development

T lymphocytes are able to generate a wide variety of different TCR from the same genomic sequence by a process known as somatic recombination[3]. In this way, unique antigen-binding sites are determined randomly, and some of them might be able to recognize auto-antigens. To avoid immune responses towards self-antigens that could harm the organism, auto-reactive lymphocytes are inactivated or eliminated directly. During thymocyte development, T cell precursors acquire self-tolerance to prevent autoimmunity[4]. Bone marrow-derived T cell progenitors are attracted to the thymus (by adhesion molecules and chemokines), where they pass through different developmental stages and corresponding TCR quality control checkpoints to establish a non-self-reactive T cell pool[5]. Two general types of T cells can be distinguished. The majority (95%) of the T cells belong to the αβ T cell lineage; only about 5% express the alternative γδTCR[6].

During the first stage of T cell development, double negative T cell precursors ($CD4^-CD8^-$; DN) start with the recombination of TCR gene segments, resulting in preTCR expression. Ligand-independent signals provided by the preTCR lead to CD4/CD8 co-expression ($CD4^+CD8^+$; double positive; DP) and further recombination of TCR genes[7]. Once a functional antigen receptor is expressed, thymocyte development is continued in the thymus and the survival of $TCR\alpha\beta^{low}CD4^+CD8^+$ cells depends critically on the TCR affinity for self-peptide:MHC complexes.

1.2.1 Central Tolerance

The thymic microenvironment has several mechanisms to ensure T cell tolerance before releasing mature T cells to peripheral tissues. This so-called central tolerance is established by positive and negative selection processes[8] (*"affinity model of selection"*).

In the thymic cortex, $CD4^+CD8^+$ DP immature T cells undergo ligand-dependent selection by binding self-peptide:MHC complexes on cortical thymic epithelial cells (cTEC). Thymocytes expressing TCR molecules that are not able to bind self-peptide:MHC complexes are deleted by apoptosis. In contrast, low-affinity engagement of the TCR selectively induces survival (**positive selection**) and subsequent differentiation to mature CD4/CD8 single positive thymocytes[9] (**SP**; $TCR\alpha\beta^{high}CD4^+CD8^-$ and $TCR\alpha\beta^{high}CD4^-CD8^+$); the respective co-receptor not involved in MHC recognition is lost.

Positively selected SP T cells travel on towards the thymic medulla, where they are exposed to a diversity of tissue-specific self-antigens presented by medullary thymic epithelial cells (mTEC) and DC. SP thymocytes that harbor high affinity TCR to self-antigens are potentially harmful; these auto-reactive cells are eliminated from the T cell pool by apoptosis (**negative selection**). In contrast, low affinity interaction of the TCR with self-peptide:MHC complexes ensures T cell survival and subsequent release of functional, mature T cell clones to peripheral tissues[10].

Nonetheless, high affinity interaction of TCR molecules with self-peptide:MHC complexes in the presence of survival cytokines such as IL-2 or TGFβ induces the development of another important T cell type, the $CD4^+CD25^+$ naturally-occurring regulatory T cells (nT_{reg}). This process, called **clonal diversion,** requires the expression of the transcription factor FoxP3 and rescues potentially harmful auto-reactive clones, providing them with suppressive or regulatory functions[11] (*see also 1.3.2*).

1.2.2 Peripheral Tolerance

As not all self-antigens are thymically expressed (such as food-derived or developmental antigens) and some potentially auto-reactive T cells manage to escape central tolerance, additional immune surveillance mechanisms operate in the periphery, preserving the state of tolerance and preventing inappropriate T cell reactions[12].

Activation of naïve mature T cells as well as subsequent proliferation and cytokine expression require, in addition to TCR engagement, positive co-stimulatory signals mediated by CD28 binding to B7 molecules (CD80/B7-1 or CD86/B7-2) expressed on APC. In the absence of an inflammatory response, quiescent APC present low surface levels of B7 molecules. When auto-reactive T cells are exposed to self-peptide MHC complexes in absence of CD28-co-stimulatory signals, activation

of naïve T cells fails and a state of hypo-responsiveness, also known as **clonal anergy**, is induced. Anergic cells are characterized by their inability to proliferate and to produce IL-2 due to insufficient TCR signaling, and hence remain unresponsive to antigens[13].

Besides the positive second signal provided by CD28, other molecules provide **negative regulation** to limit anti-self T cell responses and to establish tolerance. One of these negative receptors is CTLA-4: like CD28, it presents high affinity for B7 family co-stimulatory molecules and thus restricts B7 interaction with CD28 in a competitive way. In consequence, CTLA-4 mediates negative signals to prevent expansion of autoreactive T cell clones[14]. Another essential inhibitory co-stimulatory molecule is PD-1 (programmed death 1). By interaction with one of its ligands (PD-L1 or PD-L2), efficient TCR engagement is prevented and self-reactive T cells remain in an anergic state[15]. Both CTLA-4 and PD-1 are crucial for inducing and preserving functional inactivation of auto-reactive T cell clones in an antigen-specific manner. The absence CTLA-4 or PD-1 leads to impaired anergy induction and finally to development of autoimmune diseases[16-19].

Another type of tolerance mechanism acts when potentially autoreactive naïve T cells migrate to the periphery but the respective antigen is isolated within inaccessible tissues. This physical separation (e.g., blood-brain barrier) prevents an encounter with the antigen and subsequent activation of the auto-reactive T cell, a phenomenon known as **clonal ignorance**.

Other cell types, such as **regulatory T cells (T_{reg})**, are also involved in mediating peripheral tolerance. T_{reg} suppress auto-reactive T cells by expression of immunosuppressive cytokines such as TGFβ and IL-10 and thus prevent autoimmune responses[20].

Upon activation of an autoreactive T cell, an intrinsic tolerance mechanism known as **activation-induced cell death (AICD)** is triggered. Repeated T cell stimulation by self-antigens induces the co-expression of a death-domain-containing receptor named Fas (CD95) and its cognate ligand FasL (CD95L)[21,22]. In the presence of high IL-2 levels, Fas-FasL interaction triggers T cell apoptosis by activating caspase 8 (*for details see 1.5.1*).

Together, these tolerance mechanisms cooperate to ensure the generation of a diverse pool of naïve mature T cells able to induce effective immune responses to pathogen-derived antigens in the context of MHC molecules, while tolerating the self-antigens present. This fine balance of self-tolerance is precisely controlled to avoid autoimmune pathology; failure of any of these tolerance mechanisms leads to an inappropriate T cell response towards self-antigens and thus results in development of autoimmune diseases (*see 1.4.3*).

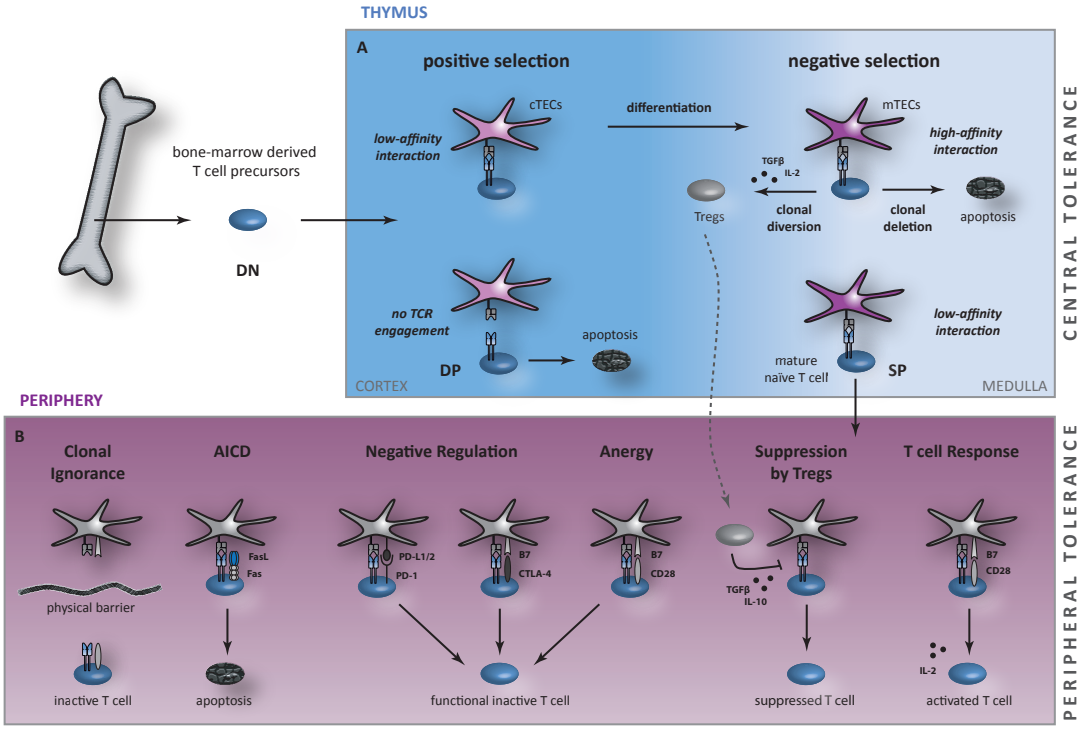

Figure 1.1. Overview of the tolerance mechanisms that shape the T cell repertoire. A. Central tolerance. Bone marrow-derived T cell precursors undergo a strict selection process in the thymus to establish an efficient T cell pool. In the thymic cortex, numerous $CD4^+CD8^+$ DP T cells undergo apoptosis because they are unable to bind to self-peptide:MHC complexes; only clones that recognize self-peptide:MHC complexes survive (*positive selection*) and develop to $CD4^+$ or $CD8^+$ SP T cells. In the thymic medulla, T cells that engage self-peptide:MHC complexes with low affinity are eliminated by apoptosis (*negative selection*), whereas low-affinity interaction leads to survival and release of mature T cells to the periphery. **B. Peripheral tolerance.** Different strategies help to prevent an immune response of mature T cells towards auto-antigens in the periphery, including suppression by regulatory T cells, anergy, negative regulation (via CTLA-4 or PD-1), activation-induced cell death (AICD) or clonal ignorance.

1.3 T cell activation

1.3.1 TCR activation pathways

Antigen-specific interaction of the TCR with peptide:MHC II complexes on APC, together with co-stimulatory signals provided by CD28, lead to T cell activation[23,24] (*Fig. 1.2A*). Following TCR stimulation, the tyrosine kinases Lck and Fyn are activated and phosphorylate CD3 ζ-chain ITAM (immunoreceptor tyrosine-based activation motif) as well as ZAP70[25], which in turn recruits several downstream molecules such as the two adaptor proteins SLP-76 and LAT to form an active signaling complex[26]. Phospholipase C gamma (PLCγ) is bound and activated by this complex, and in consequence mediates the hydrolysis of PIP_2 (phosphatidylinositol 4,5bisphosphate) into the second messengers IP_3 (inositol trisphosphate) and DAG (diacylglycerol)[27]. IP_3 mainly induces nuclear translocation of NFAT (nuclear factor of activated T cells), whereas DAG influences different T cell activation pathways.

The hydrophilic second messenger IP_3 diffuses through the cytosol and binds to its receptor (IP_3R) on membranes of the ER (endoplasmic reticulum), which triggers depletion of ER Ca^{2+} stores into the cytosol and promotes a transient elevation of intracellular free Ca^{2+} levels (*Fig.1.2B*). Accumulation of cytosolic Ca^{2+} activates calmodulin (CaM), which in turn activates the protein phosphatase calcineurin. Activated calcineurin dephosphorylates NFAT proteins[28], which appear to be heavily phosphorylated and thereby retained within the cytoplasm of resting T cells. Dephosphorylated NFAT proteins undergo conformational changes, leading to exposure of a nuclear localization sequence (NLS), which finally permits NFAT nuclear translocation and induction of NFAT-mediated gene transcription. NFAT-activated genes are involved in activation of T cells and in generation of T cell tolerance[29].

The membrane-diffusible second messenger DAG recruits and activates different effector molecules. PKCθ (protein kinase C) and RasGRP (RAS guanyl nucleotide-releasing protein) are two of the best characterized DAG targets in T cells[30,31]. Together, they control the initiation of two crucial signaling branches in T cell activation; the MAPK (mitogen-activated protein kinase) cascade and the NF-κB (nuclear factor-κB) pathway.

Together with SOS (son of sevenless), the GEF (guanine exchange factor) RasGRP promotes activation of Ras-GTP (*Fig. 1.2C*), which leads to a concatenation of phosphorylation events among the MAP kinases Raf-1, Mek-1 and ERK-1/2[32]. These events finally result in the assembly of the AP-1 (activator protein 1) transcription factor complex. AP-1 is composed of homo- and heterodimers of Fos and Jun family proteins and plays a key role in T cell activation and IL-2 production[33].

The NF-κB/Rel family of transcription factors also has a central function in T cell activation. In resting T cells, NF-κB dimers are found within the cytosol bound to inhibitory IκB molecules, which prevent NF-κB translocation to the nucleus by masking its nuclear localization sequence (NLS)[34]. Besides its contribution to the activation of the MAPK pathway, PKCθ is a critical factor for initiation of the NF-κB pathway. DAG-activated PKCθ phosphorylates CARMA1, which leads to formation of the trimolecular CMB complex composed of CARMA1, Bcl10 and MALT1 (*Fig. 1.2D*)[35,36]. The CBM complex promotes activation of IKK (IκB kinase) complexes composed of the catalytic subunits IKKα and IKKβ, and IKKγ/NEMO (NF-κB essential modulator) as a regulatory subunit, which in turn mediates the phosphorylation of inhibitory IκBα molecules[37]. This is an essential step in NF-κB activation, as it leads to ubiquitinylation and subsequent proteosomal degradation of inhibitory IκBα proteins[38]. In consequence, NF-κB dimers are released in the cytosol and are allowed to translocate to the nucleus, where they regulate transcription of pro-inflammatory genes including cytokines, chemokines, cell cycle regulators and adhesion molecules[37,39].

The crosstalk between the pathways described above determines the outcome of the immune response, and cooperative interaction of the transcription factors NFAT, AP-1 and NFκB promotes T cell activation, proliferation and pro-inflammatory cytokine production. As these events are also crucial for induction and maintenance of T cell tolerance and homeostasis, a wide variety of human diseases is associated with dysregulated pathway activities.

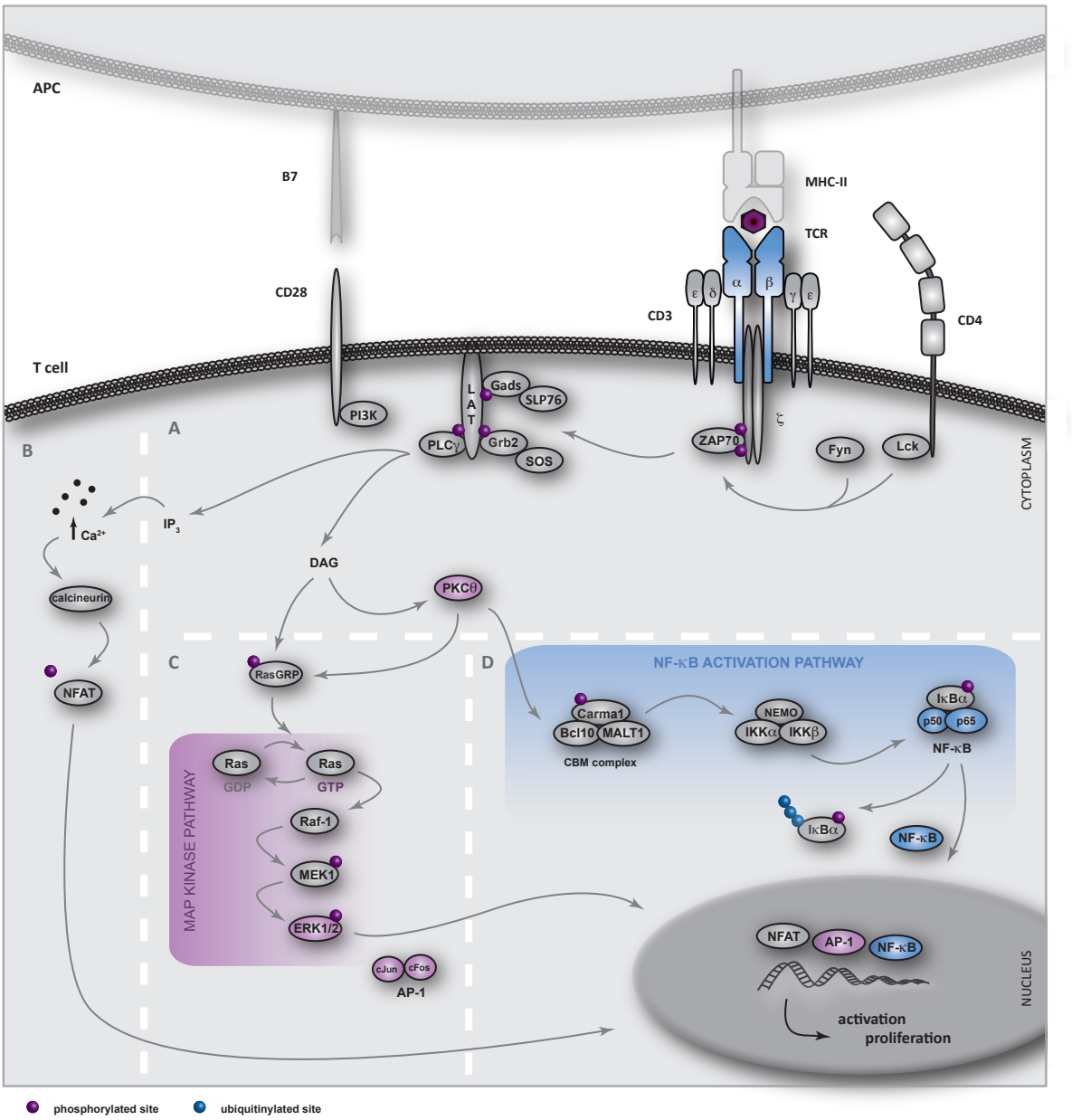

Figure 1.2. Overview of the main TCR activation pathways. A. TCR proximate events. Following interaction of the TCR with its specific peptide:MHC complex on APC, ITAM motifs within CD3 ζ-chains are phosphorylated. Activated ZAP70 and LAT induce the formation of a multi-molecular signaling complex and activation of PLCγ. The second messengers IP_3 and DAG subsequently trigger several downstream signaling pathways. **B. NFAT pathway.** IP_3 induces calcium-dependent calcineurin activation, and NFAT dephosphorylation leads to its nuclear translocation. **C. MAP kinase pathway.** Via RasGTP, DAG activates the MAPK phosphorylation cascade (Raf-1, MEK1, ERK1/2), finally resulting in AP-1 assembly. **D. NF-κB pathway.** PKCθ induces the formation of the CBM complex, which in turn promotes activation of IKK complexes. After phosphorylation and degradation of IκBα, NF-κB dimers are released and translocate to the nucleus. The transcription factors NFAT, AP-1 and NF-κB finally induce expression of pro-inflammatory cytokines and other genes involved in T cell activation and proliferation.

1.3.2 T cell subsets

After interaction with APC that present specific antigens on MHC II molecules on their surface, $CD4^+$ T cells are activated and exert their effector function via production of proinflammatory cytokines, to activate and attract B cells and macrophages towards the source of infection. During an inflammatory response, naïve $CD4^+$ T helper (T_H) cells can differentiate into several subtypes of effector T helper cells, depending on the cytokine milieu present during TCR activation and other factors such as antigen dose or co-stimulators. Based on their cytokine profile, activated $CD4^+$ T cells can be divided into the following major effector subtypes[40]: T_H1, T_H2, T_H17, and T_{reg}. Tight control among these functional subpopulations is required to establish polarized immune responses and to maintain tolerance.

In the presence of IL-12 and IFNγ, uncommitted $CD4^+$ T cells develop into mature T_H1 cells, while IL-4 favors the generation of T_H2 cells. The characteristic cytokines produced by T_H1 cells are IFNγ, IL-2 and TNFα, which activate macrophages and promote pro-inflammatory immune responses towards intracellular pathogens[40,41]. T_H2 cells typically produce large amounts of IL-4, -5, -10 and -13 to facilitate the clearance of extracellular pathogens as well as activation of eosinophils and IgE production by B cells. In addition, several transcription factors influence the differentiation towards T_H1 or T_H2 cells; T-bet, STAT1 and STAT4 promote generation of T_H1 cells, whereas GATA-3 and STAT6 support the production of T_H2 cells[40,41]. The development of T_H1/T_H2 cells is mutually antagonistic, and a fine balance is crucial to establish effective protection against pathogens and to prevent autoimmunity. Aberrant activation of T_H1 cells is linked to the development of autoimmune diseases such as systematic lupus erythematosus (SLE)[42], rheumatoid arthritis (RA) and multiple sclerosis (MS), while asthma and other allergies are induced by dysregulated T_H2 activity (*see 1.4.2*)[43].

The development of T_H17 cells is coupled to the presence of TGFβ, IL-6 and IL-23. T_H17 cells mainly secrete the pro-inflammatory cytokine IL-17, thereby facilitating innate immune responses towards extracellular bacteria and fungi[44]. Elevated IL-17 levels are associated with some autoimmune diseases[45,46].

In addition to naturally arising regulatory T cells (nT_{reg}), which develop in the thymus (*see 1.2.1 for details*), naïve $CD4^+$ T cells can convert into inducible T_{reg} (iT_{reg}) in the periphery. The presence of IL-10 and TGFβ leads to generation of iT_{reg} cells, which play a crucial role in downregulation of immune responses, maintenance of peripheral tolerance and prevention of autoimmunity[47]. Following activation, iT_{reg} cells secrete the immune-suppressive cytokines TGFβ and IL10 to regulate inflammatory responses. Defective T_{reg} functions result in development of autoimmune disorders or attenuated immunity[47].

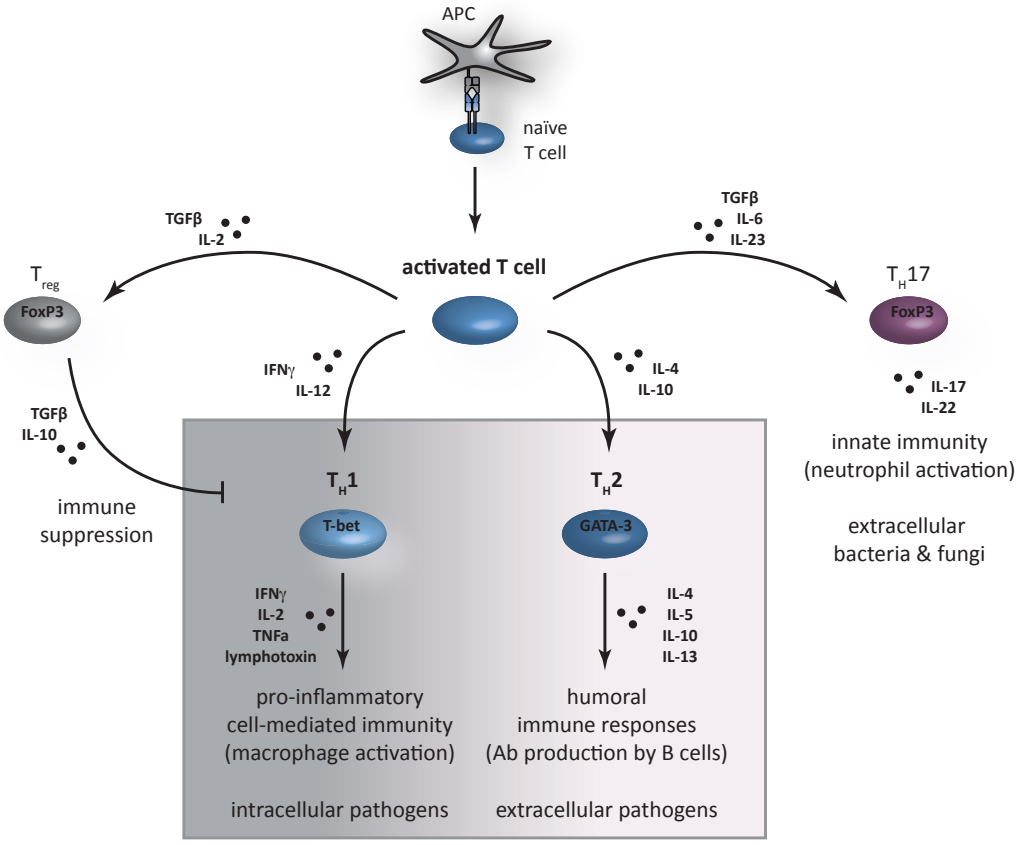

Figure 1.3. Overview of the principal T cell subsets. After activation by antigen encounter, naïve T cells differentiate into distinct effector T cells to ensure effective antigen clearance. The presence of a number of cytokines as well as transcription factor expression promote differentiation to T_H1, T_H2, T_H17 or T_{reg} cells, which in turn release particular cytokine subsets to promote (or inhibit) specific immune responses.

1.4 T cell homeostasis and its link to autoimmunity

1.4.1 T cell homeostasis during a normal immune response

Once naïve T lymphocytes (classified as $CD44^{low}$) recognize their specific antigen on MHC molecules presented by APC, they are activated and begin to proliferate intensely. This process, known as clonal expansion, amplifies the effector function by providing an elevated number of activated $CD44^{high}$ effector T cells to fight the infection[48,49].(*Fig. 1.4*). After eliminating the antigen, the activated lymphocytes undergo apoptosis during the contraction phase, to establish T cell homeostasis and prevent autoimmunity[50,51]. A small proportion of those cells survive, however, and evolve into memory T cells ($CD44^{high}CD62L^{low}$) to face subsequent infections in a faster, more efficient way. If the same antigen is recognized by the immune system, resting memory T cells differentiate immediately to activated/memory T cells ($CD44^{high}CD62L^{high}$), thus ensuring rapid antigen

clearance[52]. Inflammatory reactions must be precisely controlled to prevent overreaction of the immune system. The rapid clonal expansion of naïve T cells after antigen encounter is compensated by induced cell death of activated T lymphocytes after antigen clearance; this balance is known as T cell homeostasis[48-51]. Proliferation and apoptosis cooperate to ensure optimal immune responses and, at the same time, to protect the organism from autoimmunity. If one of these processes is defective, the proportion of naïve and memory T cells is altered. In consequence, tolerance is lost and autoimmune diseases might arise.

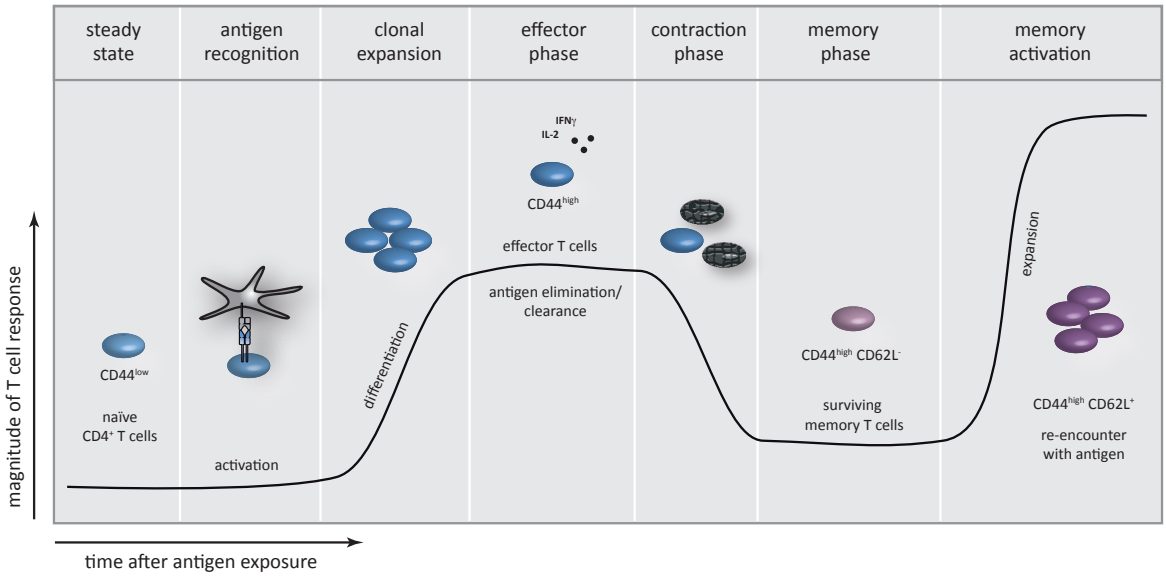

Figure 1.4. The course of a normal immune reaction. During a primary immune response, naïve T cells are activated, expand rapidly and evolve into effector T cells. After antigen elimination, effector T cells undergoapoptosis and only a few memory T cells survive. Upon re-encounter with the same antigen, activated memory T cells provide a fast, effective secondary immune response.

1.4.2 Defective T cell homeostasis leads to autoimmunity

T cell activation, proliferation and death are the three most important mechanisms involved in establishment and maintenance of T cell tolerance. Defects in any of these events cause break of tolerance, finally resulting in development of autoimmune diseases. Regulatory elements are thus crucial to restrict T cell activation, expansion and apoptosis and to keep autoimmunity at bay.

Complete T cell activation depends critically on positive co-stimulatory signals of CD28, initiating intracellular activation pathways that drive T cell proliferation. Other co-stimulatory molecules, such as PD-1 and CTLA-4, provide inhibitory signals that prevent T cell overactivation

and, in consequence, hyperproliferation (*see also 1.2.2*). Absence of PD-1 or CTLA-4 leads to loss of tolerance, massive lymphoproliferation and development of lupus-like disease in PD-$1^{-/-}$ and $CTLA^{-/-}$ mice[16,17,53], and PD-1 is implicated in human SLE[54]. Differentiation into distinct T cell subtypes after activation (*see also 1.3.2*) can also influence loss of tolerance and development of autoimmune diseases. Pro-inflammatory cytokines produced by T_H1 cells[55] (IFNγ) and T_H17 cells[45] (IL-17) are associated with anti-DNA autoantibody production in murine and human SLE.

Another crucial element in T cell tolerance and homeostasis is cell cycle control, especially the regulation of memory T cell proliferation. The absence of the cell cycle inhibitor p21 leads to development of lymphadenopathy and lupus-like autoimmune disease due to uncontrolled memory T cell expansion, as previously shown by our group[56,57] (*see also 1.6.3*). Similarly, other cell-cycle-associated molecules are crucial for maintenance of T cell tolerance, as development of autoimmune disease is observed in Gadd45$\alpha^{-/-}$, Gadd45$\beta^{-/-}$Gadd45$\gamma^{-/-}$ and $E2F2^{-/-}$ mice[58-60]. Not only memory T cells show aberrant proliferation levels; DN ($CD8^-$ $CD4^-$) T cell hyperproliferation was also observed in SLE patients[61]. Accumulating DN T cells were are implicated in the production of anti-DNA autoantibodies[62] and are responsible for elevated levels of IL-17[61].

Fas-induced apoptosis was thought to be the main regulatory mechanism of T cell restriction during the contraction phase, controlling T cell tolerance and homeostasis[63]. Several studies show that Fas-deficient T cells fail to undergo apoptosis *in vitro*, and *lpr* mice present autoimmune manifestations due to defective homeostasis[64] (*see 1.5.2*). Similar phenotypes are observed in mice that lack the pro-apoptotic molecule Bim, as well as in mice that overexpress the anti-apoptotic molecule Bcl-2[65]. Precise apoptosis regulation is thus closely linked to establishment and maintenance of T cell homeostasis.

1.5 Fas deficiency in mice and men

1.5.1 Fas-dependent apoptotic pathway

In physiological conditions, the immune system must restrict the number of activated lymphocytes after pathogen clearance to ensure T cell homeostasis and tolerance (*see 1.4.1*). This is achieved mainly by AICD via Fas (CD95, APO-1), a member of the tumor necrosis factor (TNF) receptor family, expressed as a homotrimer on the surface of T cells[66]. After T cell activation in the presence of IL-2, expression of its ligand FasL (CD95L, CD178) is induced and Fas-FasL interaction leads to the recruitment of the adaptor molecule FADD (Fas-associated death domain protein) to the death domains within the cytoplasmic tail of Fas[67,68] (*Fig. 1.5*). FADD initiates the formation of

DISC (death-inducing signaling complex), including pro-caspase-8[69] which subsequently undergoes conformational changes that allow its proteolytic autoprocessing and assembly of the enzymatically active caspase-8 form. The effector caspases-3 and -7 are then mobilized within the cytoplasm, which in turn induce morphological changes characteristic of apoptotic cells, such as chromatin condensation, cytoplasm contraction and DNA fragmentation[70]. This caspase cascade forms part of the so-called **extrinsic pathway of apoptosis** and leads to AICD.

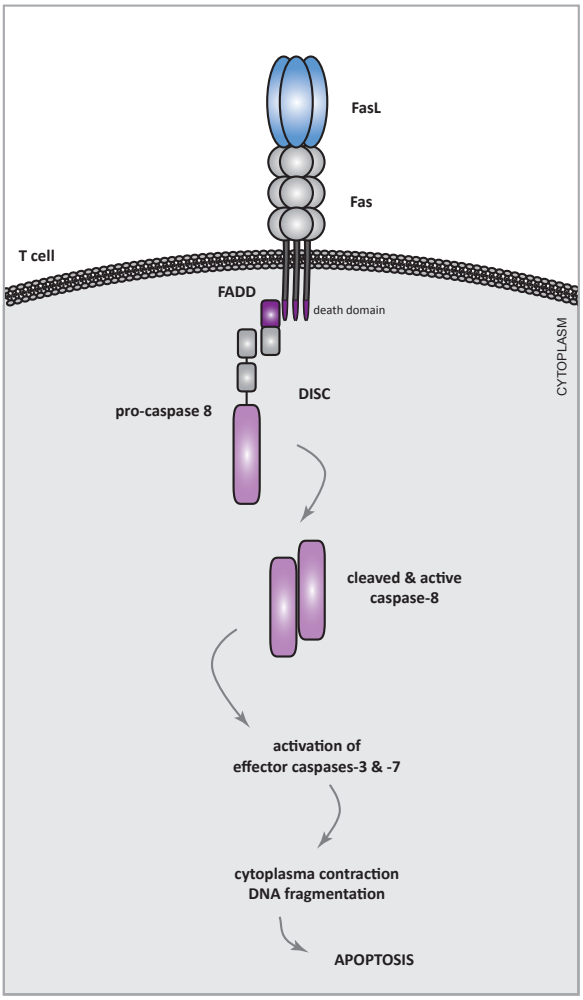

Figure 1.5. The extrinsic apoptosis pathway. Following Fas interaction with its ligand FasL, death domains within the Fas cytoplasmic tail mediate FADD recruitment and the subsequent formation of the death-inducing signaling complex (DISC). Within this complex, autoprocessing of pro-caspase 8 leads to the enzymatically active form of caspase-8, which in turn activates the downstream effector caspases3 and 7. The cell subsequently undergoes morphological changes and finally, apoptosis.

1.5.2 The B6/*lpr* mouse model of autoimmune disease

The crucial role of Fas in T cell homeostasis and tolerance maintenance is demonstrated by B6/*lpr* mice (*lpr: lymphoproliferation*). Fas deficiency due to a disruption of the *fas* gene (by insertion of a retrotransposon) causes severe defects in extrinsic apoptosis signaling and, in consequence, development of autoimmune disease[71]. These mice have a typical phenotype characterized by enlarged secondary lymphoid organs (extensive lymphadenopathy and splenomegaly) due to accumulation of DN T cells, hypergammaglobulinemia, elevated levels of anti-DNA antibodies, immune

complex precipitation in kidneys and moderate glomerulonephritis[72]. In addition, accumulation of $CD4^{+}CD44^{high}CD62L^{low}$ memory T cells is observed[73]. In *lpr* mice on the autoimmunity-prone MRL background, severity of autoimmune manifestations is increased and kidney failure leads to early death in MRL/*lpr* mice[73,74].

Development of lymphadenopathy in B6/*lpr* mice was initially attributed to defective lymphocyte apoptosis[71]; however, defects in other elements of the apoptotic pathway (such as FADD or caspase -8) lead to immunodeficiency and not to autoimmunity as in B6/*lpr* mice[75,76]. The resistance to apoptosis of B6/*lpr* T cells observed in *in vitro* studies also often fails to appear in physiological conditions[72]. Another yet unexplainable observation is the T cell hyperproliferation detected in lymph nodes of B6/*lpr* mice *in vivo*[77,78]. The autoimmune phenotype in Fas-deficient mice thus appears to be complex and cannot be justified only by the defect in apoptosis signaling; other factors might be involved to cause lupus-like disease. As several human autoimmune diseases present Fas deficiency and/or uncontrolled lymphoproliferation, the origin of autoimmunity in Fas-deficient mice is currently of special interest.

1.5.3 The autoimmune lymphoproliferative syndrome

In humans, mutations in the gene that encodes Fas –and other molecules implicated in the extrinsic apoptosis pathway– lead to development of an autoimmune lymphoproliferative syndrome (ALPS)[79-81]. Patients suffering from this rare disorder have defective apoptotic mechanisms in lymphocytes and as a result, lymphocyte accumulation and autoimmunity[82]. Onset of lymphoproliferation and autoimmune manifestations are normally detected in early childhood, but can also be diagnosed in adults. The most common ALPS-associated clinical manifestation is increased proliferation of lymphocytes (mostly DN T cells), causing enlargement of secondary lymphoid organs (lymphadenopathy and splenomegaly, presented by >80-90% of patients). Other common features of ALPS are mild to severe autoimmunity (anti-DNA antibodies as well as autoimmune cytopenias, hemolytic anemia, neutropenia, and/or thrombocytopenia) and increased risk of secondary cancers (Hodgkin and non-Hodgkin lymphomas; carcinomas)[82,83].

1.6 The cell cycle inhibitor p21 and its implication in autoimmunity

1.6.1 Regulation of cell cycle progression

After activation by antigen encounter, T lymphocytes begin to proliferate in order to exert their specific effector function (clonal expansion; *see 1.4.1*). During the division cycle, T cells pass through four distinct phases: cell growth (G1), DNA replication (S), chromosome distribution to daughter cells (G2) and mitosis (M).

External events, such as TCR activation, initiate the replication process, and the progression from one stage to the next is governed by several internal control mechanisms. At these cell cycle checkpoints, different cyclins associate with cyclin-dependent kinases (CDK) to coordinate cell cycle events[84]. Activated CDK phosphorylate and thus activate other regulatory molecules involved in cell cycle progression. G1 to S phase transition is characterized by activation of cyclinD/CDK4, cyclinD/CDK6 and cyclinE/CDK2 complexes[85] (*Fig. 1.6*). By phosphorylating retinoblastoma proteins (pRb), these cyclin/CDK complexes enable the release of E2F2 transcription factors and thus facilitate the transcription of genes required for cell cycle progression[86].

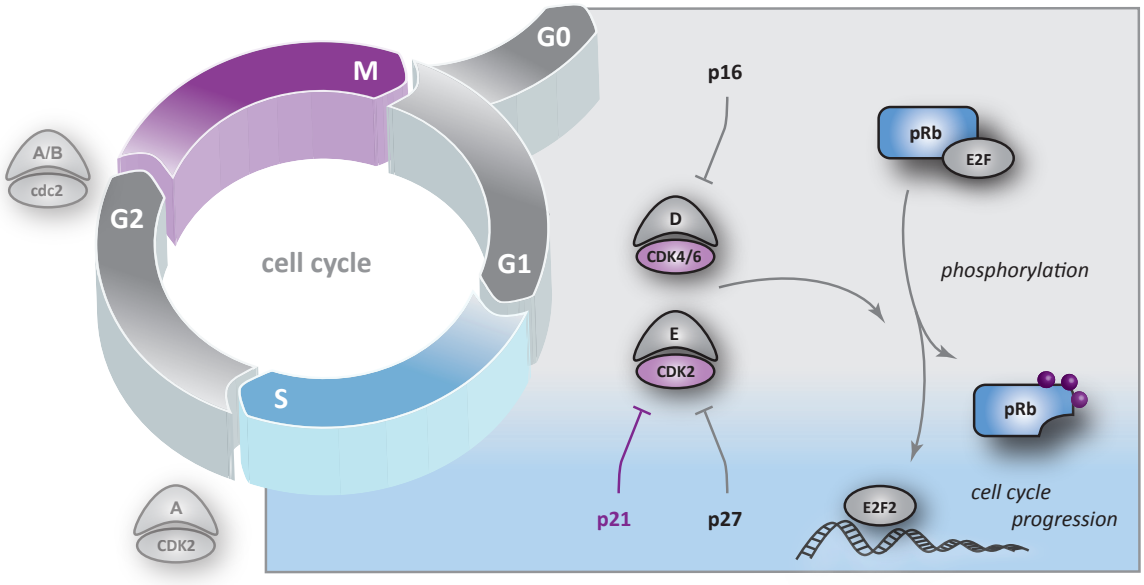

Figure 1.6. The G1/S checkpoint of the eukaryotic cell cycle. CDK associate with different cyclins (cyclinD/CDK4,6 and cyclinE/CDK2 complexes) to promote transition from G1 to S phase, inactivating the transcriptional repression of E2F2 transcription factors by retinoblastoma proteins (pRb). E2F2 transcription factors subsequently induce genes required for cell cycle progression. The activity of cyclinE/CDK2 complexes is repressed by CDK inhibitors p21 and p27; p16 selectively inhibits cyclinD/CDK4,6 complex activity.

There are nonetheless various regulatory molecules that block cell cycle progression to restrain proliferation of activated T lymphocytes or to prevent the generation of compromised T cells due to DNA damage. CDK activation is inhibited by negative regulators known as CDK inhibitors, which act at different checkpoints during the cell cycle. Entry into S phase is controlled by two families of CDK inhibitors[86]; p15, p16, p18 and p19 form part of the INK4 family and bind to CDK4 or CDK6 to inhibit their interaction with cyclinD[87], whereas the Cip/Kip family members p21, p27 and p57 prevent the formation of cyclinE/CDK2 complexes[88]. In consequence, pRb remains unphosphorylated, E2F2 downstream activities are repressed and the cell cycle is arrested. In the absence of p16 or p27, lymphoid organs are enlarged or lymphocyte selection in the thymus is impaired, but break of tolerance is not observed[89-91]. In contrast, p21 deletion leads to loss of tolerance and autoimmunity development, indicating a specific role for p21 in cells of the immune system (*see below*).

1.6.2 The cell cycle inhibitor p21

In the early 1990s, p21 was the first molecule identified as a CDK inhibitor[92] and as a p53 effector in response to DNA damage[93,94]. At present, the Cip/Kip family of cell cycle inhibitors is comprised of p21, p27 and p57, which act mainly at the G1 checkpoint. By binding to CDK2 via specific sequences in its N-terminal domain, p21 acts as negative regulator of cyclin/CDK complex activity and induces cell cycle arrest in G1[95,96]. In addition to its most prominent role as a CDK2 inhibitor, p21 has important functions in multiple cellular processes such as differentiation, apoptosis and transcription[97].

One of the most important p21 functions is its implication in the cell response to DNA damage[98]. Detection of DNA lesions leads to p53-dependent transcription of the gene CDNKN1A, which encodes p21. Increased amounts of p21 then inactivate G1 phase cyclin/CDK complexes and halt the cell cycle to allow DNA repair[97,99]. Following environmental stress, p21 is activated in a p53-independent manner to prevent malignant cell transformation due to genomic instability. p21 is also able to inhibit cell cycle progression directly. Due to the strong affinity of its C-terminal domain for the polymerase co-factor PCNA (proliferating cell nuclear antigen), p21 can interrupt the PCNA interaction with DNA synthesis molecules and thus blocks DNA replication pathways[100].

The role of p21 in regulation of programmed cell death is currently debated. p21 might have pro- or anti-apoptotic functions, depending on cellular context and stress conditions, e.g., magnitude of DNA damage[101,102]. Apoptosis is also promoted or inhibited depending on the subcellular localization of p21. Within the cytoplasm, p21 interacts with caspase-2, pro-caspase-3

and other stress-induced MAP kinases such as ASK1 (apoptosis signal-regulating kinase 1), impeding their activation and thereby inhibiting apoptosis[103,104], whereas nuclear localization favors p21 degradation and thus promotes apoptosis induction after DNA damage[105]. Not only p21 downmodulation but also its overexpression induces apoptotic signaling pathways in response to irradiation[106-108]. Overall, p21 has a fine-tuned role in cell death regulation, although the modulating mechanism remains elusive[109].

As p21 inhibits cell cycle progression, its absence was thought to promote cancer development. Nonetheless, $p21^{-/-}$ mice are not more tumor-prone than normal mice[56,110,111]. In addition, CDKN1A is rarely deleted in human tumors, and p21 is usually only partially downregulated and not completely lost in tumor cells[112]. These findings indicate that oncologic transformation of p21-deficient cells is caused by other elements, and suggest a tumor-suppressive role for cytoplasmic p21.

1.6.3 p21 as suppressor of autoimmunity

To determine the role of p21 in induction of autoimmune diseases, we generated p21deficient mice on a neutral C57BL/6 background. $p21^{-/-}$ mice develop normally, but lose tolerance to DNA over time and finally develop moderate, non-lethal autoimmunity including mild glomerulonephritis[56]. The appearance of the autoimmune phenotype in these mice was linked to defective homeostasis in effector/memory T cells and macrophage hyperactivation[56,111].

In other studies, deletion of p21 in mice with a mixed background (C57BL/6 x Sv/129) led to severe lupus-like autoimmunity and death at less than one year of age. Some characteristics observed in these mice, such as lymphadenopathy, splenomegaly, glomerulonephritis, T cell accumulation and high levels of anti-DNA antibodies, are similar to the phenotype presented by B6/*lpr* mice[57] (*see 1.5.2*), although the severe disease outcome was attributed to the mixed genetic background enhancing the effect of p21 deletion.

Also in humans, p21 deficiency is related to autoimmune diseases. Mutations in CDKN1A (which encodes p21) and other genes located on chromosome 6 (e.g., HLA class I+II and STAT4) were associated with SLE[113-115]. These mutations are inherited in some cases, but can also appear *de novo*. Not only genetic susceptibility, but also environmental factors are thought to be responsible for the occurrence of this systemic autoimmune disease[116]. In general, SLE affects women at higher rates than men (9:1), and disease usually manifests at age 15 - 35 years. In SLE patients, defective apoptosis leads to generation of anti-nuclear antibodies (ANA), subsequent precipitation of immune complexes, and inflammatory responses. As a result of chronic inflammation, tissues of multiple organs such as skin, liver, kidney, joints, blood vessels, heart and the nervous system

can be damaged[116]. Elevated levels of pro-inflammatory cytokines such as IL-17 were linked to development of lupus nephritis[61]. At the cellular level, hyperproliferation of T lymphocytes due to altered TCR signaling[117] and accumulation of DN T cells is observed[61]. SLE is not currently curable and immunosuppressive drugs such as cyclophosphamide or corticosteroids are common treatments[116].

2. OBJECTIVES

2. OBJECTIVES

To avoid development of autoimmunity, the maintenance of T cell tolerance is fundamental for the organism. This tolerance is established by the fine balance between T cell activation, proliferation and death, processes in which a broad variety of molecules are involved. Their activity must be strictly controlled, as any dysregulation leads to severe immune defects. One example is the cell cycle inhibitor p21; C57BL/6 $p21^{-/-}$ mice (hereafter, $p21^{-/-}$) develop normally, but continuously lose tolerance to DNA until they finally develop mild autoimmune disease[56,57]. An important characteristic of $p21^{-/-}$ mice is the hyperactivation and subsequent *in vitro* hyperproliferation of $CD4^+$ memory T cells, as previously reported by our group[56]. This massive proliferation was not detectable *in vivo* however; here, we established an *in vitro* stimulation system that approximates the results of the T cell responses observed *in vivo*. As p21 was implicated in effector/memory T cell activation, an event often dysregulated in autoimmune diseases, understanding the regulatory function of p21 is of considerable interest.

For the present study, the following **objectives** were defined:

1. To study the effect of p21 on T cell activation in diverse *in vitro* systems and identify the activation pathways controlled by p21.

2. To examine whether p21 regulates T cell activation independently of its role as a cell cycle inhibitor.

3. To define the influence of p21 on T cell activation in response to low affinity antigens, an event considered critical for development of autoimmunity.

4. To analyze the effect of p21 deficiency on T cell activation in parallel with the autoimmunity-inducing *lpr* defect.

5. To determine the therapeutic effect of T cell-specific p21 overexpression on lupus-prone B6/*lpr* mice.

3. MATERIALS & METHODS

3. MATERIALS & METHODS

3.1 Mice

C57BL/6 mice (hereafter, B6) were obtained from Harlan Interfauna Ibérica (San Felíu de Codines, España). Fas-deficient **C57BL/6-*lpr*** mice (B6/*lpr*) were provided by Jackson Laboratory (ME, USA). **C57BL/6-p21$^{-/-}$** mice (p21$^{-/-}$) were generated by crossing p21$^{-/-}$ 129/Sv mice (laboratory of Dr. Gregory Hannon, Cold Spring Harbor Laboratory, NY, USA) with C57BL/6 mice over eight generations. Background analysis via microsatellite markers confirmed >99% identity with the C57BL/6 background[56]. **C57BL/6-*lpr*-p21$^{-/-}$** mice (B6/*lpr*-p21$^{-/-}$ were generated by crossing C57BL/6-*lpr* with C57BL/6-p21$^{-/-}$ mice.

C57BL/6-p21tg mice (B6p21tg) were a gift from Dr. Arun Fotedar's laboratory (Sidney Kimmel Cancer Center, San Diego, CA, USA)[106]. **C57BL/6-*lpr*-p21tg** mice (B6/*lpr*-p21tg) were generated from C57BL/6-*lpr* and C57BL/6-p21tg mice by crossing for at least eight generations. As transgene expression is controlled by the Lck promotor, human p21 expression is resticted to T cells in both C57BL/6-*lpr*-p21tg and C57BL/6-p21tg mice[106].

pcc.TCRtg mice express a transgenic TCR specific for pigeon cytochrome C (PCC 88-104) and were kindly provided by Dr. Mark M. Davis (Stanford University School of Medicine, Stanford, CA, USA)[118]. These mice have an I-A^{k} haplotype and 90% of all T cells express the TCR variable regions Vα11 and Vβ3. **pcc.TCRtg-p21$^{-/-}$** mice were generated by crossing pcc.TCRtg and C57BL/6-p21$^{-/-}$ for several generations, conserving the IA^{k} haplotype. **B10BR** mice present an I-A^{k} haplotype and were provided by the Jackson Laboratory. **OT-II** mice (I-A^{b} haplotype) were also purchased from the Jackson Laboratory and express a transgenic TCR (Vα2) specific for chicken ovalbumin (OVA 323-339)[119,120]. **p21$^{-/-}$ OT-II** mice were generated in our laboratory by crossing OT-II and C57BL/6-p21$^{-/-}$ for several generations, conserving the I-A^{k} haplotype.

All strains were maintained at the CNB animal facility in pathogen-free conditions. Unless otherwise specified, mice were approximately 8-10 weeks old when used for experiments. All animal experiments complied with European regulations and were approved by the CNB Bioethics Committee.

3.2 Cell culture

3.2.1 Isolation of $CD4^+$ T cells

To obtain a single-cell suspension, spleens were segregated using 40 μm nylon filters (BD Biosciences) with RPMI-1640 medium (Gibco Life Technologies) containing HEPES (10 mM). Erythrocytes were subsequently lysed by treatment with an ammonium chloride solution (0.83% NH_4Cl, 0.1% $KHCO_3$ and 0.004% EDTA [ethylenediaminetetraacetic acid]) for 4 min at RT (room temperature). For isolation of $CD4^+$ T cells by negative selection, the cell suspension was incubated with magnetic beads coated with anti-CD8 and -B220 antibodies (pan-B220 and anti-CD8 Dynabeads; Dynal Biotech, Invitrogen) for 40 min at 4ºC with gentle shaking. A magnetic field was then applied and the supernatant (containing $CD4^+$ cells) was separated. The purity of $CD4^+$ cells was confirmed by flow cytometry and was routinely >80%.

3.2.2 Cell culture medium

Purified $CD4^+$ T cells were cultured in RPMI-1640 medium supplemented with 10% FCS (fetal calf serum; Harlan Bioproducts, SeraLab), 2 mM Lglutamine, 100 U/ml penicillin, 100 μg/ml streptomycin, 1 mM sodium pyruvate, 10 mM HEPES pH 7.4, 0.1 mM nonessential amino acids and 50 mM β-mercaptoethanol (all from Gibco Life Technologies).

3.2.3 Repeated *in vitro* stimulation protocol

For **primary stimulation**, previously purified $CD4^+$ T cells were plated (1 x 10^6 cells/ml) and stimulated with 1.5 μg/ml concanavalin A (ConA; Sigma Aldrich) in the presence of human recombinant interleukin-2 (hrIL-2; 20 ng/ml; PeproTech) for 24 h *in vitro*. Cells were washed and replated in fresh RPMI medium (0.5 x 10^6 cells/ml) supplemented with 20 ng/ml hrIL-2 for a total of 6 days; medium was changed after 3 days to prevent nutrient and IL-2 depletion. After this IL-2 expansion phase, cells were restimulated with ConA (1.5 μg/ml) for the indicated time (**secondary stimulation**). As rechallenge of $CD4^+$ T cells with the same antigen induces AICD, secondary stimulation was usually carried out with the apoptosis inhibitor zVAD (benzyloxycarbonyl-Val-Ala-Asp-fluoromethlketone; Bachem) at indicated concentrations[121].

In some experiments, cells were stimulated with PMA (phorbol 12-myristate 13acetate, 20 ng/ml; Calbiochem) and ionomycin (0.5 μg/ml; Sigma), with plate-bound anti-CD3 (0.5 μg/ml; PharMingen) in 0.1 M Tris-HCl and soluble anti-CD28 (1 μg/ml; PharMingen) or with

IL-12 (10 µg/ml) and IL-18 (10 µg/ml; both from Sigma Aldrich). Some cell cultures were carried out in the presence of different inhibitors, such as the inhibitor of ERK1/2 phosphorylation, U0126 (1,4-diamino-2,3-dicyano-1,4-bis[2- aminophenylthio] butadiene; Cell Signaling) at 10 mM final concentration[122], the inhibitor of IκBα phosphorylation $BAY_{11\text{-}7082}$ ((E)-3-(4-methylphenylsulfonyl)-2-propenenitrile, Sigma Aldrich) at 10 mM final concentration[123], or the inhibitor of CDK2 activation CVT-313 (CDK2 inhibitor III; Calbiochem) at 2.5 mM final concentration[124,125].

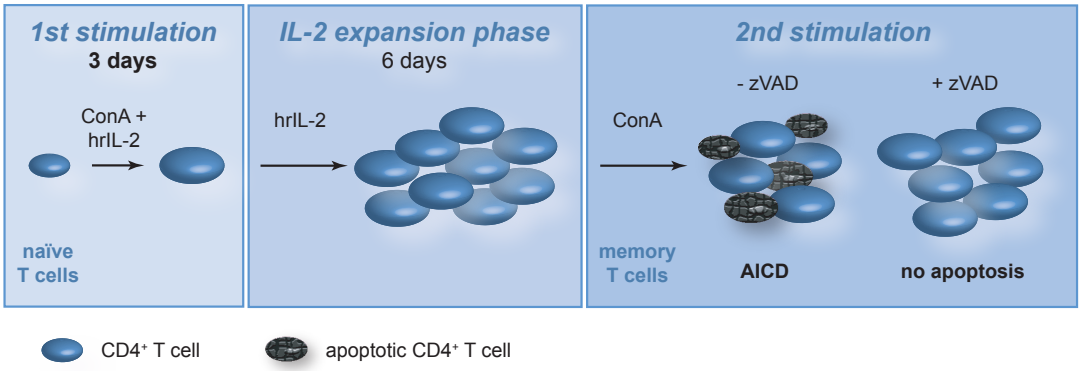

Figure 3.1. Repeated *in vitro* stimulation protocol. $CD4^+$ cells isolated from murine spleens were stimulated for 24 h with ConA (1.5 µg/ml), expanded for 6 days in hrIL-2 (20 ng/ml), and restimulated under varying conditions. To avoid AICD, secondary stimulation was carried out in the presence of zVAD (12.5 mM).

3.2.4 Generation of bone marrow-derived dendritic cells

Bone marrow extracted from mouse femur and tibia was segregated using 40 µm nylon filters (BD Biosciences) in RPMI-1640 medium containing HEPES (10 mM). After erythrocyte lysis, bone marrow progenitor cells were cultured with GM-CSF (granulocyte/macrophage colony-stimulating factor; 20 ng/ml) to promote DC differentiation and proliferation. GM-CSF was obtained from supernatant of the melanoma tumor D5-G6 cell line (a kind gift of Dr. Abul Abbas, Universidad de California, San Francisco, CA, USA). After three days, fresh medium and GM-CSF (20 ng/ml) were added. At day 6, slightly attached cells were lifted with 3 mM EDTA in 1x PBS (1 min) and, together with non-adherent cells (supernatant), washed and transferred to new plates. In addition to GM-CSF (20 ng/ml), IL-4 (1 ng/ml), generated from supernatant of I3L6 cells (a kind gift of Dr. Abul Abbas), was added to the cell culture. The next day, 1 mg/ml LPS (lipopolysaccharide, *Escherichia coli* O26:B6; Sigma Aldrich) and 1 mM peptide (ovalbumin, OVA 323-339) were added to promote DC maturation and protein presentation. After 20 h, non-adherent cells were collected and stained for CD86 (B72) and $I\text{-}A^b$ (MHC II) to test the yield of DC by flow cytometry (normally >60%).

3.2.5 Mixed cultures of pcc.TCRtg CD4⁺ T cells with APC

To stimulate CD4⁺ T cells in more physiological conditions, APC were used to present agonist peptides with high (PCC, KAERADLIAYLKQATAK) or low affinity (A96I, KAERADLIIYLKQATAK; isoleucine replaced alanine at position 96 of the PCC peptide)[126,127] for the transgenic TCR of naïve CD4⁺ T cells isolated from spleens of pcc.TCRtg or pcc.TCRtg-p21$^{-/-}$ mice (*see 3.2.1*). APC were obtained from B10BR mice by segregation of spleens on 40 μM nylon filters and subsequent lysis of erythrocytes (*described in 3.2.1*). Finally, APC were irradiated at 30 Gy to prevent proliferation during culture. For the **first stimulation**, CD4⁺ TCRtg T cells (0.5 x 10^6 cells/ml) were plated at a 1:3 ratio with irradiated APC. As naïve CD4⁺ T cells show less affinity to MHC II molecules presenting peptides than memory T cells[128], an agonist peptide with high affinity for the TCR (PCC; 3 mM) was used to stimulate naïve CD4⁺ TCRtg T cells in the presence of hrIL-2 (20 ng/ml). After 24 h, cells were washed and replated at a final concentration of 0.5 x 10^6 cells/ml in fresh RPMI medium supplemented with hrIL-2 (20 ng/ml) for a total of 6 days. Medium was changed every 2 days to avoid nutrient and hrIL2 depletion. After this expansion phase, cells were washed and restimulated with irradiated APC (1:3 ratio of 1 x 10^6 CD4⁺ TCRtg T cells/ml to APC). For the **secondary stimulation**, different concentrations of agonist peptides with high or low affinity for the TCR were used (PCC or A96I) in the presence of hrIL-2 (20 ng/ml) and zVAD (12.5 mM) (*Fig. 3.2*).

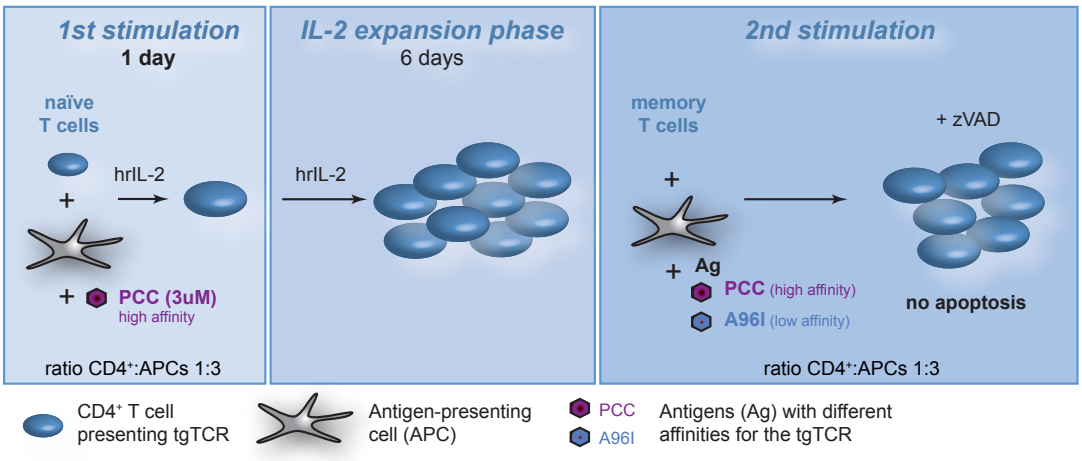

Figure 3.2. ***In vitro*** **system of repeated stimulation of pcc.TCRtg and pcc.TCRtg-p21$^{-/-}$ CD4⁺ T cells with irradiated APC, presenting peptides with high or low affinity for the TCR.**

3.2.6 Mixed cultures of OT-II CD4⁺ T cells with DC

Similar to the mixed cell cultures of pcc.TCRtg T cells (*3.2.5*), purified naïve OT-II and p21$^{-/-}$ OTII CD4⁺ T cells were stimulated with their specific peptide (OVA 323-339)[119,120], in this case presented by DC obtained from C75BL/6 mice (*see 3.2.4*). After 24 h primary stimulation with DC

presenting OVA (CD4⁺:DC ratio 10:1), CD4⁺ T cells were expanded in hrIL-2 (20 ng/ml) for a total of 6 days and subsequently restimulated with OVA-loaded DC (in conditions as for the primary stimulation) for the indicated times in the presence of zVAD (12.5 mM) (*Fig.3.3*).

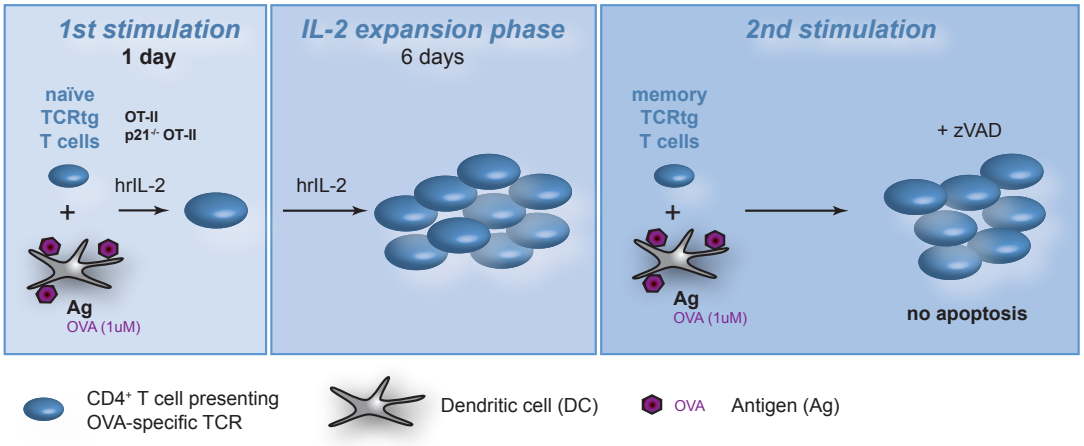

Figure 3.3. ***In vitro*** **system of repeated stimulation of OT-II and p21$^{-/-}$ OT-II CD4⁺ T cells with DC presenting OVA peptide.**

3.3 Adoptive transfer of OT-II CD4⁺ T cells

Purified naïve OT-II and p21$^{-/-}$ OT-II CD4⁺ T cells were CFSE (carboxyfluorescein succinimidyl ester; Molecular Probes)-labeled (*see 3.5.2*) and adoptively transferred (1 x 10^6 CD4⁺ T cells/mouse) to recipient mice of the same haplotype (B6). After 24 h, OVA-loaded DC were injected to stimulate the previously transferred CD4⁺ TCRtg T cells *in vivo*. After 3 days, mice were sacrificed and cells from secondary lymphoid organs were analyzed or restimulated *ex vivo* with 1 mM OVA for the indicated times (*Fig. 3.4*)[129].

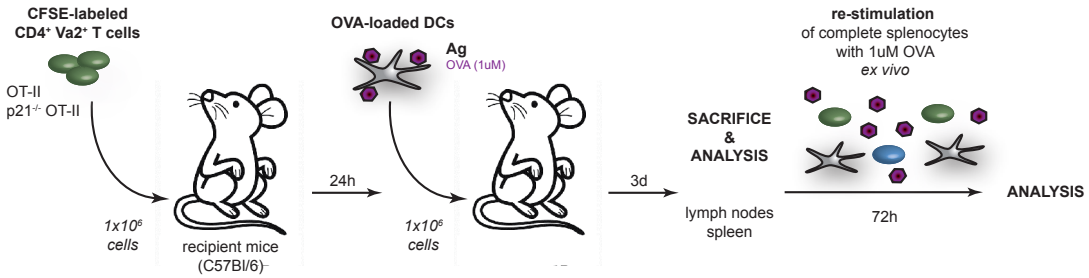

Figure 3.4. Adoptive transfer of TCRtg CD4⁺ T cells. Purified OT-II and p21$^{-/-}$ OT-II CD4⁺ (Vα2⁺) were injected into C57BL/6 recipient mice (1 x 10^6 cells/mouse), followed 24 h later by injection of DC presenting OVA peptide (1 x 10^6 cells/mouse). After 3 days, mice were sacrificed, and T lymphocytes obtained from spleens and lymph nodes were analyzed or restimulated *ex vivo*.

3.4 Flow cytometry (fluorescence-activated cell sorting, FACS)

3.4.1 Extracellular staining

For extracellular staining, 0.5-1 x 10^6 cells were harvested into FACS tubes and incubated with 30 µl of different antibody mixtures depending on the experiment, for 20 min at 4ºC in the dark. Antibodies were diluted following the manufacturer's instructions in staining PBS (1x PBS, 5% FCS, 1% BSA, 5 mM EDTA). Cells were then washed with 1 ml staining PBS, resuspended in 300 µl of staining PBS and analyzed on a cytometer (FC 500 or Gallios; Beckman Coulter).

The following antibodies were used routinely for extracellular staining: anti-B220-APC, -CD4-FITC, -CD4-SPRD, -CD8-PE, -CD44-FITC (all from Beckman Coulter), -CD4-PeCy7, CD62LAPC, -CD69-FITC (all from eBioscience), -B7-2-PE (CD86), -CD25-FITC, -CD69-PE, TCRβFITC, Vα2-PE, -Vβ3-FITC, -Vβ3-PE (all from PharMingen) and -I-A^k-FITC (Serotec).

For further analysis, FlowJo software was used (Tree Star, Inc.; version 8.8.3).

3.4.2 Intracellular cytokine staining

For intracellular cytokine staining, cells were isolated from murine spleens, plated (5 x 10^6 cells/ml) and stimulated (1 h, 37ºC) in culture medium containing PMA (50 ng/ml) and ionomycin (2 µg/ml). Brefeldin A (GolgiPlug, 2 mg/ml; BD Pharmingen) was added and cells were incubated for an additional 3 h at 37ºC. After surface marker staining (CD4, CD8, CD44, CD62L), cells were washed with staining PBS, fixed, and permeabilized with 100 µl Cytofix/Cytoperm (Cytofix/Cytoperm-Fixation/Permeabilization kit, BD Biosciences) at 4ºC for 20 min. Cells were then washed with 1x Perm/Wash buffer and stained with anti-IFNγ-APC, IL-17-APC and -IL-2-APC antibodies (1/100; all from PharMingen). After incubation (30 min, 4ºC), cells were washed twice with 1x Perm/Wash before FACS analysis.

3.5 *In vitro* proliferation assays

3.5.1 [^{3}H] thymidine incorporation

Cells were cultured in 96-well plates (1 x 10^6 cells/ml) for indicated times, with addition of [^{3}H] thymidine (1 µCi/well; Perkin Elmer) during the last 16 h of culture. To measure T cell proliferation, cell fragments were transferred onto fiber filters (Wallac) using a semi-automatic cell

harvester (Wallac) and [^{3}H] thymidine uptake was quantified by a beta-plate counter (b1205 Wallac, Perkin Elmer). Incorporation of [^{3}H] thymidine into DNA is proportional to DNA synthesis.

3.5.2 CFSE fluorescence dilution assay

CFSE is a fluorescent dye for intracellular proteins bearing amino groups. After cell division, the label is inherited by daughter cells and thus can be used to monitor proliferation over time[130].

For intracellular staining, T cells were resuspended in prewarmed 1x PBS + 0.1% BSA at a final concentration of 1 x 10^6 cells/ml and incubated with 2.5 µM CFSE for 45 min at 37ºC. The reaction was terminated by incubating cells on ice for 10 min. Cells were then washed three times with cold RPMI-1640 medium and stimulated according to the requirements of each experiment (1 x 10^6 cells/ml). CFSE fluorescence decay at the indicated times was measured by flow cytometry, gating on live PI (propidium iodide)-negative cells. A decrease in CFSE fluorescence intensity correlates with number of cell divisions.

In some experiments, CD4$^+$ TCRtg cells were CFSE-labeled before injection or stimulation with APC *in vitro* (*see 3.2.5-7*).

3.5.3 Cell cycle analysis

To analyze the different phases of the cell cycle at indicated time points, 0.5-1 x 10^6 cells were harvested into FACS tubes and permeabilized by incubation with 50 µl detergent. DNA was stained with 400 µl of PI (10 mg/ml; both reagents from the DNA-Prep Reagent Kit, Beckman Coulter) for 30 min at 37ºC. In some experiments, cells were fixed with 70% EtOH (20ºC, overnight). The next day, cells were washed with 1x PBS, incubated with 400 µl PI (30 min, 37ºC) and analyzed by flow cytometry (FC500, Beckman Coulter).

To analyze cell cycle profiles within specific T cell subsets, extracellular staining was performed prior to permeabilization in some experiments (*see 3.3.1*). Cells were then stained with 2 µg DAPI (4',6-diamidino-2-phenylindole) diluted in staining PBS (30 min, 37ºC) and analyzed directly by flow cytometry (Gallios, Beckman Coulter).

3.5.4 *In vitro* BrdU assay

Cells were plated at 1 x 10^6 cells/ml and stimulated depending on experimental needs (usually 24 h). For the last 3 h of cell culture, 20 mM BrdU (5-bromo-2´deoxyuridine, Sigma Aldrich)

was added to the culture. BrdU is a thymidine analogue and is incorporated into the DNA of proliferating cells[131]. After harvesting the cells, extracellular staining was performed (*see 3.3.1*) to monitor proliferation in different T cell subsets. Cells were then permeabilized in 0.15 M NaCl + 95% EtOH and stored at -20ºC overnight. The next day, cells were washed and treated with fixing buffer (1x PBS, 1% paraformaldehyde and 1% Tween20) for 30 min at RT and another 30 min at 4ºC. DNA was digested with DNase I (100 U/ml, Roche) diluted in 0.15 M NaCl, 4.2 mM MgCl and 10 mM HCl for exactly 10 min at RT. After several washing steps, BrdU was used for intracellular staining, incubating each sample with 10 µl anti-BrdU-FITC for 1 h at RT (*see 3.4.2*). Cells were washed with staining PBS prior to FACS analysis (Gallios, Beckman Coulter).

3.6 *In vivo* BrdU administration

T cell proliferation in physiological conditions was analyzed in an *in vivo* BrdU incorporation assay. BrdU was administered orally to the mice via drinking water (0.8 mg BrdU/ml) for a total of 9 days (renewing the solution every 2 days). After sacrificing the mice, T cell populations of spleens and lymph nodes were analyzed as described in *3.5.4*.

3.7 Calcium (Ca^{2+}) mobilization assay

Cells were harvested, washed with 1x PBS and resuspended in medium containing 10% FCS (2.5×10^6 cells/ml). After addition of 7 µl Fluo-3 AM (250 µM stock solution in DMSO (dimethylsulfoxide)), cells were incubated at 37ºC for 30 min. Cells were then washed and resuspended in complete medium (*see 3.3.2*) containing 2 mM $CaCl_2$ (0.5×10^6 cells/ml). Prior to FACS analysis (Epics XL-MCL, Beckman Coulter), cells were incubated at 37ºC for 5 min. After establishing the baseline, cells were stimulated with 5 µg/ml anti-CD3 and 1 µg/ml anti-CD28 antibodies. For direct store depletion, 1 µg/µl ionomycin was added.

3.8 Protein biochemistry

3.8.1 Western blot

Protein lysates of cultured cells (5×10^6 cells/sample) were obtained by lysis of $CD4^+$ T cells for 20 min on ice using a 0.2% NP-40 lysis buffer (10 mM TrisHCl pH 7.5, 150 mM NaCl, 0.2% NP40) supplemented with Phosphatase Inhibitor Cocktail (PhosStop) and Complete Protease Inhibitor Cocktail (both from Roche). After quantification of protein concentration by Bradford

assay (Bio-Rad), equal protein amounts (5-15 µg) were separated on 12% acrylamide gels and transferred to a nitrocellulose membrane (BioRad). Membranes were blocked in 5% low fat milk (1x TBS + 0.05% Tween20) and incubated with primary antibody dilutions as recommended by the manufacturer. Primary antibodies were purchased from Cell Signaling (anti-pERK, -ERK, -histone H3), Santa Cruz Biotechnology (anti-p21, -CDK2) or Sigma (anti-β-actin). After incubation with appropriate peroxidase-conjugated secondary antibodies (all from Dako), proteins of interest were detected by chemiluminescence (ECL, Perkin Elmer) on X-ray film (Kodak Minolta).

3.8.2 CDK2 kinase activity assay

T cells (10 x 10^6 cells/sample) were lysed for 15 min on ice in 250 µl lysis buffer (50 mM Tris-HCl pH 7.5, 150 mM NaCl, 1 mM NaF, 100 mM orthovanadate, 0.5% NP50, 1x protease inhibitor cocktail [Roche]). After centrifugation (10 min, 4ºC, maximum speed), protein concentration of supernatants was quantified by Bradford assay. Protein (70-150 µg/sample) was precleared by incubation with 25 µl protein G Sepharose beads (Invitrogen). For immunoprecipitation of CDK2, precleared cell lysates were incubated with 7.5 µl anti-CDK2 antibody (clone sc-163, Santa Cruz Biotechnology) overnight at 4ºC with rotation. In addition, 25 µl protein G Sepharose beads per sample were blocked in 3% milk + lysis buffer for 1 h at 4ºC, washed with lysis buffer and stored at 4ºC overnight.

The next day, 25 µl blocked Sepharose beads were added to each sample, and incubation continued for another 2 h. CDK2 proteins attached to beads were then washed 2x with lysis buffer and 2x with kinase buffer (20 mM Tris-HCl pH 8, 10 mM $MgCl_2$, 1 mM EGTA, 1 mM DTT, 1 mM NaF, 1 mM orthovanadate, 1x protease inhibitor cocktail). Sepharose-coupled CDK2 (10 µl), 20 µl kinase buffer, 0.5 mM adenosine triphosphate (ATP) and 10 µCi [γ^{32}P]-ATP (3000 Ci/mmol, 10 mCi/mL; Perkin Elmer) were incubated with 5 µg histone H1 (Boehringer) as substrate for CDK2 at 30ºC for 30 min. Samples were resolved by 15% SDS-PAGE, blotted on nitrocellulose membranes and visualized by autoradiography. To confirm loading and total amount of CDK2 in each sample, Western blot analysis of total cell lysates was performed (*see 3.7.1*).

3.8.3 Electrophoretic mobility shift assay (EMSA)

For cell lysis, pellets (10 x 10^6 cells per sample) were defrosted on ice and resuspended in 500µl buffer A (10 mM Hepes pH 8, 50 mM NaCl, 0.2 mM saccharose, 1 mM EDTA, 0.5 mM spermidine, 0.15 mM spermine, 0.5% Triton X100, 1 mM PMSF, 2 ng/µl aprotinin, 0.5 ng/µl pepstatin, 7 mM β-mercaptoethanol). After incubation on ice for 5 min, cells were centrifuged and

the supernatant (cytosolic fraction) was separated. The pellet, containing nuclei, was washed with 300 µl of buffer B (10 mM Hepes pH8, 50 mM NaCl, 0.1 mM EDTA, 25% glycerol, 1 mM PMSF, 2 ng/µl aprotinin, 0.5 ng/µl pepstatin, 7 mM βmercaptoethanol) without resuspending. After centrifuging, the supernatant was discarded and the pellet was resuspended in 60 µl of buffer C (10 mM Hepes pH8, 350 mM NaCl, 0.1 mM EDTA, 0.5 mM spermidine, 0.15 mM spermine, 25% glycerol, 1 mM PMSF, 2 ng/µl aprotinin, 1 ng/µl pepstatin, 7 mM β-mercaptoethanol) and incubated on ice for 30 min to obtain nuclear lysates. Protein concentration was determined by Bradford assay, and aliquots were stored at 80ºC. Radioactive labeling of double-stranded probes (200 ng) was carried out in 10x T4 kinase buffer and catalyzed by T4-polynucleotide kinase (30 min, 37°C).

Equal amounts of nuclear protein extracts (4-7 µl) were incubated with binding buffer (37.5 mM Hepes, 0.25 mM EDTA, 5 mM $MgCl_2$, 1.75 M NaCl, 2.5 mM DTT (dithiothreitol), 43.1% glycerol), 1.4 µl poly(dI-dC) and 1 µl [γ-^{32}P]-ATP-labeled probe containing the required transcription factor consensus sequence (NF-κB: 5´AGTTGAGGGGACTTTCCCAGGC-3´, Promega; AP-1:5´-CGCTTGATGAGTCAGCCGGAA-3´,Promega;NFAT:5´-GCGCCAAAGAGGAAAATTTGTTTCATA-3´, Santa Cruz Biotechnology) to analyze DNA-protein interactions. After incubation for 20 min at 25ºC (with shaking), samples were resolved on a 5% acrylamide gel in 0.5x TBE buffer. Gels were then dried and exposed to X-ray film (Kodak Minolta) at -80ºC for up to 17 h. A probe containing the NF-Y consensus sequence was used as loading control.

3.9 Confocal microscopy

For secondary stimulation, cells were cultured on collagen-I-covered chamber slides (Lab-Tek) and stimulated with 1.5 µg/ml ConA, 20 ng/ml hrIL-2 and 50 µM zVAD (24 h, 37ºC). To terminate stimulation, cells were incubated at 4ºC, fixed, and permabilized with Cytofix/Cytoperm solution (BD Biosciences; 30 min, 4ºC). After washing twice with 1x Perm/Wash solution (BD Biosciences), cells were incubated with blocking solution (1x PBS + 1% BSA + 10% goat serum; 45 min, RT) in a humidified chamber. Cells were then washed with 1x Perm/Wash solution and incubated with anti-phospho-ERK1/2 (Cell Signaling) and -p21 antibodies (Santa Cruz Biotechnology) for 45 min at RT in a humidified chamber. Cells were washed three times with 1x PBS to remove unbound primary antibody; anti-goat IgG (Santa Cruz Biotechnology) and -rabbit IgG (Molecular Probes) secondary antibodies were added (1 h, RT). After mounting cells in DAPI-containing mounting medium (Vectashield; Vector Laboratories), fluorescence was documented on a confocal microscope (Olympus).

3.10 Serological and histological analysis

3.10.1 Kidney cryosections and glomerulonephritis evaluation

Kidneys were isolated and incubated in fixing solution prior to embedding in paraffin blocks. Cryosections were prepared by the CNB Histology Facility, and glomerulonephritis grade was evaluated by Dr. Juana Flores, Animal Biology Department, School of Veterinary Medicine (Universidad Complutense de Madrid, Spain) according to the following scale[132]: (0) no glomerular lesions, (I) minimal mesangial lupus nephritis with mesangial accumulation of immune complexes, (II) mesangial proliferative lupus nephritis with increases in mesangial and glomerular cellularity, (III) focal lupus nephritis characterized by segmental endocapillary proliferative lesions and subendothelial immune deposits, and (IV) diffuse segmental or global lupus nephritis characterized by segmental or global glomerulonephritis in >50% of all glomeruli and diffuse subendothelial immune deposits.

3.10.2 Cytokine quantification in cell culture supernatants or serum

For analysis of IL-2, IL-17 and IFNγ cytokine secretion levels, cell culture supernatants or sera were collected and incubated with microbeads specific for each cytokine (kit from Milliplex Mouse Cytokine/Chemokine Immunoassay, Millipore). Samples were analyzed in duplicate by Luminex 100 IS.

3.10.3 Protein quantification in urine samples

For determination of protein levels in urine of 9-month-old mice (or older), Urispec GP+A strips (Henry Schein, Port Washington, NY, USA) were used as indicated by the manufacturer.

3.11 Statistical analysis

Values shown represent mean ± SD, where applicable. Statistical significance was calculated with the Student's *t* test. Differences were considered significant for $p < 0.05$ and are represented as *** $p < 0.001$, ** $p < 0.01$ and * $p < 0.05$.

4. RESULTS

4. RESULTS

4.1 p21 is involved in activation of CD4$^+$ memory T cells

In the first part of the present study, p21-deficient mice on the autoimmunity-free C57BL/6 background were used define the role of p21 in immune responses of T lymphocytes and induction of autoimmunity. Several studies with mixed background (C57BL/6 x 129xSv) p21$^{-/-}$ mice showed that p21 is crucial for the maintenance of tolerance, as these mice develop acute lupus-like disease that leads to death in most cases[57]. Lupus is caused by a combination of genetic and environmental factors. The mixed genetic background, which predisposes to autoimmunity[57], therefore enhances the outcome of the autoimmune manifestations in the absence of p21. The C57BL/6 p21$^{-/-}$ model allows us to study the role of p21 independently and to avoid background interference with data interpretation. As described in section 1.6.2, C57BL/6 p21$^{-/-}$ mice (p21$^{-/-}$) develop normally, but continuously lose tolerance to DNA until they finally develop mild autoimmune disease[56,57]. Age-matched C57BL/6 (B6) mice were used as controls for this part of the study.

4.1.1 p21 expression and function during primary stimulation of naïve T cells

To mimic the *in vivo* situation of continuous TCR challenge by specific auto-antigens in autoreactive T cells, a **repeated stimulation system** was used in the *in vitro* section of this study. For this purpose, purified naïve CD4$^+$ splenocytes were activated with ConA in a TCR-dependent manner (**first stimulation**). The CD4$^+$ T cells were subsequently expanded in the presence of hrIL-2 for a total of 6 days (**IL-2 expansion phase**) before they were restimulated with ConA (**second stimulation**) (*for details see 3.2.3*). After two successive TCR stimulations *in vitro*, cells were considered to be effector/memory T cells (CD44^{high}), presenting an effector (CD44^{high}CD62l^{high}) or memory phenotype (CD44^{high}CD62^{low}).

In a previous study, naïve B6 and p21$^{-/-}$ CD4$^+$ T cells were stimulated for 3 days prior to the IL-2 expansion phase, to examine the p21 effect on memory T cells[56]. Applying this methodology, we found p21-deficient effector/memory T cells to be overactivated, resulting in their extreme proliferation. These findings were not entirely reflected in a physiological situation, however, as this massive proliferation was not detectable *in vivo*. We thus considered the *in vitro* conditions

to be too vigorous, leading to overstimulation of T cells. Our objective was thus to develop an *in vitro* stimulation system that approximates the results observed in the *in vivo* T cell responses. We first reviewed the p21 expression pattern during primary stimulation of naïve $CD4^+$ T cells. Western blot analysis revealed that p21 is not expressed until 48 h after stimulation in naïve B6 $CD4^+$ T cells (*Fig. 1A*). As p21 is a direct inhibitor of the cell cycle regulator CDK2, we analyzed the activity of this kinase after stimulating naïve $CD4^+$ T cells, and observed comparable activation levels in B6 and $p21^{-/-}$ $CD4^+$ T cells until 48 h (*Fig. 4.1B*). Less CDK2 activity was observed in B6 $CD4^+$ T cells at 72 h after stimulation, probably due to expression of its inhibitor p21 after 48 h. In the absence of p21, CDK2 activity cannot be controlled and thus reached higher activation levels in $p21^{-/-}$ $CD4^+$ T cells (*Fig. 4.1B*).

These results led to the final study design of stimulating primary T cells only for 1 day (24 h), while the rest of the protocol remained the same (*see Fig. 4.4A*). In this way, we avoided possible interference by differential p21 expression during the initial stimulation phase, and both B6 and $p21^{-/-}$ $CD4^+$ T cells can be cultured in equivalent conditions until the secondary stimulation. By shortening the first stimulation, we also avoided possible restimulation of the same cells during this cell culture phase. Compared to our previous system, we considered this methodology a physiologically relevant protocol for *in vitro* studies.

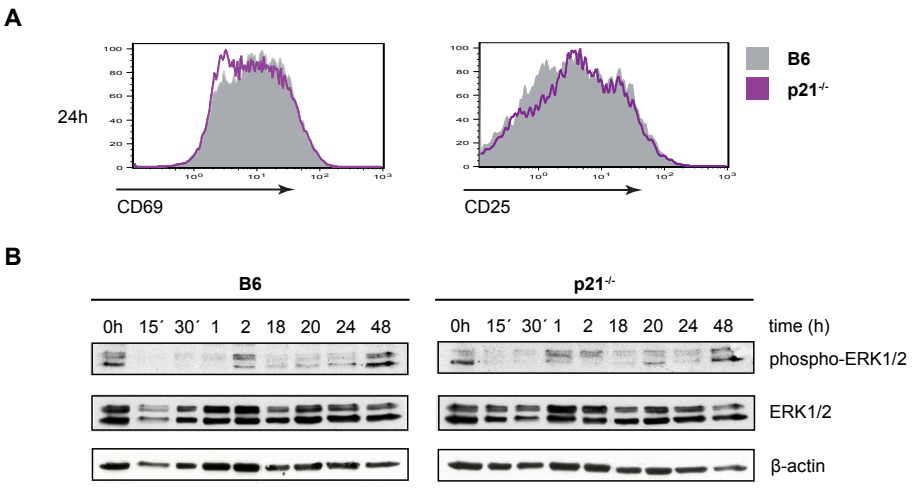

Figure 4.1. Late expression of p21 controls CDK2 activity in naïve T cells. A. Western blot showing endogenous p21 expression at indicated times after first stimulation of naïve B6 and $p21^{-/-}$ $CD4^+$ T cells. β-actin was used as a loading control. **B.** Kinetics of CDK2 kinase activity in naïve B6 and $p21^{-/-}$ $CD4^+$ T cells during first ConA stimulation. Histone H1 was used as substrate for the kinase assay. Total expression of CDK2 and β-actin was analyzed by Western blot and served as control. Representative experiments are shown (n = 2).

4.1.1.1 p21 deletion does not affect activation of naïve CD4⁺ T cells

To determine the role of p21 in the activation of naïve T cells, we compared the activation state of purified naïve B6 and p21$^{-/-}$ CD4⁺ splenocytes at 24 h after primary TCR challenge, and detected no differences in expression levels of surface activation markers such as CD69 or CD25 (*Fig. 4.2A*). In addition, we used phosphorylated ERK1/2 (phospho-ERK1/2) as an intracellular indicator of the T cell activation state and observed a similar pattern for ERK1/2 phosphorylation up to 48 h after primary stimulation (*Fig. 4.2B*). These results indicate that lack of p21 does not influence activation of naïve T cells at 24 h after the first stimulation.

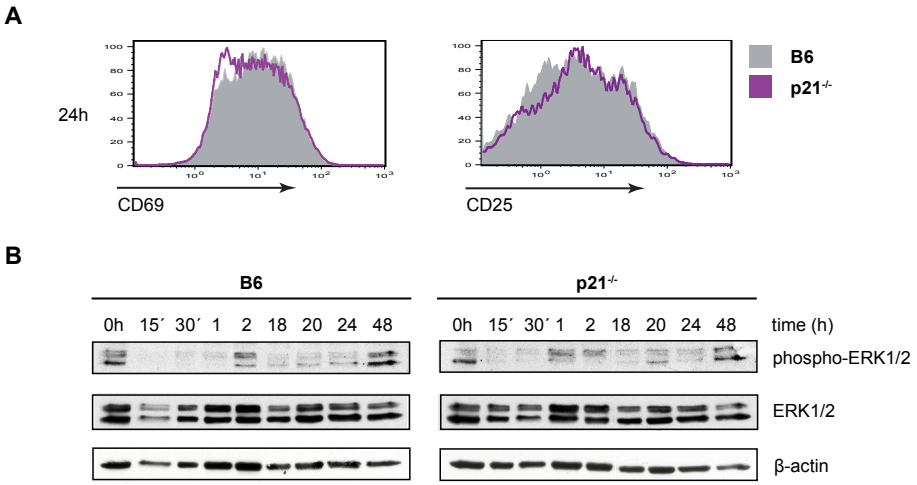

Figure 4.2. Activation of naïve CD4⁺ T cells after primary TCR stimulation. A. Surface expression of CD25 and CD69 activation markers on naïve B6 and p21$^{-/-}$ CD4⁺ T cells stimulated for 24 h with ConA, as determined by flow cytometry. Representative histograms are shown (*n* = 2). **B.** ERK1/2 phosphorylation in naïve B6 and p21$^{-/-}$ CD4⁺ T cells was detected by Western blot at indicated times after primary stimulation with ConA. Total ERK1/2 and βactin expression were used as loading controls. A representative experiment is shown (*n* = 2).

4.1.1.2 Absence of p21 does not affect proliferation of naïve CD4⁺ T cells

As T cell activation results in proliferation, we analyzed proliferation rates of naïve B6 and p21$^{-/-}$ CD4⁺ T cells following TCR challenge. After 24 h of primary stimulation with ConA, cell cycle profiles of naïve CD4⁺ T cells showed no differences in proliferation or apoptosis (*Fig. 4.3A*). [^{3}H] thymidine incorporation confirmed similar proliferation rates of B6 and p21$^{-/-}$ CD4⁺ T cells (*Fig. 4.3B*). TCR-specific stimulation with anti-CD3/CD28 antibodies gave results similar to those observed after ConA stimulation (*Fig. 4.3C,D*), which verified ConA as a representative TCR-stimulating agent in our system. Finally, CFSE dilution assay showed the same number of cell divisions in both cell types

after primary stimulation (*Fig. 4.3C*), suggesting that lack of p21 does not influence proliferation of naïve T cells after primary TCR challenge.

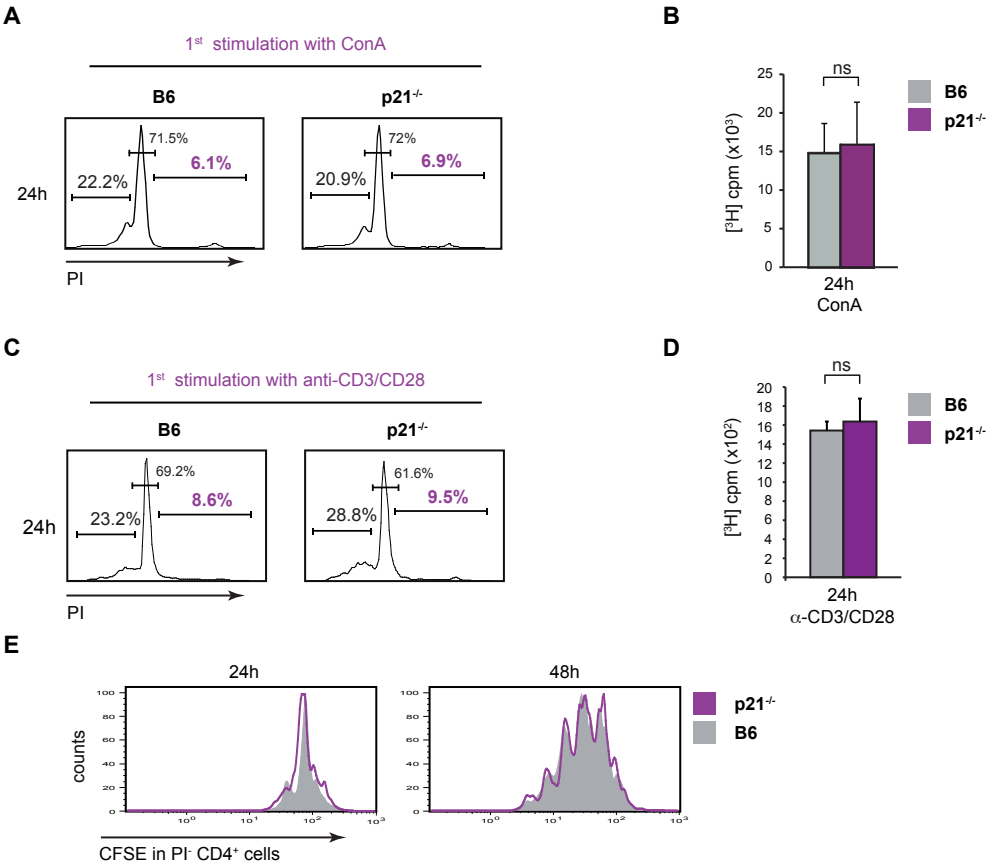

Figure 4.3. Similar proliferative response of naïve B6 and p21$^{-/-}$ CD4^{+} T cells to primary TCR challenge. A,C. Cell cycle analysis of B6 and p21$^{-/-}$ CD4^{+} T cells at 24 h after primary stimulation with ConA (**A**) or with anti-CD3/CD28 antibodies (**C**). Representative histograms are shown (ConA: *n* = 6; anti-CD3/CD28: *n* = 2). **B,D.** Proliferation rates of B6 and p21$^{-/-}$ CD4^{+} T cells were detected by [^{3}H] thymidine incorporation at 24 h after primary TCR challenge with ConA (**B**) or with anti-CD3/CD28 antibodies (**D**). Values show mean ± SD (**B**: *n* = 3, *p* = 0.449; **D**: *n* = 2, *p* = 0.563). **E.** CFSE dilution of gated live (PI^{-}) naïve WT and p21$^{-/-}$ CD4^{+} T cells at 24 and 48 h after first ConA stimulation. Representative histograms are shown (*n* = 3).

4.1.2 The role of p21 in activation of memory-phenotype T cells after secondary TCR challenge

4.1.2.1 Differential expression of p21 in effector/memoryT cells

To analyze the behavior of B6 and p21$^{-/-}$ memory CD4^{+} T cells after secondary stimulation *in vitro,* we used the repeated stimulation system (*described in 4.1.1*) (*Fig. 4.4A*). In this step of the culture process, a large number of cells undergo AICD. To obtain clearer results regarding the role of p21 in T cell activation, we complemented the culture with the caspase inhibitor zVAD (Z-Val-Ala-

DL-Asp-fluoromethylketone)[121]. In apoptosis-free conditions, p21 was clearly expressed in memory-phenotype T cells even before 4 h post-TCR challenge (*Fig. 4.4B*). Compared to naïve B6 T cells, in which p21 was not detectable before 48 h (*Fig. 4.1A*), effector/memory T cells expressed p21 shortly after TCR stimulation.

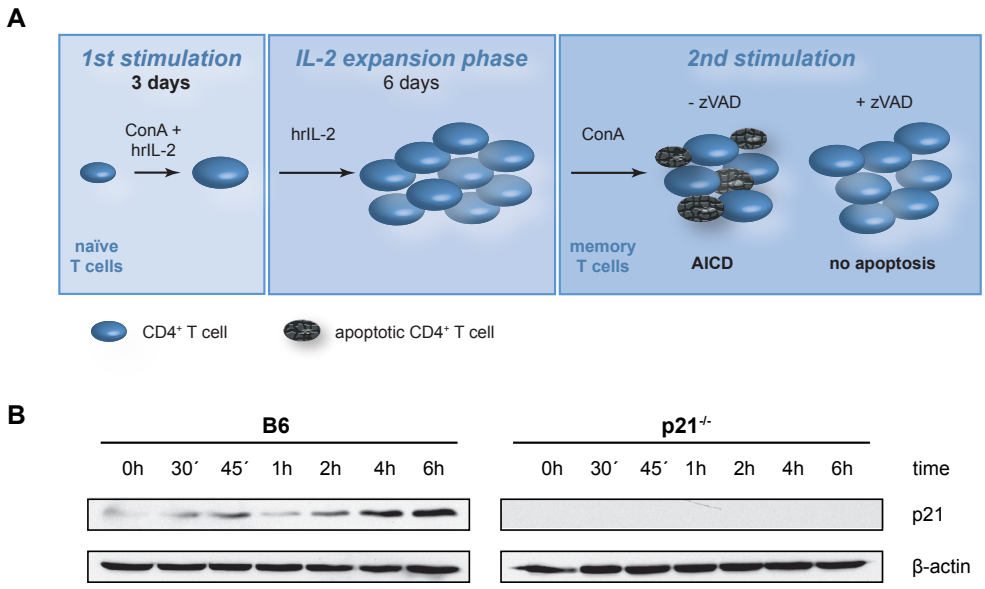

Figure 4.4. p21 is expressed early in memory-like T cells after secondary TCR challenge. A. $CD4^+$ splenocytes were isolated, ConA-stimulated for 24 h, expanded in hrIL-2 for 6 days and restimulated for the indicated times in minimal cell death conditions (zVAD concentrations indicated). **B.** Western blot showing endogenous p21 expression in B6 and $p21^{-/-}$ $CD4^+$ effector/memory T cells after secondary stimulation. β-actin was used as a loading control. A representative experiment is shown (n = 2).

4.1.2.2 p21-deficient memory-like T cells are hyperactivated after secondary stimulation

Effector/memory T cells that lack p21 accumulate and hyperproliferate in culture conditions similar to the *in vitro* system used in this thesis[56], suggesting an additional role of the cell cycle inhibitor p21 in effector/memory T cell activation. In accordance with these data, we observed elevated surface CD69 expression levels in $p21^{-/-}$ $CD4^+$ T cells after secondary TCR challenge (*Fig. 4.5A*). As the MAPK pathway is an important activation pathway in lymphocytes, we analyzed the ERK1/2 phosphorylation pattern and found sustained hyperphosphorylation of ERK1/2 in $p21^{-/-}$ effector/memory T cells at short (12 h) as well as at late time points (14-24 h) after repeated stimulation (*Fig. 4.5B*).

The transcription factor AP-1, an important downstream effector of the MAPK pathway, is activated by phospho-ERK1/2 and induces –together with other transcription factors– the production

of pro-inflammatory cytokines in response to T cell activation. After 24 h secondary stimulation *in vitro*, restimulated p21-deficient CD4⁺ T cells showed higher AP1 activity levels (*Fig. 4.5C*), confirming the finding that early p21 expression controls activation events in effector/memory T cells.

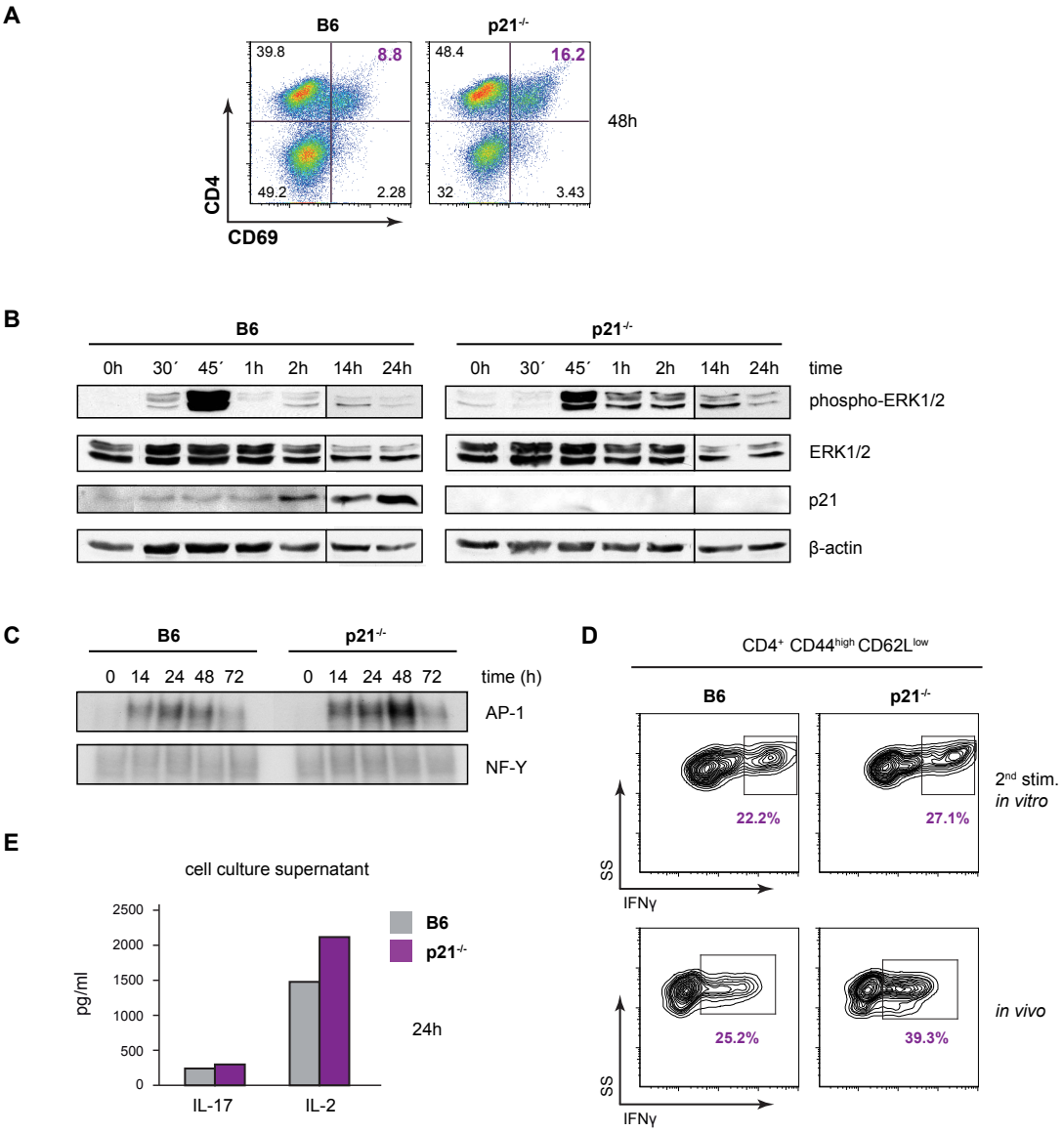

Figure 4.5. Early p21 expression after TCR stimulation controls early activation events in effector/memory T cells. A. CD4 and CD69 double staining at 48 h after secondary stimulation of B6 and p21$^{-/-}$ CD4^{+} effector/memory T cells. Representative histograms are shown (*n* = 2). **B.** Differential ERK1/2 phosphorylation in B6 and p21$^{-/-}$ CD4^{+} effector/memory T cells was detected by Western blot at indicated times after secondary TCR challenge (+ 50 µM zVAD). Total ERK1/2 and β-actin were used as loading controls. A representative experiment is shown (*n* = 4). **C.** Electrophoretic mobility shift assay (EMSA) detected AP-1 activity in B6 and p21$^{-/-}$ effector/memory T cells after secondary ConA stimulation in the presence of zVAD (50 µM). A probe containing the NF-Y consensus sequence was used as a control for sample quality in all EMSA. A representative experiment is shown (*n* = 2). **D**. Intracellular staining for IFNγ in B6 and p21$^{-/-}$ CD4^{+}CD44^{high}CD62L^{low} T cells after secondary stimulation with PMA (40 ng/ml) and ionomycin (1 µg/ml) for 4 h (1 x 10^{6} cells/ml) *in vitro* (top panel) and in splenocytes isolated from 1year-old B6 and p21$^{-/-}$ mice (bottom panel). A representative experiment is shown (*n* = 2). **E.** Amount of proinflammatory cytokines IL-17 and IL-2 (pg/ml) measured by Luminex in cell culture supernatants of B6 and p21$^{-/-}$ CD4^{+} T cells at 24 h after secondary TCR challenge with ConA (*n* = 2).

The data showing higher ERK1/2 phosphoryation and AP-1 activation in the absence of p21 suggested possible induction of cytokine expression in $p21^{-/-}$ T cells. Indeed, we detected elevated intracellular expression of the pro-inflammatory cytokine IFNγ in $p21^{-/-}$ $CD4^+$ T cells *in vitro* (*Fig. 4.5D,* top panels). In freshly isolated splenocytes from 1-year-old mice, the difference was even more evident (*Fig. 4.5D*, bottom panels). Larger amounts of IL-17 (B6, 243.1 pg/ml *vs.* $p21^{-/-}$, 298.6 pg/ml) and IL-2 (B6, 1478.6 pg/ml *vs.* $p21^{-/-}$, 2116.9 pg/ml) were also measured in cell culture supernatants of effector/memory T cells at 24 h after secondary stimulation (*Fig. 4.5E*).

Overall, these data support the hypothesis that lack of p21 leads to increased T cell activation and indicate indirectly that p21 modulates T cell activation via ERK1/2 phosphorylation. Whether p21 controls inflammatory cytokine expression by activated effector/memory T cells (*in vitro*) directly or indirectly requires further research.

4.1.2.3 Hyperactivation results in hyperproliferation of $p21^{-/-}$ effector/memory T cells after secondary stimulation

As activation precedes proliferation, we examined the proliferation rates of B6 and $p21^{-/-}$ effector/memory T cells after secondary stimulation. Cell cycle profiles showed hyperproliferation of p21-deficient effector/memory T cells compared to their control counterparts. Apoptosis was inhibited efficiently by zVAD in both cell types (*Fig. 4.6A*). This finding was confirmed by increased [^{3}H] thymidine incorporation in $p21^{-/-}$ $CD4^+$ T cells compared to B6 $CD4^+$ T cells after 48 h, with significant differences in proliferation rates whether or not the inhibitor zVAD was present (-zVAD: B6, 20701 cpm *vs.* $p21^{-/-}$, 52734 cpm; p = 0.011; +zVAD: B6, 41758 cpm *vs.* $p21^{-/-}$, 115767 cpm, p = 0.017) (*Fig 4.6B*). Any interference of zVAD with the results can thus be excluded. Finally, CFSE dilution assay showed that restimulated p21-deficient effector/memory T cells undergo more rounds of cell cycle division over time than controls (*Fig. 4.6C*). To verify the ConA stimulation results, we used anti-CD3/CD28 antibodies to stimulate the cells in a TCR-specific manner. Again, $p21^{-/-}$ $CD4^+$ effector/memory T cells proliferated more in response to TCR challenge, as determined by [^{3}H] thymidine incorporation (-zVAD: B6, 6642 *vs.* $p21^{-/-}$, 10723 cpm, p = 0.001; +zVAD: B6, 7868 *vs.* $p21^{-/-}$, 13282 cpm, p = 0.012) (*Fig. 4.6D*) and CFSE dilution assay (*Fig. 4.6E*). These data showed that lack of p21 leads to hyperactivation of memory-phenotype T cells and thus to their hyperproliferation.

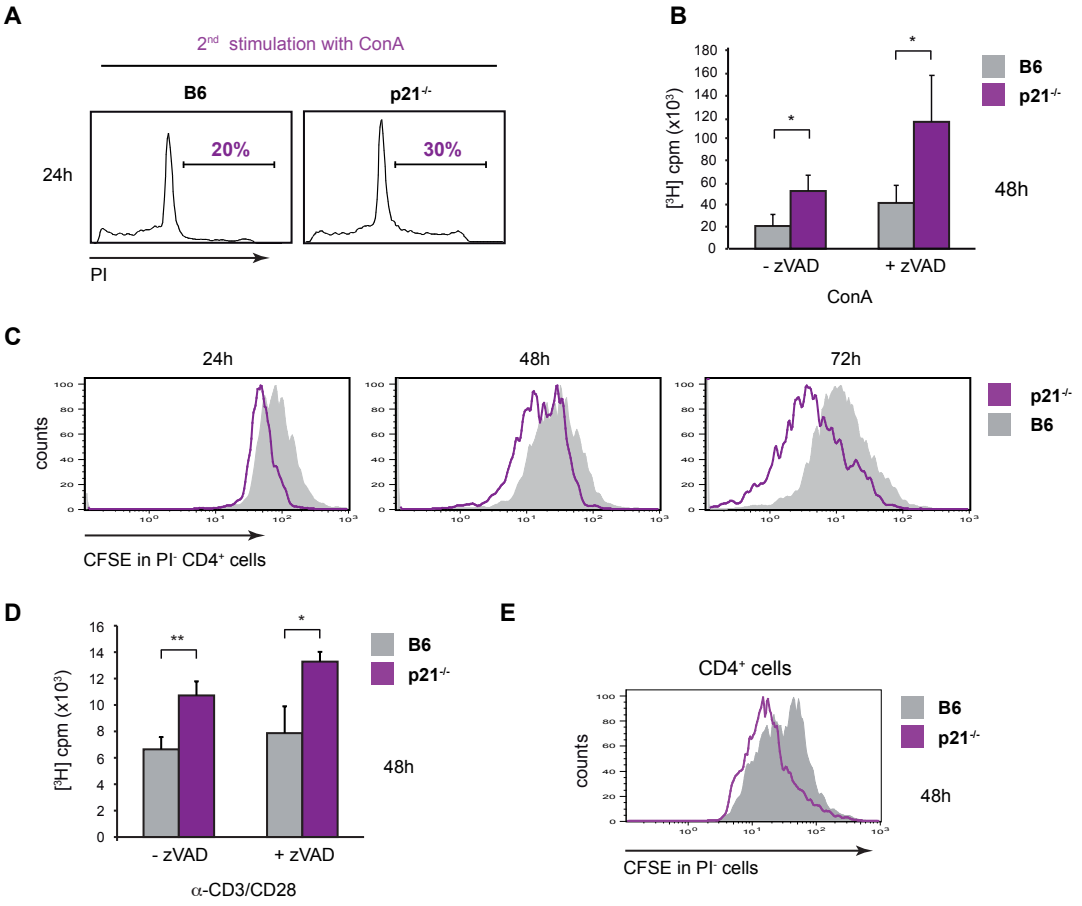

Fig. 4.6. p21-deficient effector/memory T cells hyperproliferate after secondary TCR stimulation. A. Cell cycle analysis of B6 and p21$^{-/-}$ CD4^{+} effector/memory T cells at 24 h post-secondary stimulation in the presence of zVAD (50 µM). Representative data are shown (n = 8). **B.** [^{3}H] thymidine uptake at 48 h after secondary stimulation with ConA, alone or with zVAD (50 µM). Values show mean ± SD (n = 8; -zVAD: p = 0.011; +zVAD: p = 0.017). **C.** CFSE dilution rate of gated PI-negative cells after 24, 48 and 72 h of secondary stimulation with ConA in the presence of zVAD (50 µM). Representative histograms are shown (n = 4). **D.** Hyperproliferation of p21$^{-/-}$ effector/memory T cells measured by [^{3}H] thymidine incorporation at 48 h after a second stimulation with anti-CD3/CD28 antibodies (+ 12.5 µM zVAD). Values show mean ± SD (n = 2; -zVAD: p = 0.001; +zVAD: p = 0.012). **E.** Dilution rate of CFSE-labeled PI-negative WT and p21$^{-/-}$ effector/memory T cells at 48 h post-restimulation with anti-CD3/CD28 antibodies (+ 12.5 µM zVAD). Representative data are shown (n = 2).

4.1.2.4 Hyperproliferation of p21-deficient effector/memory T cells is CDK2-independent

After observing hyperactivation and hyperproliferation of effector/memory T cells in the absence of p21, we tested whether increased CDK2 activity might be the reason for this behavior, as p21 is a direct inhibitor of this kinase[88]. In such a case, increased kinase activity would induce hyperproliferation, and continous proliferation could lead to hyperactivation of effector/memory T cells. Kinase activity experiments supported our hypothesis and showed no notable changes

in CDK2 activity in the absence of p21, either at early (*Fig. 4.7A*) or at later times after secondary stimulation (*Fig. 4.7B*) in our culture conditions.

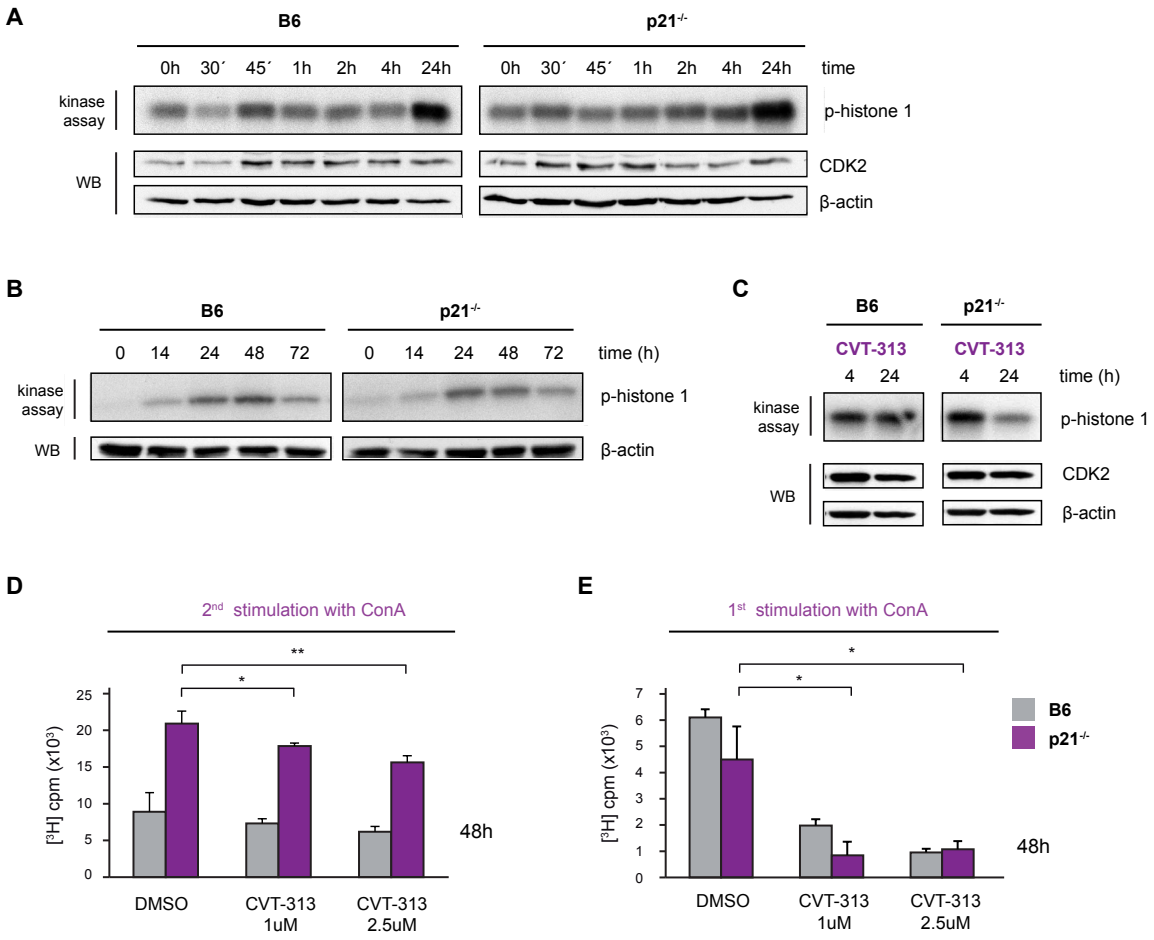

Figure 4.7. Lack of p21 does not influence CDK2 activity in effector/memory T cells. A,B. CDK2 activity levels in WT and p21$^{-/-}$ effector/memory T cells at short (**A**) and long times (**B**) after secondary ConA stimulation in the presence of zVAD (12.5 μM), as determined by kinase assays. Histone H1 was used as substrate. Western blot analysis of total CDK2 and β-actin expression was used as loading control. Representative experiments are shown (n = 2). **C.** Kinase assay to determine CDK2 activity during a secondary stimulation in the presence of the CDK2 inhibitor CVT-313 (2.5 μM). **D,E.** [^{3}H] thymidine uptake at 48 h after secondary (**D**) or primary stimulation (**E**) with ConA in untreated (DMSO) or CVT-313-treated (1 μM or 2.5 μM) cells. Values show mean ± SD (n = 2; **D**: p21$^{-/-}$ DMSO *vs.* CVT-313 1 μM, p = 0.022; p21$^{-/-}$ DMSO *vs.* CVT-313 2.5 μM, p = 0.0012; B6 DMSO *vs.* CVT-313 2.5 μM, p = 0.081; **E**: p21$^{-/-}$ DMSO *vs.* CVT-313 1 μM, p = 0.0148; p21$^{-/-}$ DMSO *vs.* CVT-313 2.5 μM, p = 0.0145; B6 DMSO *vs.* CVT-313 2.5 μM, p = 0.00001).

To further show that p21 does not control CDK2 activity in CD4$^+$ effector/memory T cells, we used the specific CDK2 inhibitor CVT-313[124,125] during the repeated stimulation protocol and monitored T cell proliferation. The difference in CDK2 activity observed at 4 and 24 h in normal conditions (*Fig. 4.7A*) was minimized in the presence of CVT-313, confirming inhibitor function (*Fig. 4.7C*). During secondary TCR challenge, proliferation of both strains in the presence of CVT-313 was only

slightly reduced (*Fig. 4.7D*), which suggests that in fact p21 controls the cell cycle via pathways other than classical CDK2 inhibition in effector/memory T cells. In contrast, proliferation of naïve T cells was almost abolished in the presence of CVT313 (*Fig. 4.7E*), in accordance with our previous observation that p21 controlled CDK2 activity after first stimulation (*Fig. 4.1B*). CDK2 activity thus appears to be irrelevant for proliferation after a secondary stimulation.

4.1.2.5 p21 is unrelated to TCR proximate events

As p21 appeared to be involved in T cell activation, we analyzed the effect of p21 on T cell activation pathways more closely. Using the phorbol ester PMA (phorbol 12-myristate 13-acetate), which mimics the function of the second messenger diacylglycerol (DAG) and stimulates protein kinase C (PKCθ)[133], we are able to bypass TCR proximate events and can activate intracellular molecules directly. To test whether p21 has a role in early events after TCR activation or in downstream pathways, we restimulated B6 and $p21^{-/-}$ $CD4^+$ T cells simultaneously with distinct stimulating agents, ConA and a combination of PMA and the calcium ionophore ionomycin. After ConA stimulation, we observed hyperphosphorylation of ERK1/2 in $CD4^+$ T cells that lacked p21, confirming previous experiments (*Fig. 4.8A*). We nonetheless detected a similar ERK1/2 phosphorylation pattern after stimulating cells with PMA/ionomycin (*Fig. 4.8B*). This finding suggested that p21 does not have a TCR proximal role and is more likely to act on PCKθ or in downstream T cell activation pathways.

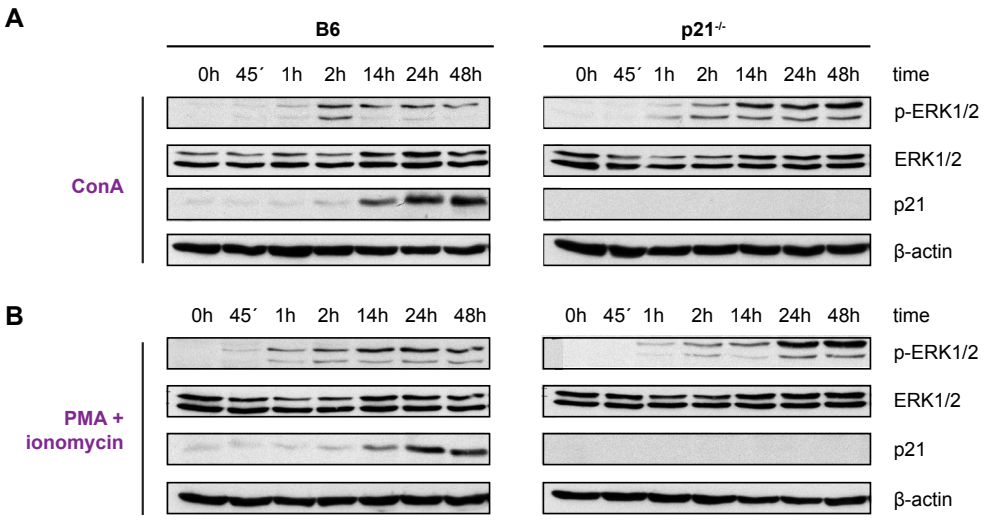

Figure 4.8. p21 does not play a TCR proximal role. A,B. B6 and $p21^{-/-}$ $CD4^+$ T cells were restimulated in parallel in a TCR-dependent manner with ConA (**A**) and in a TCR-independent manner with PMA/ionomycin (**B**); +50 µM zVAD was present in both conditions. Western blot detection of ERK1/2 phosphorylation and p21 expression showed similar kinetics during secondary stimulation in both cases. Total ERK1/2 and β-actin were used as loading controls. A representative experiment is shown (*n* = 2).

4.1.2.6 p21 is located in cytosol of memory-phenotype T cells

To determine whether p21 acts within the cytosolic or the nuclear compartment of memory T cells, we separated lysates from restimulated B6 and p21$^{-/-}$ CD4^{+} T cells into cytosolic and nuclear fractions prior to Western blot analysis. p21 was detected mainly within the cytosol of B6 CD4^{+} effector/memory T cells, and ERK1/2 appeared to be hyperphosphorylated in the cytoplasm of p21-deficient CD4^{+} effector/memory T cells (*Fig. 4.9A*). Within the nuclear fraction, p21 was hardly detectable in B6 CD4^{+} T cells and ERK1/2 was hyperphosphorylated in the absence of p21 (*Fig. 4.9B*).

To confirm these results, we performed confocal microscopy and found p21 in the cytoplasm of B6 CD4^{+} effector/memory T cells (*Fig. 4.9C*); as predicted, p21 was not detectable in p21$^{-/-}$ CD4^{+} T cells. In B6 CD4^{+} T cells, phospho-ERK1/2 concentrated around the nucleus, whereas phospho-ERK1/2 was visible in both cytoplasm and nucleus of p21-deficient CD4^{+} T cells (*Fig. 4.9C*). These observations indicate that p21 exerts its role within the cytosol, and that its absence leads to increased levels of phosphorylated ERK1/2 in nucleus and cytoplasm.

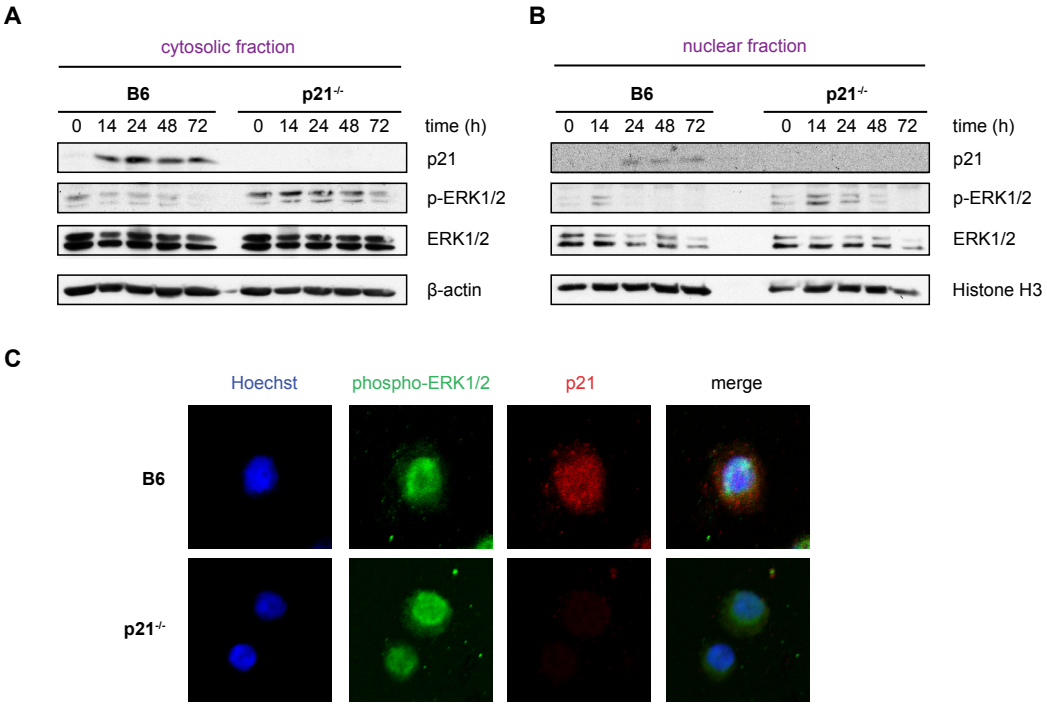

Figure 4.9. Cytoplasmic localization of p21 and phosphorylated ERK1/2 in memory-like T cells after secondary stimulation. A,B. Western blot analysis of cell fractions from ConA-restimulated B6 and p21$^{-/-}$ CD4^{+} T cells, showing cytoplasmic (**A**) and nuclear (**B**) localization of p21, phosphorylated ERK1/2 and total ERK1/2. β-actin and histone H3 were used as loading controls, respectively. A representative experiment is shown (*n* = 2). **C.** Confocal analysis of phosphorylated ERK1/2 and p21 localization in cells at 24 h after secondary ConA stimulation. Cells were antibody-stained to detect phospho-ERK1/2 (green) and p21 (red) and mounted with DAPI (blue)-containing mounting medium for confocal microscopy. Representative results are shown (*n* = 2).

4.1.2.7 Implication of p21 in the NFAT activation pathway

Another pivotal pathway in T cells leads to activation of the transcription factor NFAT, which together with AP-1 and NF-κB is essential for proinflammatory cytokine production[134,135]. As NFAT activation is mediated by a rapid increase in free intracellular calcium (Ca^{2+}) upon TCR stimulation, we tested whether the lack of p21 affected calcium release in effector/memory T cells. TCR stimulation with anti-CD3/CD28 antibodies led to comparable Ca^{2+} influx levels in both B6 and p21-deficient $CD4^+$ T cells (*Fig. 4.10A*). We next analyzed direct NFAT activity. EMSA showed higher NFAT activity in restimulated $p21^{-/-}$ effector/memory T cells after 24 h, which was maintained (*Fig. 4.10B*). In comparison, NFAT activity in B6 effector/memory T cells decreased after 24 h post-secondary TCR challenge.

Consistent with previous findings (*Fig. 8A,B*), Ca^{2+} flux analysis indicated that p21 was not implicated in TCR proximal events and was thus not directly responsible for higher NFAT levels in $p21^{-/-}$ memory T cells. A possible explanation for elevated NFAT activity in p21-deficient effector/memory T cells is a feedback mechanism induced by other activation pathways that are dysregulated in the absence of p21.

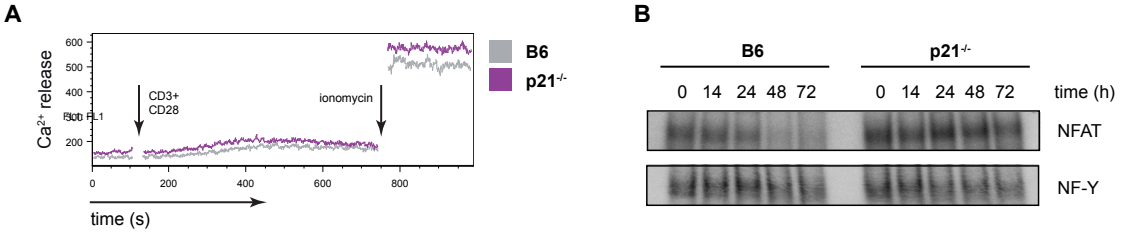

Figure 4.10. p21 is not involved in early Ca^{2+} responses or NFAT activation after TCR-mediated cell activation. **A.** Intracellular calcium responses of B6 and $p21^{-/-}$ effector/memory T cells to TCR-specific stimulation with anti-CD3/CD28 antibodies (5 µg/ml and 1 µg/ml, respectively) after a 6-d IL-2 expansion phase. For direct store depletion, T cells were stimulated with ionomycin (1 µg/µl). Representative fluorescence traces from Fluo3-AM-loaded cells are shown (*n* = 2). **B.** Elevated NFAT activation levels in $p21^{-/-}$ effector/memory T cells after secondary ConA stimulation in the presence of zVAD (50 µM), as detected by EMSA. A representative experiment is shown (*n* = 2).

4.1.2.8 p21 controls ERK activation in effector/memory T cells

To show that increased ERK phosphorylation in $p21^{-/-}$ T cells constitutes a critical pathway for their hyperactivation and proliferative advantage, we inhibited ERK1/2 phosphorylation. To study the direct effect of absence of ERK1/2 activation on $p21^{-/-}$ effector/memory T cell hyperproliferation, we treated both B6 and $p21^{-/-}$ $CD4^+$ T cells with the MEK inhibitor U0126 during secondary ConA stimulation. This molecule selectively interrupts MAPK cascade signal transduction and thus impedes ERK1/2 phosphorylation[122]. In the presence of U0126, we observed a clear reduction in ERK1/2 phosphorylation, which confirmed inhibitor efficiency in our model (*Fig. 4.11A*). We subsequently monitored division rates of CFSE-labeled B6 and $p21^{-/-}$ $CD4^+$ T cells over time after secondary stimulation, and found reduced proliferation in both cell types in the presence of U0126 (*Fig. 4.11B*). Restimulated $p21^{-/-}$ memory T cells were more susceptible to the inhibitor, however, as their proliferation was reduced to a greater extent compared to B6 effector/memory T cells (*Fig. 4.11B*). Significantly reduced proliferation of p21-deficient $CD4^+$ T cells in the presence of U0126 was also evident in [^{3}H] thymidine incorporation assays, whereas the decrease in B6 $CD4^+$ T cell proliferation was not significant ($p21^{-/-}$: -U0126, 102,546 *vs.* +U0126, 26893 cpm, $p = 0.0002$; B6: U0126, 18390 *vs.* +U0126, 7704 cpm, $p = 0.177$) (*Fig. 4.11C*). These findings confirmed the result that hyperproliferation of effector/memory T cells lacking p21 is dependent on ERK phosphorylation.

To analyze the effect of the inhibitor U0126 specifically on effector/memory T cells, we performed a BrdU incorporation assay *in vitro*. Whereas the proliferation of B6 $CD4^+CD44^{high}CD62L^{low}$ memory T cells was almost the same in the presence of the inhibitor, we observed a great reduction in $p21^{-/-}$ $CD4^+CD44^{high}CD62L^{low}$ memory T cells (*Fig. 4.11D*). These results indicate that autoreactive p21-deficient effector/memory T cells were more sensitive to inhibitor treatment and that p21 controls proliferation of effector/memory T cells via ERK1/2 phosphorylation.

Finally, we examined the kinase activity of CDK2 in the presence of U0126 and detected similar CDK2 activity levels in B6 and $p21^{-/-}$ $CD4^+$ T cells treated with DMSO or U0126 (*Fig. 4.11E*). These data indicate that hyperproliferation of p21-deficient effector/memory T cells is ERK-dependent, and that p21 does not control the proliferation via the classical CDK2 pathway.

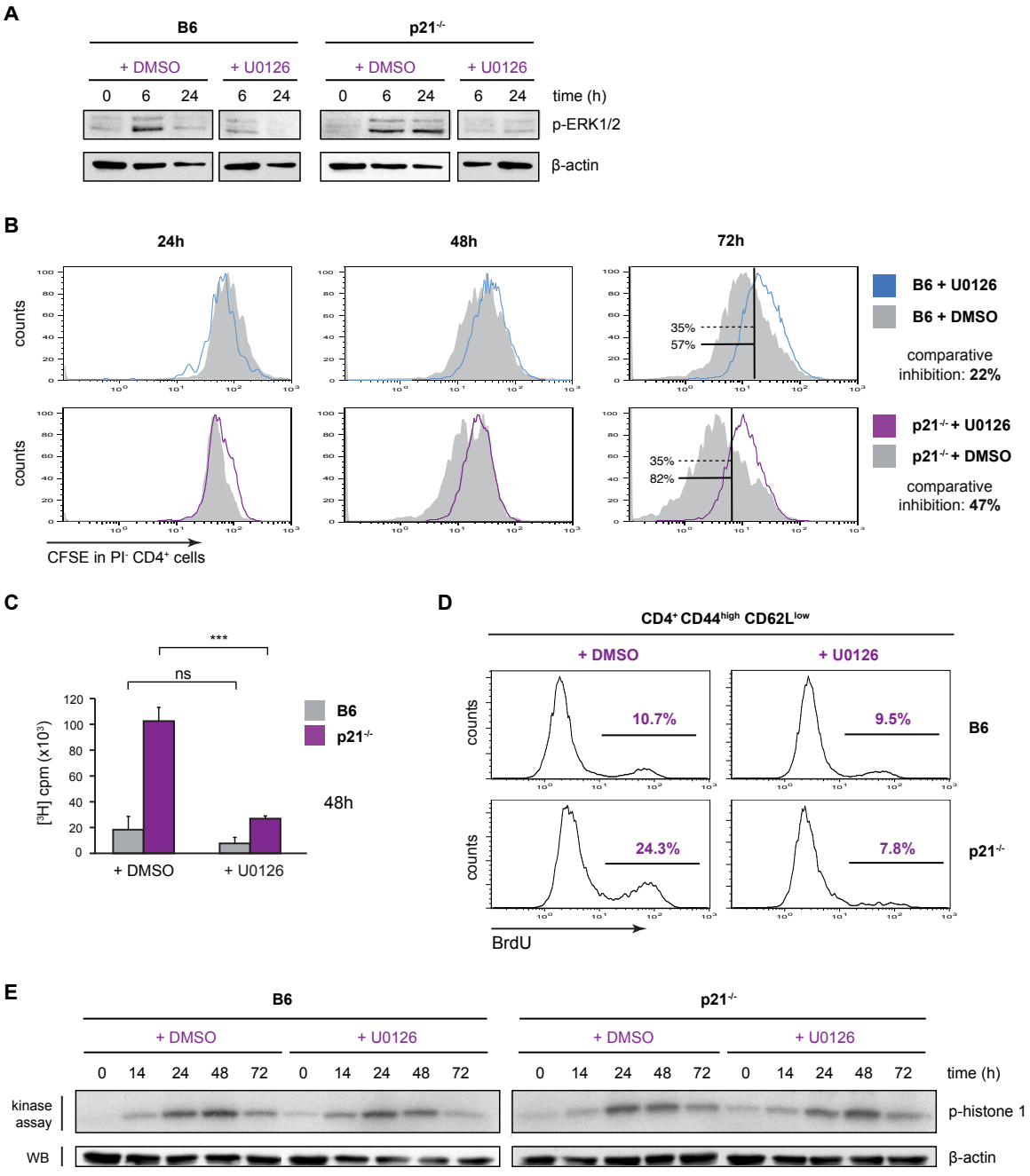

Figure 4.11. p21 controls proliferation of effector/memory T cells via ERK1/2 activation. A. Western blot reflecting the reduction in ERK1/2 phosphorylation in B6 and p21$^{-/-}$ effector/memory T cells in the presence of U0126 (10 mM) after ConA secondary stimulation. β-actin was used as a loading control. A representative experiment is shown (*n* = 4). **B.** CFSE dilution experiments in p21$^{-/-}$ and B6 memory T cells at 24, 48 and 72 h after secondary ConA stimulation in the presence of U0126 (10 mM) and zVAD (50 μM). In all cases, representative data are shown (*n* = 2). **C.** [^{3}H] thymidine incorporation of U0126-treated (10 mM) restimulated B6 and p21$^{-/-}$ CD4$^+$ effector/memory T cells at 48 h after secondary ConA stimulation. Values show mean ± SD (*n* = 5; B6, *p* = 0.177; p21$^{-/-}$, *p* = 0.0002). **D.** *In vitro* BrdU incorporation by CD4$^+$CD44^{high}CD62L^{low} B6 and p21$^{-/-}$ T cells restimulated with ConA for 24 h in the presence of zVAD (50 μM) and U0126 (10 mM) compared to DMSO-treated cells. A representative experiment is shown (*n* = 2). **E.** Kinase assay showing CDK2 activity in both B6 and p21$^{-/-}$ effector/memory T cells during secondary ConA stimulation in the presence of zVAD (50 μM) and U0126 (10 mM) or

DMSO. Histone H1 was used as substrate. Western blot analysis of total CDK2 and β-actin expression was performed as loading control. A representative experiment is shown (*n* = 2).

Although ERK1/2 phosphorylation is one of the earliest events following TCR engagement, a second phase of ERK1/2 activation is thought to play an important role in mediating sustained T cell activation[136]. To study whether the early ERK1/2 phosphorylation phase is sufficient to induce the hyperproliferation observed in p21$^{-/-}$ memory T cells or if later hyperactivation (between 14 h and 24 h) is relevant for hyperproliferation, we added U0126 to the cell culture at different time points of secondary stimulation, and compared the results to DMSO-treated cells. Western blot detection of phospho-ERK1/2 confirmed inhibitor efficiency in all conditions tested (*Fig. 4.12A*).

In terms of proliferation, [^{3}H] thymidine incorporation showed a significant reduction in restimulated p21-deficient CD4$^+$ T cells when U0126 was added at 6 h post-secondary stimulation (p21$^{-/-}$, 102,546 *vs.* 31227 cpm, $p = 0.0003$). We observed similar proliferation levels in B6 and p21$^{-/-}$ CD4$^+$ T cells cultured with inhibitor from the start of stimulation (time 0) compared to cells treated with U0126 after 6 h. In B6 CD4$^+$ T cells, the reduction was not significant (B6, 18390 *vs.* 8871 cpm, $p = 0.207$) (*Fig.12B*). Dilution assays that compared proliferation rates of CFSE-labeled B6 and p21$^{-/-}$ effector/memory T cells confirmed fewer cell divisions in p21-deficient CD4$^+$ T cells, regardless of the time at which inhibitor was added to the culture (*Fig. 4.12C*). We conclude that continuous ERK phosphorylation is necessary for hyperactivation and subsequent hyperproliferation of p21-deficient memory T cells.

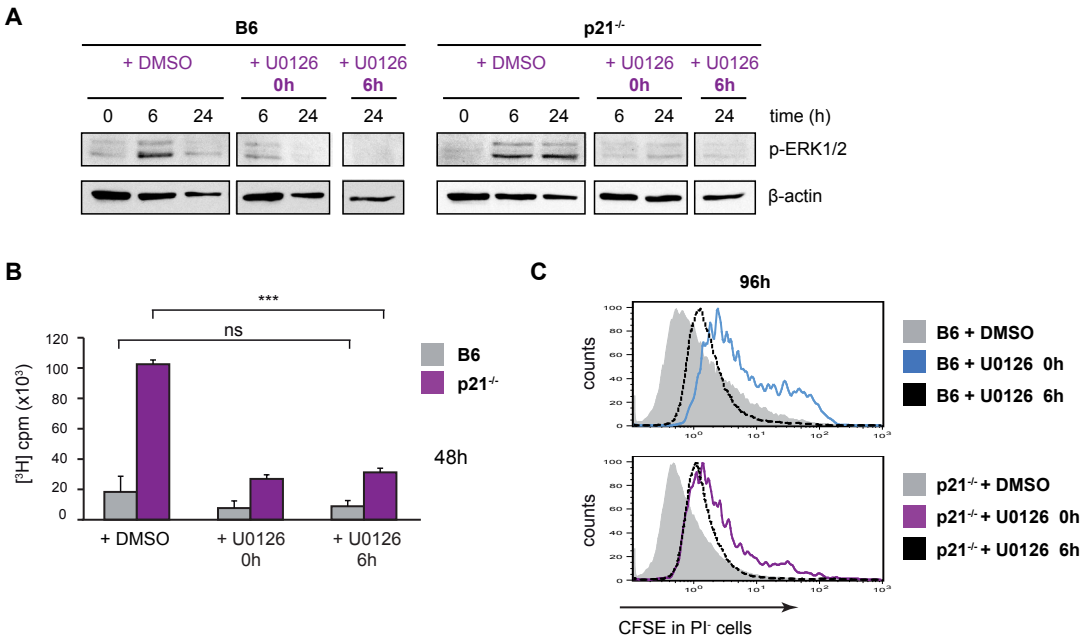

Figure 4.12. p21 controls late ERK activation and proliferation of effector/memory T cells. A. Western blot confirming reduced ERK1/2 phosporylation in the presence of the ERK1/2 inhibitor U0126 (10 mM) added at 0 h or 6 h of ConA

restimulation. β-actin was used as loading control. A representative experiment is shown (n = 5). **B.** [^{3}H] thymidine uptake at 48 h after the second TCR challenge in B6 and p21$^{-/-}$ effector/memory T cells, with U0126 (10 mM) added at 0 h or 6 h post-stimulation (p = 0.0003). Values show mean ± SD (n = 5). **C.** Dilution rate of CFSE-labeled PI-negative B6 (top panel) and p21$^{-/-}$ memory T cells (bottom panel) at 96 h after the second ConA stimulation and U0126 treatment at 0/6 h or DMSO control. Representative data are shown (n = 3).

4.1.2.9 p21 regulates activation of NF-κB in memory-phenotype T cells

As we observed an increase in AP-1 activity and subsequent cytokine release *in vitro* (*Fig. 4.5C-E*) as well as higher NFAT activity (*Fig. 4.10B*) in the absence of p21, we evaluated whether p21 also influenced the activity of the transcription factor NF-κB, another important T cell activation marker crucial for cytokine production[37]. We found hyperactivated NF-κB in p21$^{-/-}$ effector/memory T cells at 14 h after secondary stimulation, with maximum activation at 24 h (*Fig. 4.13A*). We also tested whether this hyperactivation was detectable in earlier stages post-secondary TCR challenge, and observed elevated levels of active NF-κB at early times (30 min) after secondary stimulation (*Fig. 4.13B*). p21 thus has an essential role in early activation of effector/memory T cells, and controls both MAPK and NF-κB activation pathways.

As we found that p21 also regulates effector/memory T cell activation and proliferation via the NF-κB pathway, we used the NF-κB inhibitor BAY$_{11\text{-}7082}$ to study its effect on p21-deficient T cell hyperproliferation. BAY$_{11\text{-}7082}$ selectively inhibits IKKα and subsequent IκBα phosphorylation, thus retaining NF-κB dimers in their inactive state[123]. In the presence of BAY$_{11\text{-}7082}$, NF-κB activity was greatly reduced, confirming similar inhibitor efficiency in B6 and p21$^{-/-}$ CD4$^+$ T cells (*Fig. 4.13C*). [^{3}H] thymidine incorporation assays showed significantly reduced p21-deficient T cell proliferation levels in the presence of BAY$_{11\text{-}7082}$ (13500 *vs.* 6549 cpm, p = 0.004), whereas B6 memory T cell proliferation diminished only moderately (7088 *vs.* 4284 cpm, p = 0.10) (*Fig. 4.13D*). To examine whether early or late NF-κB activation was responsible for the p21$^{-/-}$ effector/memory T cell hyperproliferation observed previously (*Fig. 4.6*), we added BAY$_{11\text{-}7082}$ at 6 h after secondary TCR challenge and compared the proliferation rates to cells treated at 0 h with DMSO or BAY$_{11\text{-}7082}$. At 6 h post-TCR stimulation, we found that proliferation was nearly abolished in both cell types (B6: -BAY$_{11\text{-}7082}$, 14041 *vs.* +BAY$_{11\text{-}7082}$, 1510 cpm, p = 0.055; p21$^{-/-}$: -BAY$_{11\text{-}7082}$, 50757 *vs.* +BAY$_{11\text{-}7082}$, 2216 cpm, p = 0.0005) (*Fig. 4.13E*). These data suggest that in addition to ERK1/2 phosphorylation, hyperproliferation of p21-deficient effector/memory T cells depends on late hyperactivation of NF-κB.

To determine whether CDK2 activity influenced NF-κB activation, we performed secondary stimulation in the presence of the CDK2 inhibitor CVT-313. EMSA showed elevated NF-κB activation levels in p21$^{-/-}$ effector/memory T cells after CVT-313 treatment compared to controls (*Fig. 4.13F*).

As NF-κB activity was unaffected by CDK2 inhibition, we propose that NFκB activation is independent of CDK2 in effector/memory T cells.

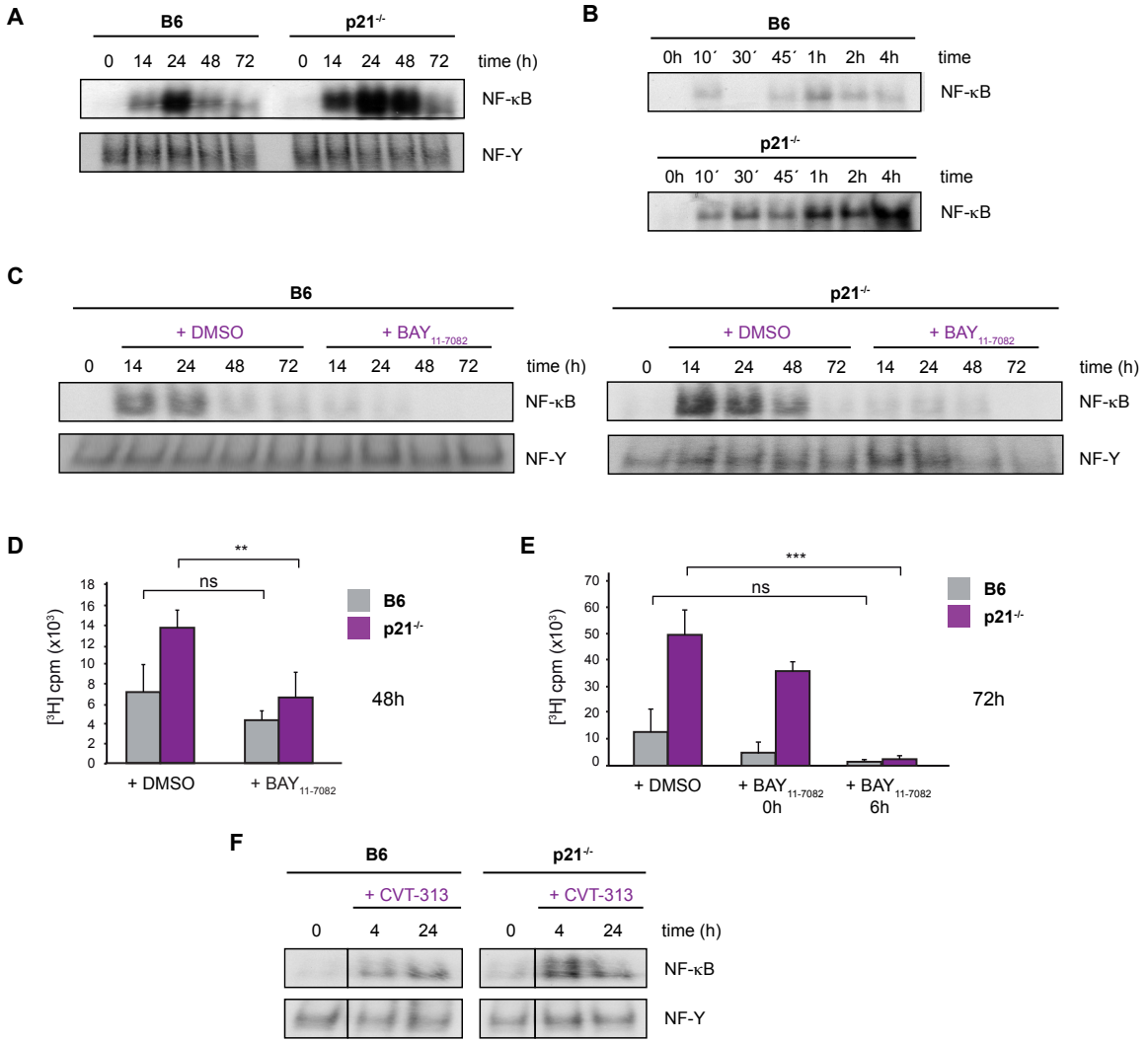

Figure 4.13. Increased NF-κB activation in effector/memory T cells in the absence of p21. A,B. NF-κB activation in p21$^{-/-}$ effector/memory T cells compared to B6 controls, as determined by EMSA at long (**A**) and short times (**B**) after secondary ConA stimulation in the presence of zVAD (50 μM). Probe containing the NF-Y consensus sequence was used as a loading control. Representative experiments are shown (n = 4). **C**. EMSA showed reduced NF-κB activation after $BAY_{11\text{-}7082}$ (10 μM) treatment of B6 and p21$^{-/-}$ effector/memory T cells during secondary stimulation in the presence of zVAD (12.5 μM). A representative experiment is shown (n = 2). **D**. Proliferation of B6 and p21$^{-/-}$ effector/memory T cells treated with $BAY_{11\text{-}7082}$ (10 μM) at 48 h post-secondary ConA stimulation in the presence of zVAD (50 μM), determined by [^{3}H] thymidine incorporation (B6: p = 0.10, p21$^{-/-}$: p = 0.004). Values show mean ± SD (n = 2). **E.** Proliferation of B6 and p21$^{-/-}$ effector/memory T cells treated with $BAY_{11\text{-}7082}$ (10 μM) at 0 h or 6 h in the presence of zVAD (12.5 μM), measured at 72 h post-secondary stimulation by [^{3}H] thymidine incorporation. Values show mean ± SD (n = 2; B6: p = 0.055, p21$^{-/-}$: p = 0.0005). **F.** Elevated NF-κB activity in p21$^{-/-}$ effector/memory T cells after treatment with CVT-313 (2.5μM), as detected by EMSA. A representative experiment is shown (n = 2).

4.2 $p21^{-/-}$ memory-like T cells hyperproliferate in response to specific antigens

As shown above, p21-deficient $CD4^+$ memory T cells present a hyperactive state and proliferate intensely in response to repeated TCR stimulation with ConA *in vitro*. To confirm our previous results, we next used a specific antigen (Ag) for repeated *in vitro* stimulation, to approximate a physiological stimulation model. We purified $CD4^+$ T cells that expressed a transgenic TCR (TCRtg) for chicken ovalbumin (OVA 323-339; OVA)[119,120] from p21-deficient ($p21^{-/-}$ OT-II) and control mice (OT-II) and cultured them *in vitro* with dendritic cells (DC) previously loaded with OVA (1 µM) (*see 3.2.6*). These $CD4^+$ T cells can be tracked by surface expression of the alpha chain (Vα2) in their transgenic TCR.

4.2.1 Similar proliferative response of naïve OT-II and $p21^{-/-}$ OT-II $CD4^+$ T cells to primary stimulation with specific antigens *in vitro*

We first analyzed the *in vitro* response of purified naïve OT-II and $p21^{-/-}$ OT-II $CD4^+$ T cells to TCR-specific stimulation with OVA peptide presented by DC in mixed cell cultures (*Fig. 4.14A*). [^{3}H] thymidine incorporation was similar for both T cell types at 24 h after stimulation (naïve OT-II, 1911 *vs.* $p21^{-/-}$ OT-II, 1774 cpm, $p = 0.615$) (*Fig. 4.14B*). Comparison of cell cycle profiles of $CD4^+Vα2^+$ T cells at 24 h after primary stimulation showed no differences in proliferation or apoptosis induction (*Fig. 4.14C*). CFSE dilution assay showed that T cells of both types undergo the same number of cell divisions in response to specific antigen stimulation (*Fig. 4.14D*). Activation markers such as CD69 were expressed at similar levels on the surface of naïve OT-II and $p21^{-/-}$ OT-II $CD4^+$ T cells (*Fig. 4.14E*), confirming comparable activation states in both cell types after primary TCR challenge.

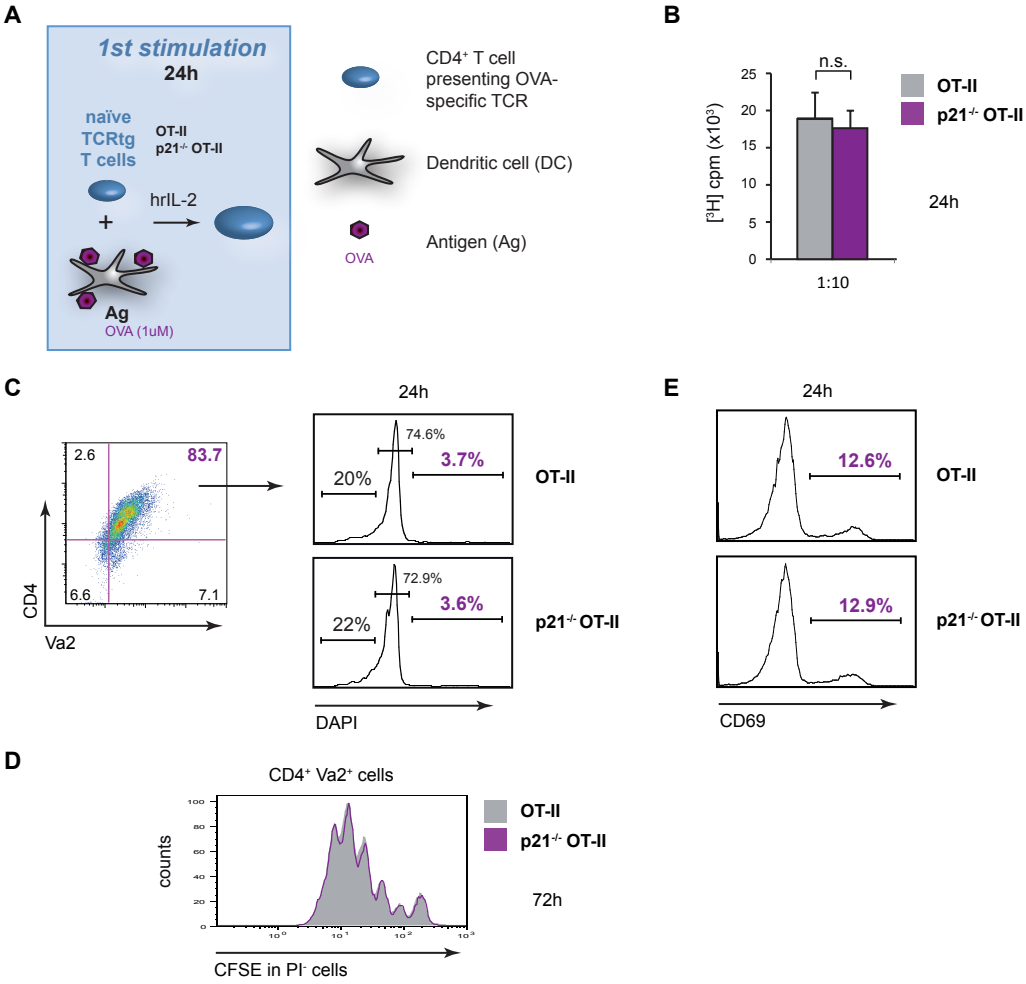

Figure 4.14. Naïve OT-II and p21$^{-/-}$ OT-II CD4^{+} T cells show similar proliferation rates and activation states during first stimulation with OVA-presenting DC. A. Primary stimulation *in vitro* of purified naïve OT-II and p21$^{-/-}$ OT-II CD4^{+} T cells with DC presenting OVA (1 µM) in the presence of hrIL-2. Cells were co-cultured at 1 x 10^{6}/ml CD4^{+} and 1 x 10^{5}/ml DC (10:1) final concentration. **B.** [^{3}H] thymidine incorporation in naïve OT-II and p21$^{-/-}$ OT-II T cells at 24 h post-primary TCR challenge with OVA presented by DC. Values show mean ± SD (n = 2; p = 0.615). **C.** Cell cycle profiles of naïve OT-II and p21$^{-/-}$ OT-II (CD4^{+} Vα2^{+}) T cells at 24 h after first stimulation. Fixed cells were stained with DAPI (2 µg/ml) for DNA quantification. Representative histograms are shown (n = 4). **D.** CFSE dilution of gated live (PI^{-}) CD4^{+} Vα2^{+} cells of naïve OT-II and p21$^{-/-}$ OT-II T cells at 72 h after first stimulation. Representative histograms are shown (n = 2). **E**. Surface expression of the CD69 activation marker on naïve OT-II and p21$^{-/-}$ OT-II CD4^{+} Vα2^{+} T cells stimulated for 24 h with OVA-presenting DC, as determined by flow cytometry. Representative histograms are shown (n = 2).

4.2.2 p21-deficient OT-II CD4$^+$ T cells show a proliferative advantage after a second stimulation with OVA-presenting DC *in vitro*

Auto-reactive T cells that escape thymic selection migrate to peripheral tissues, where they are activated repeatedly by encountering their cognate auto-antigen. To mimic this situation, we challenged OT-II and p21$^{-/-}$ OT-II CD4$^+$ T cells for a second time *in vitro* with OVA-presenting DC in the presence of zVAD to avoid AICD (*Fig. 4.15A*).

Repeated stimulation with the TCR-specific OVA peptide presented by DC led to hyperproliferation of p21$^{-/-}$ OT-II CD4$^+$ effector/memory T cells in comparison to control OT-II CD4$^+$ memory T cells, as seen in cell cycle analysis (*Fig. 4.15B*). A [^{3}H] thymidine incorporation assay confirmed significantly higher proliferation rates of p21-deficient OT-II effector/memory T cells at 48 h after secondary TCR challenge (OT-II, 39491 vs. p21$^{-/-}$ OT-II, 69579 cpm; p = 0.025) (*Fig. 4.15C*). In addition, an elevated number of cell divisions was observed for p21$^{-/-}$ OTII CD4$^+$ effector/memory T cells in CFSE dilution assays compared to control counterparts (*Fig. 4.15D*). In accordance with the apparent hyperproliferation of p21-deficient OT-II T cells, higher surface expression of CD69 was detected in these cells (*Fig. 4.15E*), confirming the hyperactive state of p21$^{-/-}$ OT-II CD4$^+$ effector/memory T cells after secondary TCR challenge. As a consequence of the elevated proliferation rate, we observed an accumulation of p21-deficient CD4$^+$Vα2$^+$ effector/memory T cells during restimulation (*Fig. 4.15F*).

By applying this *in vitro* model and stimulating CD4$^+$ T cells in a more physiological manner for one or two consecutive times with OVA-loaded DC, we observed results similar to those obtained with ConA. This antigen-specific stimulation model confirmed the hypothesis that p21 is involved in the cell cycle regulation of effector/memory, but not naïve CD4$^+$ T cells.

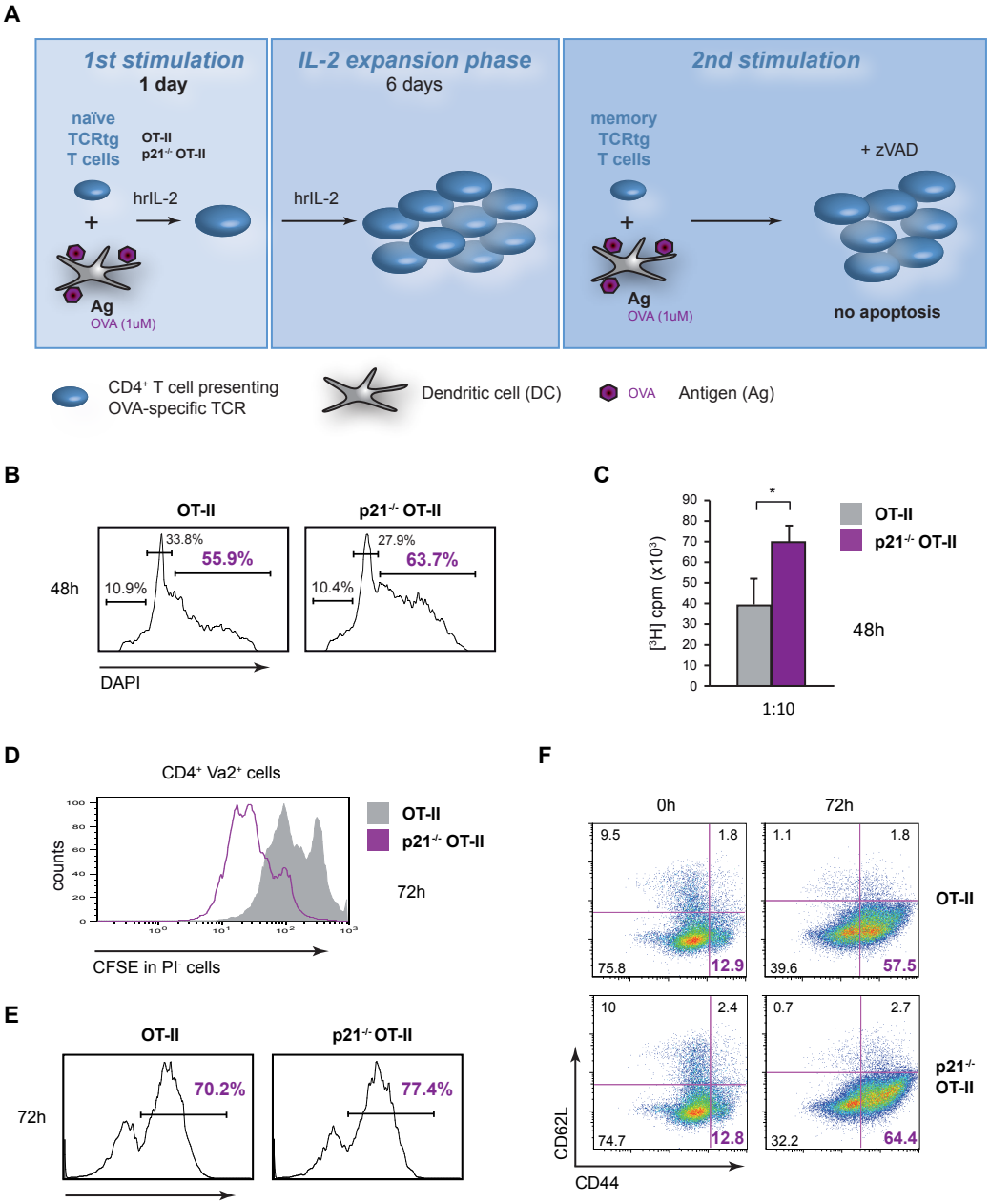

Figure 4.15. Hyperproliferation of p21$^{-/-}$ OT-II CD4^{+} effector/memory T cells in response to antigen (OVA)-specific stimulation. A. Secondary stimulation of OT-II and p21$^{-/-}$ OT-II CD4^{+} effector/memory T cells *in vitro* in the presence of DC presenting OVA (1 µM). Cells were co-cultured at 1 x 10^{6}/ml CD4^{+} and 1 x 10^{5}/ml DC (10:1) final concentration. **B.** Cell cycle analysis of CD4^{+} Vα2^{+} T cells at 48 h post-secondary stimulation (+12.5 µM zVAD). Fixed cells were stained with DAPI (2 µg/ml) to quantify DNA. Representative histograms are shown (*n* = 3). **C.** Hyperproliferation of p21$^{-/-}$ OT-II effector/memory T cells measured by [^{3}H] thymidine incorporation at 48 h after the second stimulation by OVA-presenting DC (+ 12.5 µM zVAD). Values show mean ± SD (*n* = 3; *p* = 0.025). **D.** CFSE dilution rate of gated PI-negative CD4^{+} Vα2^{+} cells at 72 h after secondary stimulation with OVA-presenting DC in the presence of zVAD (12.5 µM). Representative histograms are shown (*n* = 3). **E**. CD69 surface expression as determined by flow cytometry. Representative histograms are shown (*n* = 2). **F**. CD44/CD62L double staining to compare effector/memory T cell populations at 0 h and 72 h after secondary stimulation as determined by flow cytometry (*n* = 2).

4.2.3 Hyperproliferation of p21$^{-/-}$ OT-II CD4^{+} T cells after secondary stimulation with specific antigens *in vitro* is mediated by NF-κB, not CDK2

After *in vitro* restimulation of B6 and p21$^{-/-}$ CD4^{+} T cells with ConA, we found that p21-deficient effector/memory T cells were hyperactivated; as a result, we detected higher proliferation rates in these cells (*Fig. 4.6*). We also observed that p21 did not control T cell proliferation via its typical effector kinase CDK2 (*Fig. 4.7*), but more likely via the NF-κB activation pathway (*Fig. 4.13*). To confirm these results in physiological conditions, we analyzed CDK2 kinase activity in OT-II and p21$^{-/-}$ OT-II CD4^{+} T cells after secondary stimulation with OVA-loaded DC, and found no differences in kinase activity between T cells of both types (*Fig. 4.16A*). We nonetheless observed higher NF-κB activity in p21$^{-/-}$ OT2 effector/memory T cells (*Fig. 4.16B*), as also seen in p21$^{-/-}$ memory T cells stimulated with ConA (*Fig. 4.13A,B*).

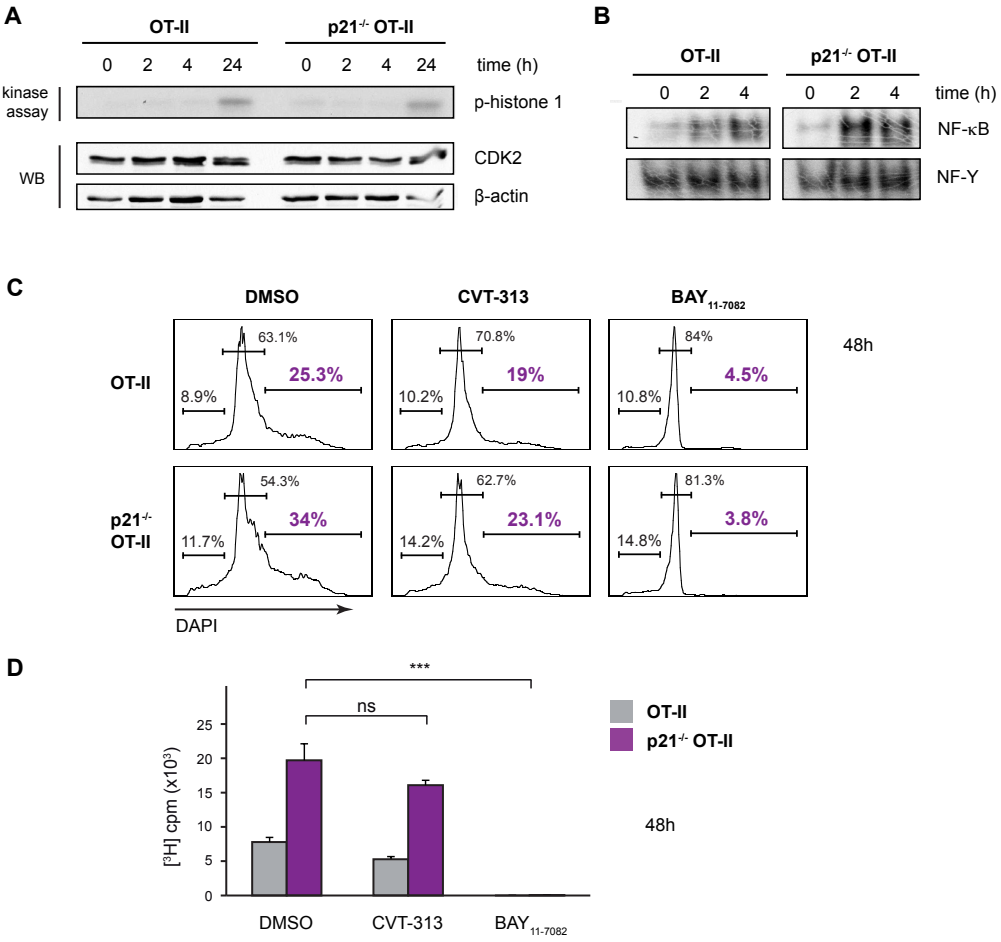

Figure 4.16. Hyperproliferation of p21$^{-/-}$ OT-II effector/memory T cells is NF-κB-dependent and independent of CDK2. A. CDK2 activity levels in OT-II and p21$^{-/-}$ OT-II effector/memory T cells during secondary stimulation with DC-presented OVA peptide in the presence of zVAD (12.5 μM), as determined by kinase assay. Histone H1 was used as substrate. Western blot analysis of total CDK2 and β-actin expression served as loading control. A representative experiment is shown (n = 2). **B.** EMSA showing NF-κB activation in OT-II and p21$^{-/-}$ OT-II effector/memory T cells after secondary stimulation. A

representative experiment is shown (*n* = 2). **C.** Cell cycle analysis of PI^- $CD4^+$ $V\alpha2^+$ T cells at 48 h after secondary stimulation in the presence of CVT-313 (2.5 µM) or $BAY_{11\text{-}7082}$ (10 µM) (+ 12.5 µM zVAD). Fixed cells were stained with DAPI (2 µg/ml) to quantify DNA. Representative data are shown (*n* = 2). **D.** Proliferation of OT-II and $p21^{-/-}$ OT-II effector/memory T cells in the presence of $BAY_{11\text{-}7082}$ (10 µM) or CVT-313 (2.5 µM), measured by [^{3}H] thymidine uptake at 48 h after secondary stimulation ($p21^{-/-}$ OT-II: CVT-313, $p = 0.0675$; $BAY_{11\text{-}7082}$, $p = 0.0001$). Values show mean ± SD (*n* = 2).

For further confirmation, T cells of both types were restimulated in the presence of the inhibitors CVT-313 (CDK2) and $BAY_{11\text{-}7082}$ (NF-κB) to study their effect on hyperproliferation of p21-deficient OT-II T cells. Cell cycle analysis showed only a moderate decrease in effector/memory T cell proliferation in the presence of CVT-313; in contrast, treatment with $BAY_{11\text{-}7082}$ completely abolished T cell proliferation in both OT-II and $p21^{-/-}$ OT-II effector/memory T cells. In both cases, apoptosis induction was unaffected (*Fig. 4.16C*). [^{3}H] thymidine incorporation assays showed that CVT-313 did not affect T cell proliferation rates ($p21^{-/-}$ OT-II, 19695 *vs.* 16065 cpm; $p = 0.0675$), whereas $BAY_{11\text{-}7082}$ completely inhibited proliferation in both OT-II and $p21^{-/-}$ OT-II $CD4^+$ T cells ($p21^{-/-}$ OT-II, 19695 *vs.* 59 cpm; $p = 0.0001$) (*Fig. 4.16D*). These findings suggest that p21 controls effector/memory T cell proliferation via NF-κB and not via CDK2.

4.2.4 *In vivo* TCR-specific stimulation of naïve $CD4^+$ T cells leads to hyperreactivity of $p21^{-/-}$ TCRtg T cells

To study the role of p21 in cell cycle control of effector/memory T cells in a more physiological context, we mimicked conditions of an immune response to allow us to monitor $CD4^+$ T cell behavior *in vivo*. We adoptively transferred TCR-transgenic naïve $CD4^+$ T cells from OT-II or $p21^{-/-}$ OT-II mice to recipient mice of the same haplotype (C57BL/6). The T cell population injected represents ~1% of all cells in secondary lymphoid organs, and can be detected and followed by the expression of the transgenic TCR ($V\alpha2$)[137,138].

For these experiments, we purified TCRtg $CD4^+$ from spleens of OT-II or $p21^{-/-}$ OT-II mice and labeled them with CFSE prior to injection into recipient mice (1×10^6 $CD4^+$ T cells/mouse). After 24 h, we challenged with OVA-loaded DC (1×10^6 DC/mouse); three days later, mice were sacrificed and cells of secondary lymphoid organs were analyzed (*Fig. 4.17A*)[129].

We examined the proliferative response of $CD4^+V\alpha2^+$ T cells to specific stimulation with OVA peptide *in vivo* by analyzing dilution of the CFSE proliferation marker in these cells. Both OT-II and $p21^{-/-}$ OT-II T cells proliferated considerably (OT-II, blue curve; $p21^{-/-}$ OT-II, purple) compared to initial CFSE loading (solid black), but were still distinguishable from the CFSE-negative peak, which

represented endogenous CD4⁺ T cells (solid grey) (*Fig. 4.17B*). No differences were observed when we compared the proliferation rates of OT-II and p21$^{-/-}$ OT-II T cells in spleen and lymph nodes. Cell cycle analysis at 3 d post-stimulation confirmed similar proliferation and apoptosis levels in OT-II and p21$^{-/-}$ OT-II T cells in spleens and lymph nodes (*Fig. 4.17C*).

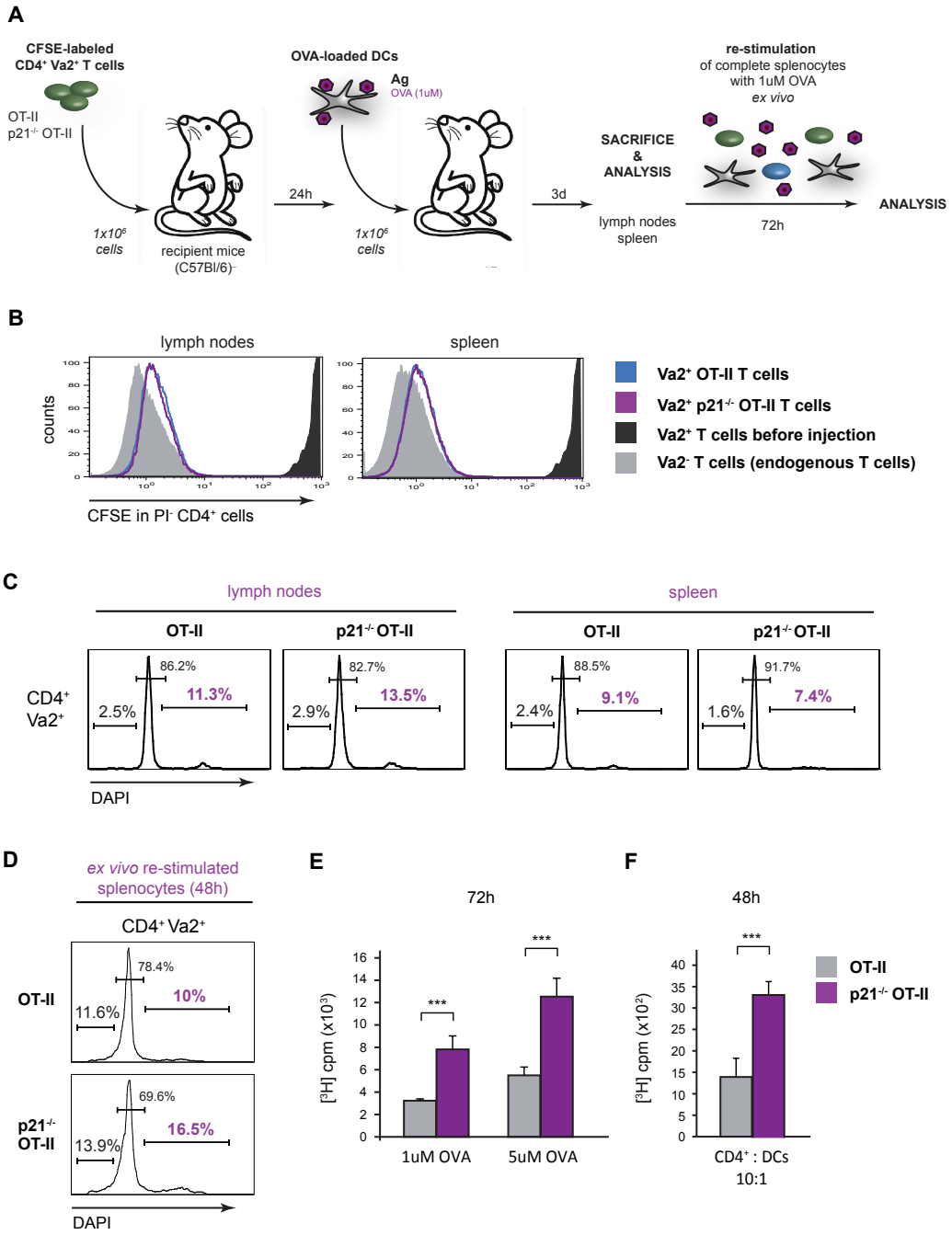

Figure 4.17. ***In vivo*** **TCR-specific stimulation does not alter naïve CD4⁺ T cell activation, but leads to hyperreactivity of p21$^{-/-}$ TCRtg effector/memory T cells** ***ex vivo*****. A.** Purified CD4⁺ splenocytes from OT-II or p21$^{-/-}$ OT-II mice were CFSE-labeled and adoptively transferred to B6 recipients. After 24 h, the cells were challenged specifically by injection of DC presenting OVA peptide. After 3 days, mice were sacrificed and the CD4⁺ T cell response was evaluated. CD4⁺ splenocytes

received an additional OVA challenge *ex vivo* as indicated. **B.** CFSE dilution of OT-II (blue) and p21$^{-/-}$ OT-II (purple) (CD4$^+$ Vα2$^+$) T cells 72 h after TCR-specific stimulation with DC *in vivo*. Endogenous T cells (Vα2$^-$; solid grey) and initial CFSE loading (CD4$^+$ Vα2$^+$; solid black) controls are shown. A representative experiment is shown (*n* = 2). **C.** Cell cycle analysis of CD4$^+$ Vα2$^+$ T cells in spleen and lymph nodes after primary stimulation *in vivo*. Fixed cells were stained with DAPI (2μg/ml) for DNA quantification. Representative histograms are shown (*n* = 2). **D.** *Ex vivo* restimulation of OT-II and p21$^{-/-}$ OT-II T cells with total splenocytes in the presence of soluble OVA peptide (1 μM) as determined by cell cycle analysis. Fixed cells were DAPI-stained for DNA quantification. Representative histograms are shown (*n* = 2). **E,F.** [^{3}H] thymidine incorporation in OT-II and p21$^{-/-}$ OT-II T cells after *ex vivo* restimulation with total splenocytes and soluble OVA peptide (1 μM/5 μM; 72 h) (**E**) or OVA-presenting DC (48 h; 10:1 CD4$^+$:DC ratio) (**F**). Values show mean ± SD (*n* = 2; 1 μM OVA, *p* = 0.0007; 5 μM OVA, *p* = 0.0004; CD4$^+$:DC 10:1: *p* = 0.025).

Following primary stimulation *in vivo*, we observed no proliferation differences between OT-II and p21$^{-/-}$ OT-II T cells; we thus stimulated the cells for a second time *ex vivo* to confirm the importance of p21 in regulating proliferation in effector/memory T cells. We restimulated total splenocytes *in vitro* with soluble OVA peptide; in this way, the spleen APC specifically stimulate the CD4$^+$Vα2$^+$ T cells. Cell cycle analysis showed high proliferation levels for p21$^{-/-}$ OT-II T cells in comparison to OT-II T cells at 48 h after secondary stimulation *ex vivo*, while apoptosis levels remained similar (*Fig. 4.17D*). [^{3}H] thymidine incorporation confirmed significantly higher proliferation levels of p21$^{-/-}$ OT-II T cells, independently of the OVA peptide dose used for restimulation (1 μM OVA: OT-II, 3240 *vs.* p21$^{-/-}$ OT-II, 7508 cpm, *p* = 0.0007; 5 μM OVA: OT-II, 5498 *vs.* p21$^{-/-}$ OT-II, 12634 cpm, *p* = 0.0004) (*Fig. 4.17E*). To exclude the possible influence of endogenous recipient mouse splenocytes on the outcome of the [^{3}H] thymidine incorporation assay, we purified CD4$^+$ T cells from spleens harvested 3 days after *in vivo* stimulation, and used OVA-loaded DC for *ex vivo* restimulation (10:1 CD4$^+$:DC ratio). We again observed p21$^{-/-}$ OT-II T cell hyperproliferation after secondary stimulation (OT-II, 39491 *vs.* p21$^{/}$ OT-II, 69579 cpm, *p* = 0.025) (*Fig. 4.17F*).

4.2.5 p21-deficient TCRtg CD4$^+$ T cells hyperproliferate in response to repeated stimulation with specific antigens of low and high affinity

The next objective was to study the regulatory effect of p21 on T cell responses to self-antigens in physiological conditions, by stimulating the cells with a specific antigen. We therefore used T cells that present a transgenic T cell receptor (TCRtg) for pigeon cytochrome C (PCC)[126,127]. Purified control (pcc.TCRtg) and p21-deficient (pcc.TCRtg-p21$^{-/-}$) CD4$^+$ T cells were cultured with irradiated APC of the same haplotype (*see 3.2.5*). These T cells can be identified by expression of transgenic alpha (Vα11) and beta (Vβ3) TCR chains[137,138].

This mixed cell culture model allowed us to stimulate the $CD4^+$ T cells with antigens that have high (PCC) or low affinity (A96I; PCC with an A>I subsitution at residue 96) for the transgenic TCR, to test whether loss of p21 expression in memory T cells affected the TCR-mediated activation threshold. In response to auto-antigens with low affinity for the TCR[139], T lymphocytes progressively lose tolerance to the antigen, leading finally to development of autoimmune diseases. Greater susceptibility of $p21^{-/-}$ $CD4^+$ T cells to stimulation by peptides with low TCR affinity would thus provide insight into the role of p21 in the $CD4^+$ T cell response to auto-antigens, maintenance of tolerance, and the induction of autoimmune disorders.

4.2.5.1 pcc.TCRtg-$p21^{-/-}$ $CD4^+$ T cells hyperproliferate in response to a secondary TCR challenge with high affinity antigens

To ensure appropriate activation of purified naïve pcc.TCRtg and pcc.TCRtg-$p21^{-/-}$ $CD4^+$ T cells, for the first stimulation we used irradiated APC presenting an antigen with high affinity (PCC) for the transgenic TCR (*Fig. 4.18A*). The A96I antigen with low affinity for the TCRtg is too weak to generate significant T cell responses and was not considered for naïve T cell stimulation (data not shown). After primary stimulation, [^{3}H] thymidine incorporation showed no significant differences between naïve pcc.TCRtg and pcc.TCRtg-$p21^{-/-}$ T cells (pcc.TCRtg, 2036 *vs.* pcc.TCRtg-$p21^{-/-}$, 2151 cpm, $p = 0.7$) (*Fig. 4.18B*). Cell cycle profiles showed similar proliferation rates in naïve pcc-TCRtg and pcc.TCRtg-$p21^{-/-}$ $CD4^+$ T cells; apoptosis levels were also similar and included dying irradiated APC in the culture (*Fig. 4.18C*). The proliferative response to primary stimulation with TCR-specific antigens *in vitro* is thus comparable in pcc.TCRtg and pcc.TCRtg-$p21^{-/-}$ naïve $CD4^+$ T cells.

To study the role of p21 in the determination of the TCR activation threshold of effector/memory T cells, we applied the repeated stimulation protocol to pcc.TCRtg and pcc.TCRtg-$p21^{-/-}$ $CD4^+$ T cells. T cells were expanded for 6 days in hrIL-2 and then restimulated with freshly isolated and irradiated APC. For secondary stimulation, we used antigens with different affinities for the TCRtg (*Fig. 4.18A*) (*see 3.2.5*).

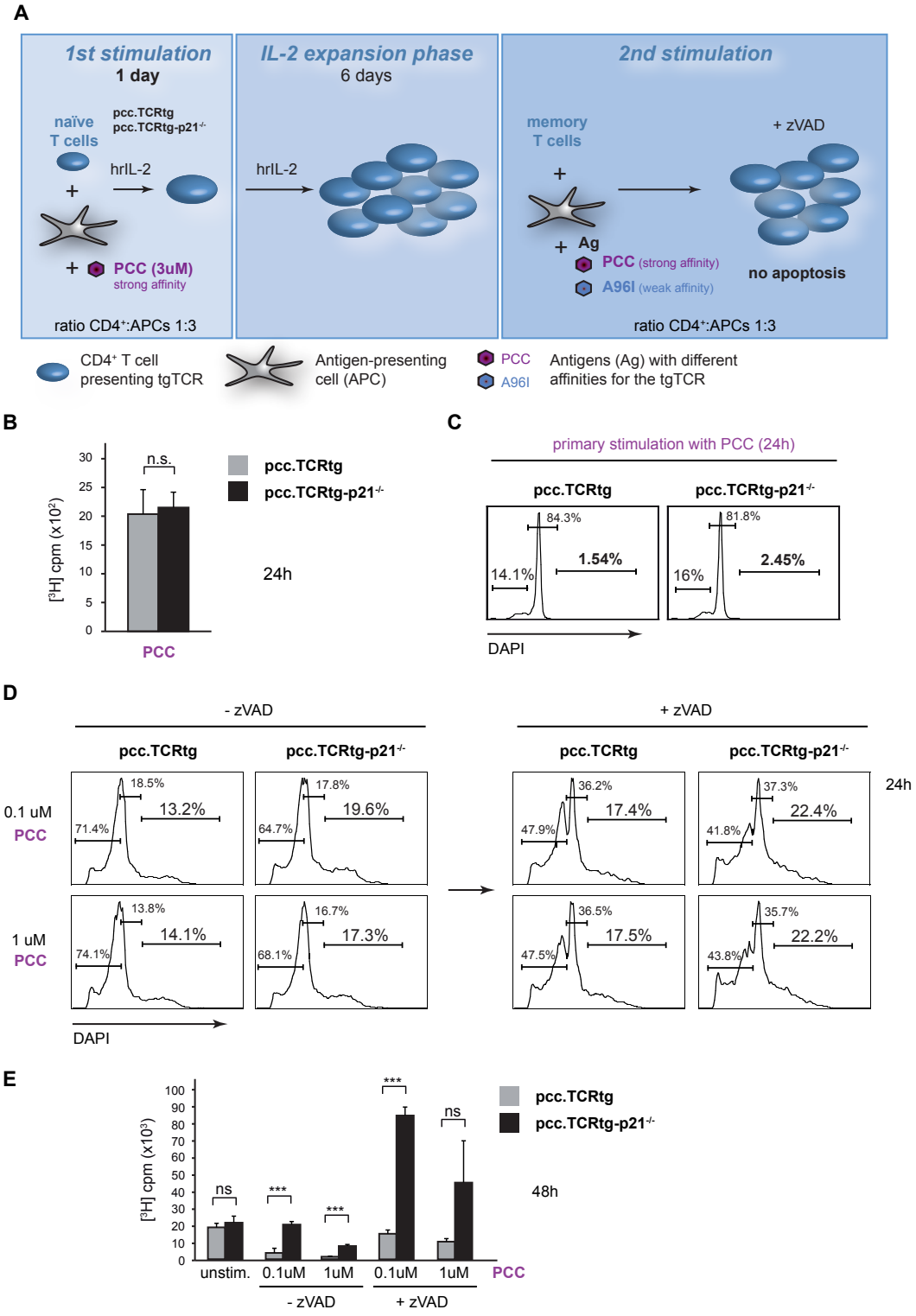

Figure 4.18. Hyperproliferation of pcc.TCRtg-p21$^{-/-}$ effector/memory T cells after a secondary TCR challenge *in vitro* with a high affinity antigen. **A.** Naïve pcc.TCRtg and pcc.TCRtg-p21$^{-/-}$ CD4^{+} T cells were stimulated *in vitro* with irradiated APC (B10BR, 30 Gy) and PCC (3 µM) in the presence of hrIL-2 (20 ng/ml). CD4^{+} T cells and APC were plated at a 1:3 ratio. After 6 days expansion with hrIL-2, CD4^{+} T cells were restimulated with freshly isolated and irradiated APC (CD4^{+}:APC ratio 1:3) and an antigen with high TCR affinity (PCC) in the presence of zVAD (12.5 µM). **B.** [^{3}H] thymidine incorporation at 24 h after primary stimulation with PCC. Values show mean ± SD, (n = 2, p = 0.7). **C.** Cell cycle analysis of pcc.TCRtg and pcc.TCRtg-p21$^{-/-}$ CD4^{+}Vb3^{+} T cells at 24 h after primary stimulation with PCC (3 µM) in mixed cell cultures (2 µg/ml

DAPI). A representative experiment is shown (*n* = 2). **D.** Cell cycle analysis (2 µg/ml DAPI) of pcc.TCRtg and pcc.TCRtg-p21$^{-/-}$ CD4^{+}Vb3^{+} T cells at 24 h after restimulation with PCC alone or with zVAD (12.5 µM). A representative experiment is shown (*n* = 2). **E.** [^{3}H] thymidine incorporation in pcc.TCRtg and pcc.TCRtg-p21$^{-/-}$ T cells at 48 h after secondary stimulation with PCC. Values show mean ± SD (*n* = 2; -zVAD: 0.1 µM, *p* = 0.0009, 1 µM, *p* = 0.0003; +zVAD: 0.1 µM, *p* = 0.00003, 1 µM, *p* = 0.071).

Whereas pcc.TCRtg and pcc.TCRtg-p21$^{-/-}$ CD4^{+} T cells showed a similar proliferative response to high affinity antigens (PCC) during primary stimulation, pcc.TCRtg-p21$^{-/-}$ effector/memory T cells hyperproliferated after secondary simulation with PCC, as observed by cell cycle analysis (*Fig. 4.18D*). In addition, restimulation with high affinity antigen induced high levels of apoptosis (*Fig. 4.18D*, left). This phenomenon, known as AICD, was slightly reduced in the presence of the apoptosis inhibitor zVAD at the usual concentration (12.5 µM) (*Fig. 4.18D*, right). The [^{3}H] thymidine incorporation assay confirmed p21-deficient pcc.TCRtg effector/memory T cell hyperproliferation in response to PCC (*Fig. 4.18E*). Low [^{3}H] thymidine incorporation in the absence of zVAD can be explained by the increased apoptosis levels observed in cell cycle profiles (0.1 µM PCC, *p* = 0.0009; 1 µM PCC, *p* = 0.0003) where, in the presence of zVAD, pcc.TCRtg-p21$^{-/-}$ CD4^{+} T cells clearly hyperproliferated compared to their pcc.TCRtg counterparts (0.1 µM PCC, *p* = 0.00003; 1 µM PCC, *p* = 0.071) (*Fig. 4.18E*). Low PCC doses (0.1 µM) induced higher proliferation levels than high PCC doses (1 µM) in pcc.TCRtg CD4^{+} T cells. This finding was more evident in pcc.TCRtg-p21$^{-/-}$ CD4^{+} T cells (*Fig. 4.18D,E*) and indicated distinct activation thresholds in p21-deficient T cells. These data suggested that second stimulation using an antigen with high affinity for the transgenic TCR leads to p21-deficient TCRtg T cell hyperproliferation, which confirmed our previous results after restimulation with ConA and anti-CD3/CD28 antibodies *in vitro* (*Fig. 4.6*).

4.2.5.2 TCRtg-p21$^{-/-}$ CD4^{+} T cells hyperproliferate in response to a second stimulation with weak affinity antigen

Self-reactive T cells that escape peripheral tolerance mechanisms (*see 1.2*) usually have low affinity for auto-antigens and play a central role in the pathogenesis of autoimmune diseases[139]. To study the role of p21 in the maintenance of tolerance and induction of autoimmunity, a specific antigen with low affinity for the TCRtg (A96I) was used for secondary stimulation of TCRtg CD4^{+} cells *in vitro*.

After restimulation of pcc.TCRtg and pcc.TCRtg-p21$^{-/-}$ effector/memory T cells with A96I, no AICD was induced (*Fig. 4.19A*, left) and apoptosis levels were hardly altered in the presence of zVAD, as observed in cell cycle profiles (*Fig. 4.19A*, right). In addition, pcc.TCRtg-p21$^{-/-}$ effector/memory

T cells clearly hyperproliferated in response to A96I compared to pcc.TCRtg CD4$^+$ Vβ3$^+$ T cells (*Fig. 4.19A*); the proliferation difference between both cell types was even greater than after secondary PCC stimulation (*Fig. 4.18D*). The elevated proliferative capacity of pcc.TCRtg-p21$^{-/-}$ effector/memory T cells was verified by [^{3}H] thymidine incorporation at 48 h after secondary stimulation with A96I (1 µM and 10 µM) alone or in the presence of zVAD (12.5 µM) (-zVAD: 1 µM A96I, p = 0.006, 10 µM A96I, p = 0.0003; +zVAD: 1 µM A96I, p = 0.001, 10 µM A96I, p = 0.03) (*Fig. 4.19B*). p21-deficient pcc.TCRtg T cells proliferated up to 2.5 times more compared to pcc.TCRtg T cells in response to high doses of A96I (10 µM). In accordance with previous results, a CFSE dilution assay confirmed the finding that pcc.TCRtg-p21$^{-/-}$ effector/memory T cells undergo more rounds of cell division than their pcc.TCRtg counterparts (*Fig. 4.19C*). The hyperproliferation of p21-deficient pcc.TCRtg CD4$^+$ T cells in response to a low affinity antigen points to a lower TCR activation threshold in these cells. pcc. TCRtg-p21$^{-/-}$ effector/memory T cells might thus be more susceptible to activation by auto-antigens, which could lead to loss of tolerance.

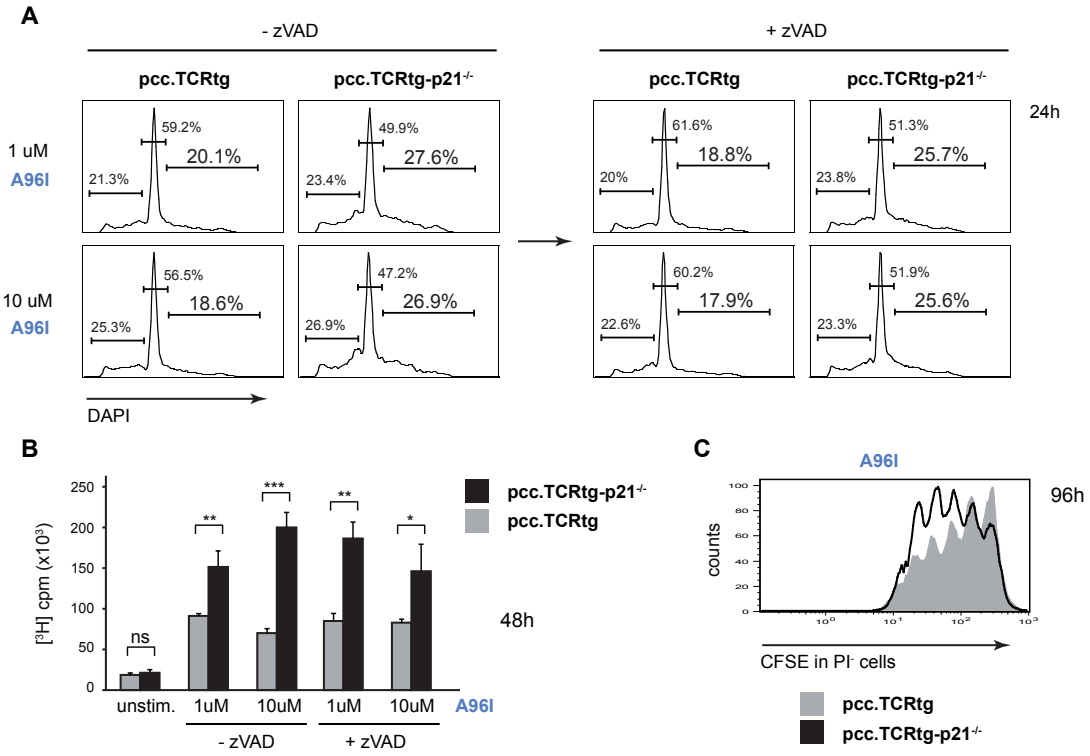

Figure 4.19. The low affinity antigen A96I induces hyperproliferation of TCRtg-p21$^{-/-}$ memory-phenotype CD4$^+$ T cells. **A.** Cell cycle analysis of pcc.TCRtg and pcc.TCRtg-p21$^{-/-}$ effector/memory T cells at 24 h after secondary stimulation with A96I (1 µM and 10 µM) alone (left) or with zVAD (12.5 µM; right) (2 µg/ml DAPI). A representative experiment is shown (n = 2). **B.** [^{3}H] thymidine incorporation in pcc.TCRtg and pcc.TCRtg-p21$^{-/-}$ effector/memory T cells at 48 h after secondary TCR challenge with A96I (1 µM and 10 µM) alone or with zVAD (12.5 µM). Values show mean ± SD (-zVAD: 1 µM A96I, p = 0.006, 10 µM A96I, p = 0.0003; +zVAD: 1 µM A96I, p = 0.001, 10 µM A96I, p = 0.03; n = 2). **C.** CFSE dilution assay of pcc. TCRtg and pcc.TCRtg-p21$^{-/-}$ effector/memory T cells at 96 h after secondary stimulation with 10 µM A96I (+ 12.5 µM zVAD). A representative experiment is shown (n = 2).

4.3 The role of p21 in the development of autoimmune disease in B6/*lpr* mice

Thus far, in addition to its known function as a cell cycle inhibitor, we identified p21 as a negative regulator of memory T cell activation and proliferation. p21 therefore appears to be important for establishment of T cell tolerance and for autoimmune suppression, as it prevents immune responses to antigens with low TCR affinity, which mimic auto-antigens.

To study the role of p21 in an *in vivo* model of autoimmunity, we used B6/*lpr* mice. These mice have Fas deficiency, which leads to defective apoptosis signaling and development of autoimmune disorders, characterized by lymphadenopathy and splenomegaly (*see 1.5.2*). In addition, elevated levels of anti-DNA antibodies in serum, immune complex formation in tissues and mild glomerulonephritis are detected. These alterations could lead to kidney failure, but in general a mild, non-lethal course of disease is observed in B6/*lpr* mice[56]. As both Fas and p21 are essential to restrain T cell activation and proliferation, we generated B6/*lpr*-p21-deficient mice on the C75BL/6 background (B6/*lpr*-p21$^{-/-}$) to study T cell responses and the development of autoimmunity in mice lacking Fas and p21.

4.3.1 Lack of p21 exacerbates the autoimmune manifestations in B6/*lpr* mice

A common characteristic in B6/*lpr* pathology is the presence of anti-DNA antibodies in serum of Fas-deficient mice (*see 1.5.2*). As a direct result of the immunological hyperactivation in the absence of p21, significantly higher levels of anti-DNA antibodies of all IgG isotypes were detected in 8-month-old B6/*lpr*-p21$^{-/-}$ mice (data not shown). High levels of IgG auto-antibodies have an important role in the development of glomerulonephritis[42,55,57], a common manifestation in pathology of B6/*lpr* mice. Autoimmune nephritis is caused by the accumulation of immune complexes composed of DNA and anti-DNA-antibodies, and subsequent activation and infiltration of inflammatory cells.

We analyzed kidney paraffin sections of 6-month-old B6, p21$^{-/-}$, B6/*lpr* and B6/*lpr*-p21$^{-/-}$ mice and observed glomerular inflammation and an increase in mesangial matrix in B6/lpr mice (grade III lupus nephritis according to Weening and co-workers[132]), whereas no alteration in the glomerulus was found in B6 controls (*Fig. 4.20A*, left). The lack of p21 caused a serious aggravation of the pathologic manifestation in p21$^{-/-}$ (grade II) and B6/*lpr*-p21$^{-/-}$ mice (grade IV) compared to B6 and B6/*lpr* mice, respectively (*Fig. 4.20A*, right). Lack of both Fas and p21 had an additional effect, with more severe disease pathology in B6/*lpr*-p21$^{-/-}$ mice.

The maintained inflammation state leads to structural degradation of the glomerulus and thus to protein precipitation in the urine of Fas-deficient mice with lupus-like disease. We confirmed increased protein levels in the urine of B6, p21$^{-/-}$, B6/*lpr* and B6/*lpr*-p21$^{-/-}$ mice (9 months and older) (*Fig. 4.20B*) corresponding to the lupus nephritis grades previously described (*Fig. 4.20A*). The absence of p21 aggravated autoimmune manifestations in B6 and B6/*lpr* mice, resulting in severe glomerulonephritis in B6/*lpr*-p21$^{-/-}$ mice.

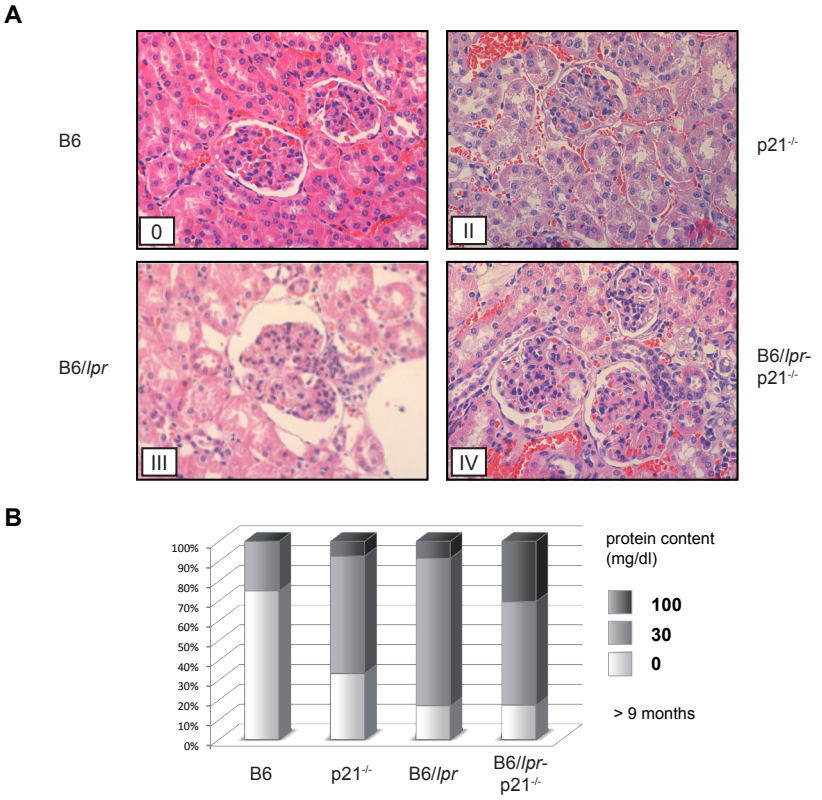

Figure 4.20. Lack of p21 aggravates autoimmune glomerulonephritis in B6 and B6/*lpr* mice. A. Light micrographs of representative kidney sections from 6-month-old female B6, p21$^{-/-}$, B6/*lpr* and B6/*lpr*-p21$^{-/-}$ mice (*n* = 4 mice/group). Lupus nephritis grades according to the scale defined by Weening *et al.*[132] are indicated. **B.** Detection of protein levels in urine of B6, p21$^{-/-}$, B6/*lpr* and B6/*lpr*-p21$^{-/-}$ mice (*n* ≥27 mice/group; 9 months and older).

To determine the effect of p21 deficiency on autoimmune manifestations at the cellular level, we analyzed several T cell populations from B6/*lpr* and B6/*lpr*-p21$^{-/-}$ mice and their implication in disease development *in vivo*. An important characteristic of the B6/*lpr* phenotype is accumulation of TCRβ^{+}CD4^{-}CD8^{-} (DN), CD4^{+}CD44^{high}CD62L^{high} (effector phenotpye) and CD4^{+}CD44^{high}CD62L^{low} (memory phenotype) T cells in secondary lymphoid organs. The excessive proliferation of DN T cells is thought to cause lymhadenopathy over time[73,77]. *In vivo* analysis of DN populations, however, did not show marked differences in the percentage of TCRβ^{+}CD4^{-}CD8^{-} T cells between B6/*lpr* and

B6/*lpr*-p21$^{-/-}$ mice (*Fig. 4.21A*). The proliferative response of DN cells *in vivo* was also comparable, as determined by a BrdU incorporation assay (*Fig. 4.21B*). The lack of p21 thus did not alter DN T cells in B6/*lpr* mice.

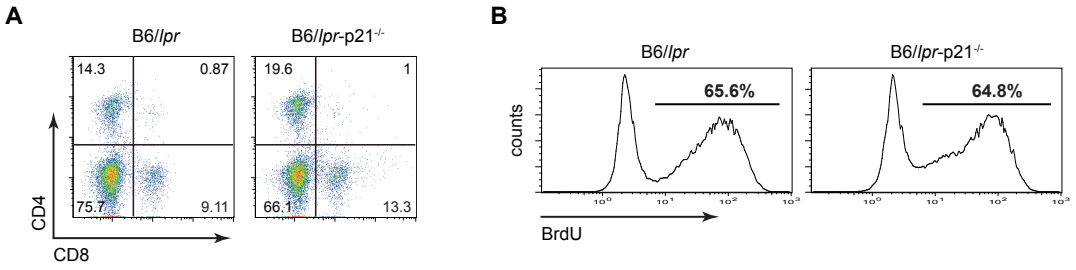

Figure 4.21. DN T cell accumulation and proliferation is similar in B6/*lpr* and B6/*lpr*-p21$^{-/-}$ mice. A. CD4 and CD8 double staining, gated on TCRβ^{+} T cells isolated from lymph nodes of 8-month-old B6/*lpr* and B6/*lpr*-p21$^{-/-}$ mice. Representative data are shown (*n* = 3 mice/strain). **B.** Similar proliferative response of B6/*lpr* and B6/*lpr*-p21$^{-/-}$ DN T cells *in vivo* (1 month old). BrdU was administered in drinking water for 9 days. A representative experiment is shown (*n* = 2).

4.3.2 Hyperactivation of CD44^{high}CD62L^{low} memory T cells in B6/*lpr*-p21$^{-/-}$ mice

We next examined whether CD44^{high}CD62L^{high} and CD44^{high}CD62L^{low} memory T cell populations were influenced by the lack of p21 in B6/*lpr* mice. At one month of age, B6/*lpr*-p21$^{-/-}$ mice already presented indications of CD44^{high}CD62L^{low} memory T cell accumulation (*Fig. 4.22A*, left). When mice reached the age of 8 months, the percentage of CD44^{high}CD62L^{low} cells was clearly increased in B6/*lpr*-p21$^{-/-}$ mice, whereas the CD44^{high}CD62L^{high} population was reduced (*Fig. 4.22A*, right). We found both memory T cell populations, and CD4^{+} T cells in general, to be hyperactivated in B6/*lpr*-p21$^{-/-}$ mice compared to B6/*lpr* mice, as indicated by staining for cell surface activation markers CD25 (*Fig. 4.22B*) and CD69 (data not shown). These findings suggest a regulatory role for p21 in activation of potentially auto-reactive memory T cells.

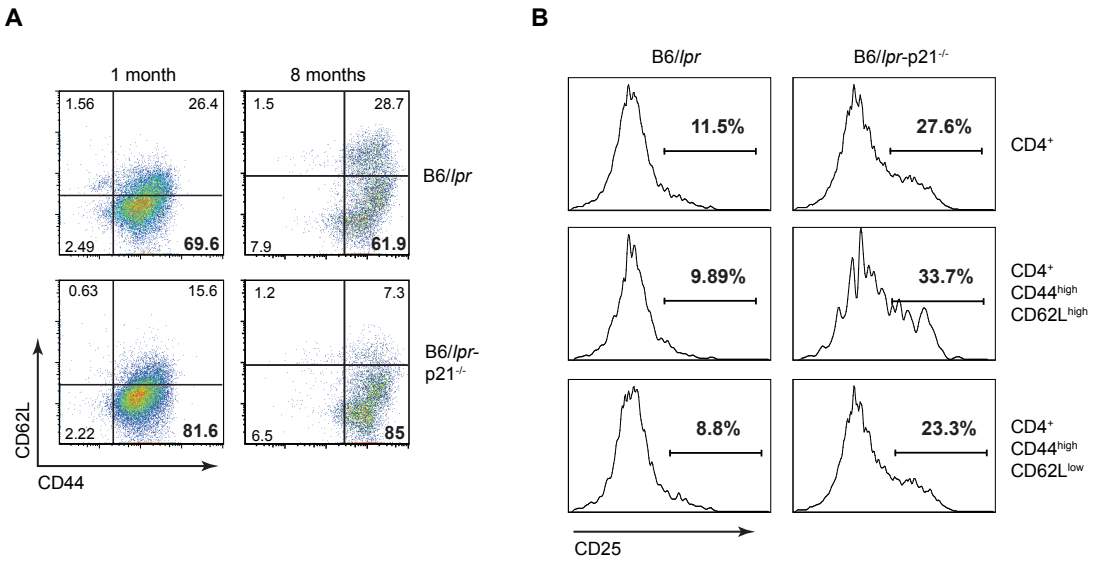

Figure 4.22. Hyperactivation and increased representation of CD44^{high}CD62L^{low} memory T cells in B6/*lpr*-p21$^{-/-}$ mice. **A.** CD44-CD62L double staining gated on CD4^{+} T cells isolated from lymph nodes of 1- or 8-month-old B6/*lpr* and B6/*lpr*-p21$^{-/-}$ mice. Representative data are shown (*n* = 3 mice/strain). **B.** Surface expression of CD25 on CD4^{+} (top panel), CD4^{+}CD44^{high}CD62L^{high} (middle) and CD4^{+}CD44^{high}CD62L^{low} (bottom) T cells from 8-month-old B6/*lpr* and B6/*lpr*p21$^{-/-}$ mice, as determined by flow cytometry. Representative histograms are shown (*n* = 3 mice/strain).

4.3.3 B6/*lpr*-p21$^{-/-}$ memory-phenotype T cells present a hyperactive state *in vitro*

To analyze the influence of p21 in B6/*lpr* T cell responses *in vitro*, we applied the repeated stimulation system to B6/*lpr* and B6/*lpr*-p21$^{-/-}$ T cells (*Fig. 4.4A*). Freshly isolated naïve CD4^{+} T cells from 2-month-old mice were stimulated twice with ConA, and factors of the most important T cell activation pathways were analyzed in response to a secondary antigen encounter.

We found that B6/*lpr*-p21$^{-/-}$ effector/memory T cells were hyperactivated compared to B6/*lpr* memory T cells, reflected by increased ERK1/2 phosphorylation levels after restimulation (*Fig. 4.23A*). We also observed elevated NF-κB activation levels in B6/*lpr*-p21$^{-/-}$ memory T cells during a secondary ConA stimulation (*Fig. 4.23B*). The activity of other key transcription factors such as NFAT was unaltered in B6/*lpr*-p21$^{-/-}$ T cells (*Fig. 4.23C*). To confirm B6/*lpr* and B6/*lpr*-p21$^{-/-}$ memory T cell hyperactivation, we analyzed pro-inflammatory cytokine production in response to a secondary TCR challenge *in vitro*, and detected elevated IFNγ, IL-17 and IL-2 production in B6/*lpr*-p21$^{-/-}$ memory T cells (*Fig. 4.23D*). These findings concur with our data for B6 and p21$^{-/-}$ memory T cells, and confirm the importance of p21 as a negative regulator of T cell activation via ERK1/2 and NF-κB.

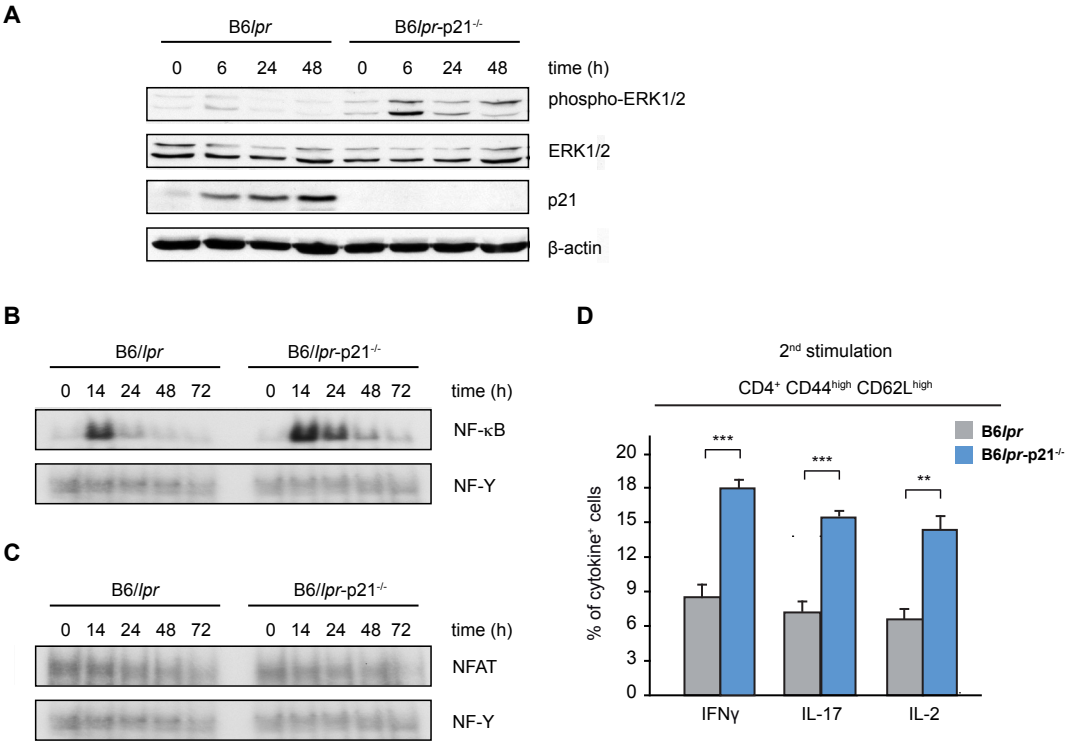

Figure 4.23. p21 controls T cell activation pathways in B6/*lpr*-p21$^{-/-}$ effector/memory T cells *in vitro*. **A.** Western blot analysis of ERK1/2 phosphorylation kinetics in B6/*lpr* and B6/*lpr*-p21$^{-/-}$ effector/memory T cells at indicated times after secondary ConA stimulation (1.5 µg/ml). A representative experiment is shown (*n* = 2). **B.** NF-κB activation levels in B6/*lpr*-p21$^{-/-}$ effector/memory T cells after secondary stimulation as detected by EMSA. A representative experiment is shown (*n* = 2). **C.** NFAT activation levels in B6/*lpr*-p21$^{-/-}$ effector/memory T cells after secondary stimulation, as detected by EMSA. A representative experiment is shown (*n* = 2). **D**. Percentage of CD44^{high}CD62L^{high} T cells positive for intracellular staining of IFNγ (left), IL-17 (middle) and IL-2 (right) at 4 h after secondary stimulation with PMA (40 ng/ml) and ionomycin (1 µg/ml) at 1 x 10^6 cells/ml (*n* = 3; *p* values are indicated: ** = < 0.01; *** = < 0.001).

4.3.4 Lack of p21 leads to hyperproliferation of B6/*lpr* CD4$^+$ memory-like T cells *in vitro*

To determine whether the T cell hyperactivation in the absence of p21 had any effect on other B6/*lpr* CD4$^+$ T cell responses, we monitored proliferation after primary and secondary stimulation *in vitro*. At 24 h after the first TCR challenge, cell cycle analysis showed comparable proliferation and apoptosis levels (*Fig. 4.24A*). No significant proliferative differences between naïve B6/*lpr* and B6/*lpr*-p21$^{-/-}$ T cells were detected by [^{3}H] thymidine incorporation (B6/*lpr*, 4309 *vs.* B6/*lpr*-p21$^{-/-}$, 3903 cpm; *p* = 0.16) (*Fig. 4.24B*).

After 6 days of IL-2 expansion, T cells were restimulated with ConA to study the proliferative capacity of B6/*lpr*-p21$^{-/-}$ in comparison to B6/*lpr* effector/memory T cells *in vitro*. As B6/*lpr* mice lack Fas, AICD is not found in B6/*lpr* T cells and low apoptosis levels were anticipated during secondary

stimulation. Use of the apoptosis inhibitor zVAD was thus not necessary during restimulation of effector/memory T cells. Comparison of cell cycle profiles at 24 h post-secondary stimulation showed higher proliferation rates for B6/*lpr*-p21$^{-/-}$ effector/memory than for B6/*lpr* T cells. Apoptosis levels were similar in both cell types, although higher than predicted (*Fig. 4.24C*). A [^{3}H] thymidine incorporation assay demonstrated 2.5-fold higher proliferation rates for B6/*lpr* effector/memory T cells (B6/*lpr*, 4142 *vs.* B6/*lpr*-p21$^{-/-}$, 10243 cpm; $p = 0.006$) at 48 h after a secondary TCR challenge (*Fig. 4.24D*). CFSE dilution assay confirmed increased cell division of B6/*lpr*-p21$^{-/-}$ effector/memory T cells compared to B6/*lpr* effector/memory T cells in the course of secondary stimulation (*Fig.4.24E*). The results obtained with B6/*lpr* lymphocytes validate previous experiments with B6 T cells showing that lack of p21 increases hyperproliferation of memory-like T cells *in vitro.*

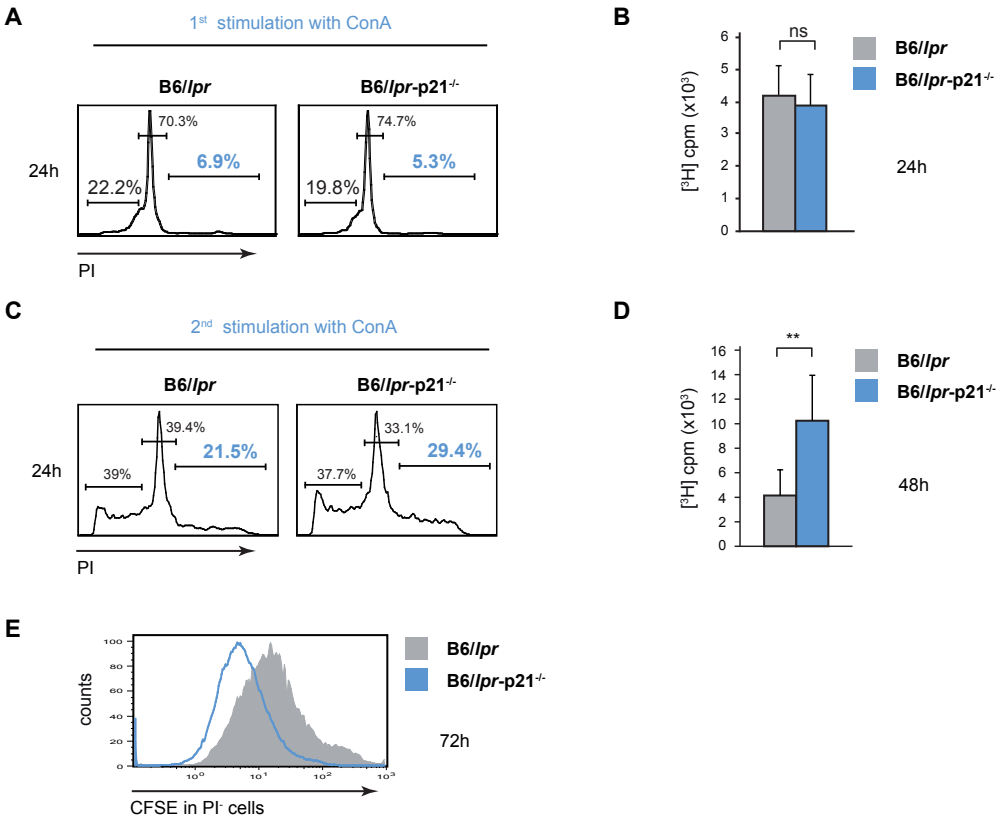

Figure 4.24. Lack of p21 leads to hyperproliferation of B6/*lpr* CD4$^+$ effector/memory T cells, but not naïve CD4$^+$ T cells *in vitro*. A. Cell cycle analysis of naïve B6/*lpr* and B6/*lpr*-p21$^{-/-}$T cells at 24 h after primary ConA stimulation. Representative histograms are shown ($n = 4$). **B.** [^{3}H] thymidine incorporation in B6/*lpr* and B6/*lpr*-p21$^{-/-}$ T cells at 24 h after primary TCR challenge ($p = 0.16$). Values show mean ± SD ($n = 4$). **C.** Cell cycle analysis of B6/*lpr* and B6/*lpr*-p21$^{-/-}$ effector/memory T cells at 24 h post-secondary stimulation. Representative data are shown ($n = 4$). **D.** [^{3}H] thymidine uptake in B6/*lpr* and B6/*lpr*-p21$^{-/-}$ effector/memory T cells at 24 h after secondary ConA stimulation ($p = 0.006$). Values show mean ± SD (n=4). **E.** CFSE dilution rate of PI$^-$ B6/*lpr* and B6/*lpr*-p21$^{-/-}$ effector/memory T cells at 72 h after secondary ConA stimulation. Representative histograms are shown ($n = 2$).

Finally, we compared the proliferative capacity of B6, p21$^{-/-}$, B6/*lpr* and B6/*lpr*-p21$^{-/-}$ effector/memory T cells after a secondary TCR challenge. A [^{3}H] thymidine incorporation assay verified higher proliferation rates for p21$^{-/-}$ and B6/*lpr*-p21$^{-/-}$ T cells compared to the respective controls (B6 or B6/*lpr*), as observed in previous experiments (B6 *vs*. p21$^{-/-}$, $p = 0.039$; B6/*lpr vs*. B6/*lpr*-p21$^{-/-}$, $p = 0.015$). Lack of Fas led to high proliferation levels for B6/*lpr* and B6/*lpr*-p21$^{-/-}$ T cells compared to B6 and p21$^{-/-}$ T cells (*Fig. 4.25A*). This finding was confirmed by a CFSE dilution assay; B6/*lpr*-p21$^{-/-}$ T cells showed more cell divisions than p21$^{-/-}$ and B6/*lpr* T cells, while B6 control cells had the lowest proliferation rate (*Fig.4.25B*). These data point to an additive effect of Fas and p21 in the control of effector/memory T cell proliferation in response to secondary TCR challenge *in vitro*.

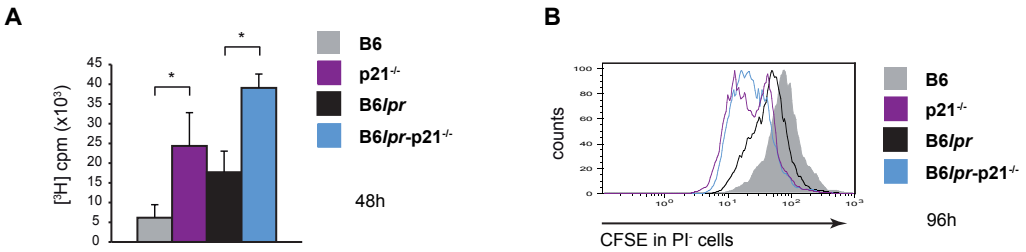

Figure 4.25. FAS and p21 synergy in the control of memory-phenotype T cell proliferation. A. Hyperproliferation of B6/*lpr*-p21$^{-/-}$ and p21$^{-/-}$ effector/memory T cells compared to their respective control T cells (B6/*lpr* and B6) at 48 h after secondary ConA stimulation was detected by [^{3}H] thymidine uptake (B6 *vs*. p21$^{-/-}$, $p = 0.039$; B6/*lpr vs*. B6/*lpr*-p21$^{-/-}$, $p = 0.015$). Values show mean ± SD ($n = 2$). **B.** Dilution rate of CFSE-labeled PI$^-$ B6, p21$^{-/-}$, B6/*lpr* and B6/*lpr*-p21$^{-/-}$ effector/memory T cells at 96 h after restimulation with ConA. Representative data are shown ($n = 2$).

4.3.5 Hyperactivated B6/*lpr*-p21$^{-/-}$ memory-phenotype T cells produce large amounts of pro-inflammatory cytokines *in vivo*

NF-κB is crucial for appropriate T cell activation and pro-inflammatory cytokine production[37]. As we previously observed NF-κB hyperactivation of B6/*lpr*-p21$^{-/-}$ effector/memory T cells, we analyzed the activation state of memory T cell populations and the corresponding cytokine production *in vivo*. To evaluate cytokine production by different lymphocyte populations in 1-month-old B6/*lpr* and B6/*lpr*-p21$^{-/-}$ mice, we stimulated cells from secondary lymphoid organs (spleen or lymph nodes) *ex vivo* for 4 h with PMA and ionomycin, before intracellular staining for flow cytometry analysis (*see 3.4.2*). In accordance with previous results, we observed higher production of IFNγ in total CD4$^+$ T cells from B6/*lpr*-p21$^{-/-}$ mice compared to B6/*lpr* mice (*Fig. 4.26A*, left). Both CD4$^+$CD44^{high}CD62L^{high} and CD4$^+$CD44^{high}CD62L^{low} memory T cell populations from B6/*lpr*-p21$^{-/-}$ mice showed high IFNγ production (*Fig. 4.26A*, middle and right). In contrast, we detected no significant differences in production of IL-17 (*Fig.4.26B*) and IL-2 (data not shown).

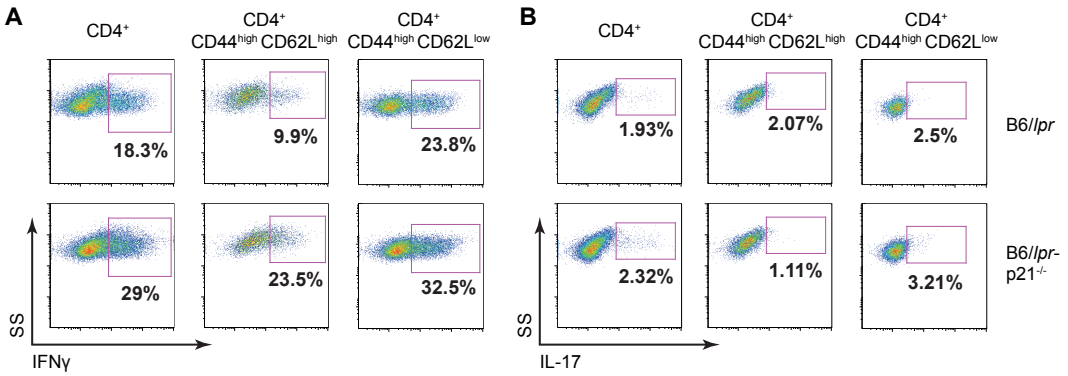

Figure 4.26. Hyperactivated B6/*lpr*-p21$^{-/-}$ memory T cells produce large amounts of pro-inflammatory cytokines. A,B. Intracellular levels of IFNγ (**A**) and IL-17 (**B**) in splenocyte CD4^{+} and memory T cell populations from 1-month-old female B6/*lpr* and B6/*lpr*-p21$^{-/-}$ mice. *Ex vivo* stimulation was performed with PMA (50 ng/ml) and ionomycin (2 μg/ml) at a concentration of 5 x 10^{6} cells/ml. A representative experiment is shown (*n* = 2).

As Fas-deficient mice are reported to develop autoimmune disease with age, we monitored aging B6/*lpr* and B6/*lpr*-p21$^{-/-}$ mice over time to analyze characteristic autoimmune parameters such as pro-flammatory cytokine production. *Ex vivo* stimulation of splenocytes isolated from 8-month-old females showed higher IL-17 levels in total CD4^{+} and memory cell populations from B6/*lpr*-p21$^{-/-}$ mice (*Fig. 4.27A*). In addition, we found a marked IL-2 increase in serum from these mice (*Fig. 4.27B*). Finally, we tested for IFNγ, a cytokine with an important role in autoimmune disease development[140], and observed nearly three-fold higher IFNγ levels in CD4^{+} and memory T cells from B6/*lpr*-p21$^{-/-}$ compared to B6/*lpr* mice (*Fig.4.27C*). Serum analysis confirmed high IFNγ levels in 6-month-old B6/*lpr*-p21$^{-/-}$ mice (*Fig.4.27D*).

We found that pro-inflammatory cytokines are produced at elevated levels in B6/*lpr*-p21$^{-/-}$ compared to B6/*lpr* T cells; this might be a reason for the severe phenotype and increased mortality observed in B6/*lpr*-p21$^{-/-}$ mice. We conclude that lack of p21 increases *in vivo* production of IFNγ, a cytokine closely linked to lupus development[55].

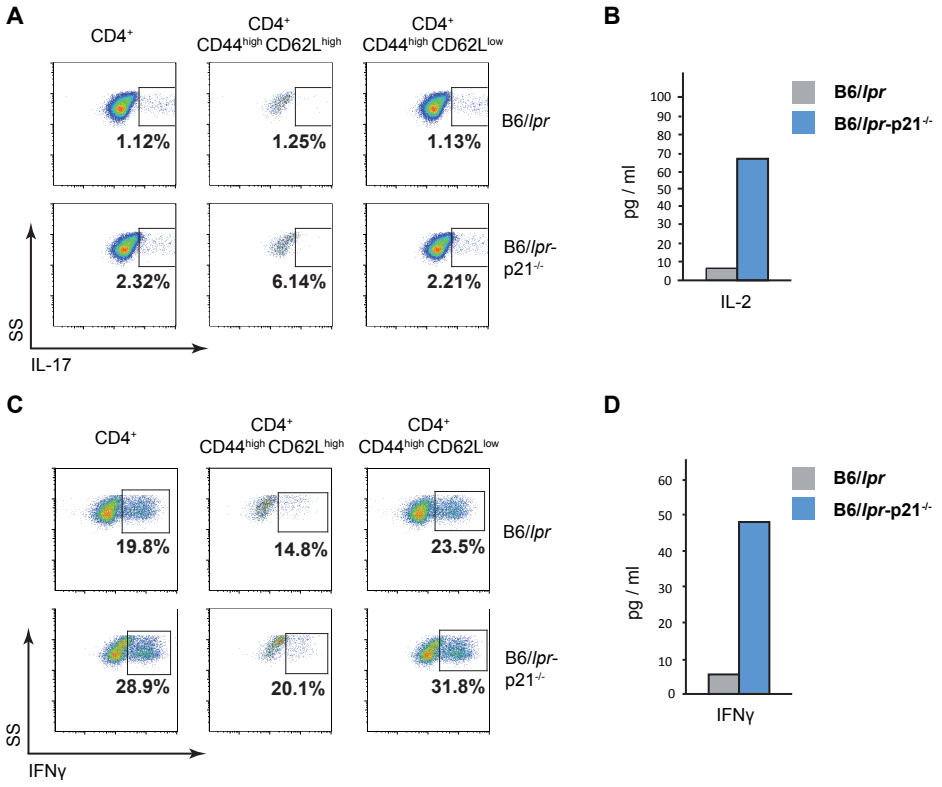

Figure 4.27. Elevated levels of pro-inflammatory cytokines produced by CD4⁺ memory T cells from aging B6/*lpr*-p21$^{-/-}$ mice. A, C. Intracellular levels of IL-17 (**A**) and IFNγ (**C**) in splenocyte CD4⁺ and memory T cell populations from 8-month-old female B6/*lpr* and B6/*lpr*-p21$^{-/-}$ mice. *Ex vivo* stimulation was performed with PMA (50 ng/ml) and ionomycin (2 µg/ml) at a concentration of 5 x 10^6 cells/ml. A representative experiment is shown (n = 2). **B,D.** IL-2 (**B**) and IFNγ (**D**) levels in serum from 4 mice/strain (pool) were quantified by Luminex.

4.4 p21 overexpression reduces T cell activation and autoimmunity development

Here we analyzed different p21-deficient mouse strains (B6, OT-II, pcc.TCRtg and B6/*lpr*) and found that $CD4^+$ T cells, and especially effector/memory T cells, are hyperactivated in these mice. This hyperactivation state is translated into hyperproliferation of restimulated memory T cells *in vitro* and increased pro-inflammatory cytokine production.

To confirm the role of p21 in the T cell alterations described above, we reversed the $p21^{-/-}$ effects seen before by generating p21-overexpressing mice on the B6 and B6/*lpr* backgrounds (B6-p21tg and B6/*lpr*-p21tg). These mice feature a human p21 transgene expressed constitutively under the T cell-specific Lck promotor[106], which allows analysis of T cell-directed p21 overexpression and its impact on autoimmune manifestations. p21-transgenic mice show normal development and T cell differentiation processes[106], and thus represent an excellent model to study the role of hyperactivation and hyperproliferation of $CD4^+$ T cells in autoimmune disease development.

4.4.1 T cell-specific p21 overexpression reduces IFNγ production in B6/*lpr* but not in B6 effector/memory T cells

Increased levels of pro-inflammatory cytokines are associated with autoimmune disease development[141]. In previous experiments, we found elevated lupus-linked IFNγ, IL17 and IL-2 in the absence of p21 (*Fig. 4.26, 4.27*). As several studies suggest a crucial role for IFNγ in autoimmune disease development in lupus models[61,140,141], we measured IFNγ production in B6 and B6-p21tg as well as B6/*lpr* and B6/*lpr*-p21tg $CD4^+$ effector and memory T cells. We found higher IFNγ levels in $CD4^+CD44^{high}CD62L^{high}$ and $CD4^+CD44^{high}CD62L^{low}$ T cells of Fas-deficient B6/*lpr* mice compared to B6 controls (*Fig. 4.28A,B*; left). IFNγ production was greatly reduced in B6/*lpr*-p21tg T cells (*Fig. 4.28A,B*; bottom), whereas p21 overexpression did not alter IFNγ levels in B6-p21tg T cells (*Fig. 4.28A,B*; top). There were no significant differences in IL-17 and Il-2 cytokine expression in B6-p21tg and B6/*lpr*-p21tg mice (data not shown).

Autoimmune disease in B6/*lpr* mice is thought to originate from accumulation of $CD4CD8^-TCR\beta^+$ (DN) and $CD4^+$ memory T cells[72,77]. In the presence of the p21 transgene in B6/*lpr* mice, both DN and memory T cell populations were substantially reduced (data not shown). Together with lower IFNγ expression, this reduction led to decreased lymphadenopathy and ameliorated autoimmune manifestations in B6/*lpr*-p21tg mice.

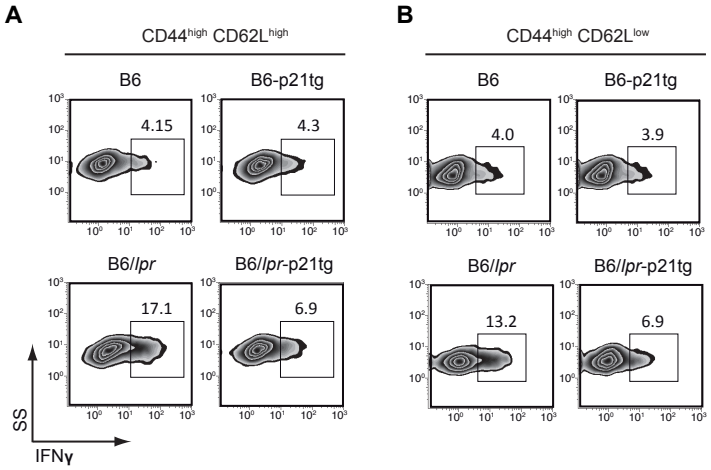

Figure 4.28. T cell-specific p21 overexpression reduces IFNγ production in B6/*lpr* but not in B6 memory T cells. Intracellular levels of IFNγ in lymph node $CD4^+CD44^{high}CD62L^{high}$ (**A**) and $CD4^+CD44^{high}CD62L^{low}$ (**B**) memory T cell populations from 4-month-old B6, B6-p21tg, B6/*lpr* and B6/*lpr*-p21tg mice, as determined by flow cytometry. *Ex vivo* stimulation was performed with PMA (50 ng/ml) and ionomycin (2 µg/ml) at a concentration of 5 x 10^6 cells/ml. A representative experiment is shown (*n* = 2; 4 mice/strain).

4.4.2 Hyperactivation of $CD4^+$ effector/memory T cells is reduced by p21 overexpression in B6/*lpr*-p21tg mice

As T cells were shown to be hyperactivated in the absence of p21 (*Fig. 4.5*), we analyzed the activation of various $CD4^+$ effector/memory T cell populations in p21-overexpressing mice using CD69 as a cell surface activation marker[143]. We observed a >4-fold higher activation level in $CD4^+CD44^{high}CD62L^{high}$ T cells from B6/*lpr* mice compared to B6 controls (*Fig. 4.29A*, left). p21 transgene expression had no effect on B6 effector T cell activation (*Fig. 4.29A*, top panels), but clearly reduced $CD4^+CD44^{high}CD62L^{high}$ T cell activation in B6/*lpr* mice (*Fig. 4.29A*, bottom panels).

Activation of $CD4^+CD44^{high}CD62L^{low}$ memory T cells was only slightly increased in Fas-deficient mice compared to B6 controls (*Fig. 4.29B*, left panels). p21 overexpression had no effect on the high activation levels of memory B6 T cells (*Fig. 4.29B*, top panels), and activation levels of B6/*lpr* memory T cells also remained unaffected (*Fig. 4.29B*, bottom panels).

Exogenous p21 expression had no effect on the activation of B6 effector/memory T cells (*Fig. 4.29A,B*; top panels), but efficiently reduced activation of B6/*lpr* $CD44^{high}CD62L^{high}$ effector T cells (*Fig. 4.29A*, bottom panels), indicating a specific role for p21 in the regulation of hyperactivated T cells.

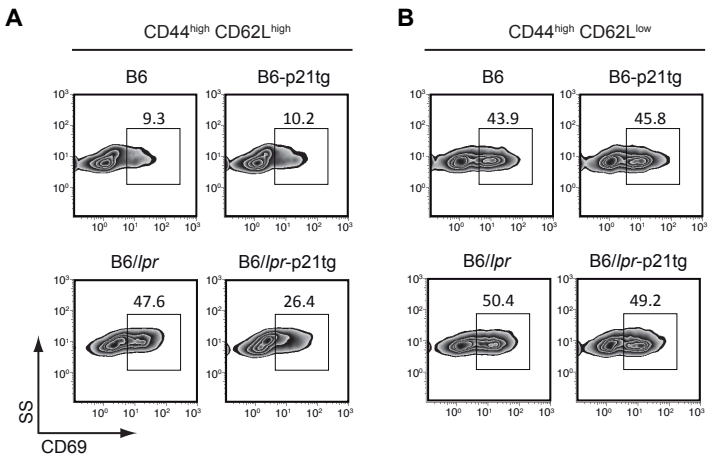

Figure 4.29. Activation of CD4⁺ effector/memory T cells is reduced by p21 overexpression in B6/*lpr*-p21tg mice. Surface expression of CD69 on lymph node $CD4^+CD44^{high}CD62L^{high}$ (**A**) and $CD4^+CD44^{high}CD62L^{low}$ (**B**) memory T cell populations from 4-month-old B6, B6-p21tg, B6/*lpr* and B6/*lpr*-p21tg mice, as determined by flow cytometry. A representative experiment is shown (*n* = 2; 4 mice/strain).

4.4.3 p21 overexpression reduces B6/*lpr* T cell proliferation after repeated *in vitro* stimulation

We previously showed the relevance of p21 in the control of T cell expansion after a secondary TCR stimulation. To analyze the effect of p21 overexpression on T cell proliferation, we subjected freshly isolated B6 and B6-p21tg $CD4^+$ T cells to our optimized repeated stimulation system *in vitro* (*Fig. 4.4A*). We observed similar percentages of proliferation and apoptosis after ConA stimulation of naïve B6 and B6-p21tg $CD4^+$ T cells (*Fig. 4.30A*), and [^{3}H] thymidine uptake was comparable between both cell types (B6, 1352 *vs.* B6-p21tg, 1240 cpm; $p = 0.652$) (*Fig. 4.30B*). In response to a secondary TCR challenge, however, B6 and B6-p21tg effector/memory T cells showed comparable proliferation levels, as indicated by cell cycle analysis (*Fig. 4.30C*). Apoptosis levels remained unaffected by p21 overexpression (*Fig. 4.31C*). A [^{3}H] thymidine incorporation assay revealed slightly decreased proliferation rates in restimulated B6-p21tg effector/memory T cells (B6, 8508 *vs.* B6p21tg, 16066 cpm, $p = 0.03$) (*Fig. 4.30D*). We detected no major difference difference in the expansion of B6 and B6-p21tg effector/memory T cells, which indicates that overexpressed p21 had little effect on T cell proliferation.

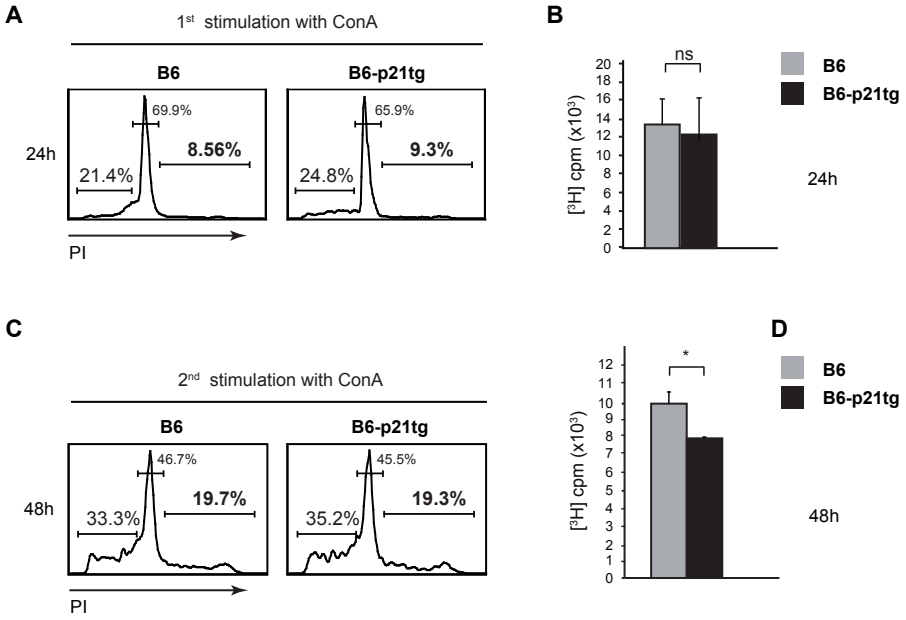

Figure 4.30. p21 overexpression does not affect effector/memory B6 T cell proliferation. A. Cell cycle analysis of B6 and B6-p21tg T cells at 24 h after primary ConA stimulation. Representative histograms are shown (*n* = 2). **B.** [^{3}H] thymidine uptake in B6 and B6-p21tg T cells at 24 h after primary TCR challenge with ConA. Values show mean ± SD (*n* = 2; *p* = 0.652). **C.** Cell cycle profiles of B6 and B6-p21tg effector/memory T cells at 48 h after secondary stimulation in the presence of zVAD (12.5 μM). Representative histograms are shown (*n* = 2). **D.** [^{3}H] thymidine uptake by B6-p21tg effector/memory T cells at 48 h after secondary TCR challenge in the presence of zVAD (12.5 μM). Values show mean ± SD (*n* = 2; *p* = 0.03).

CD4$^+$ T cells hyperproliferate in B6/*lpr* mice, a phenomenon implicated in development of autoimmune disease[55,144]; we thus examined the effect of T cell-specific p21 overexpression on B6/*lpr* T cell proliferation. Cell cycle profiles of restimulated CD4$^+$ T cells revealed a decreased percentage of proliferation of B6/*lpr*-p21tg compared to B6/*lpr* T cells (*Fig. 4.31A*). This observation was confirmed by a [^{3}H] thymidine incorporation assay, which showed a significant reduction in T cell expansion in B6/*lpr*-p21tg compared to B6/*lpr* effector/memory T cells (B6/*lpr*, 26346 *vs.* B6/*lpr*-p21tg, 15448 cpm; *p* = 0.0003) (*Fig. 4.31B*). Specific TCR stimulation with anti-CD3/CD28 antibodies led to similar results (data not shown).

To analyze activation levels of B6/*lpr* and B6/*lpr*-p21tg CD4$^+$ memory T cells following secondary TCR challenge *in vitro*, we used Western blot to monitor ERK1/2 phosphorylation over time. We observed less phospho-ERK1/2 in B6/*lpr*-p21tg T cells up to 1 h post-stimulation compared to control counterparts, with maintained ERK1/2 hyperphosphorylation after 2 h (*Fig. 4.32C*). We also detected a reduction in p21 transgene expression after secondary stimulation (*Fig. 4.32C*). High p21 expression levels at the beginning of secondary TCR challenge could explain the lower proliferative response during secondary stimulation. We found that p21 overexpression regulated

hyperactivation and resulting hyperproliferation of B6/*lpr*-p21tg effector/memory T cells *in vitro*, whereas no significant effects were observed in B6-p21tg effector/memory T cells.

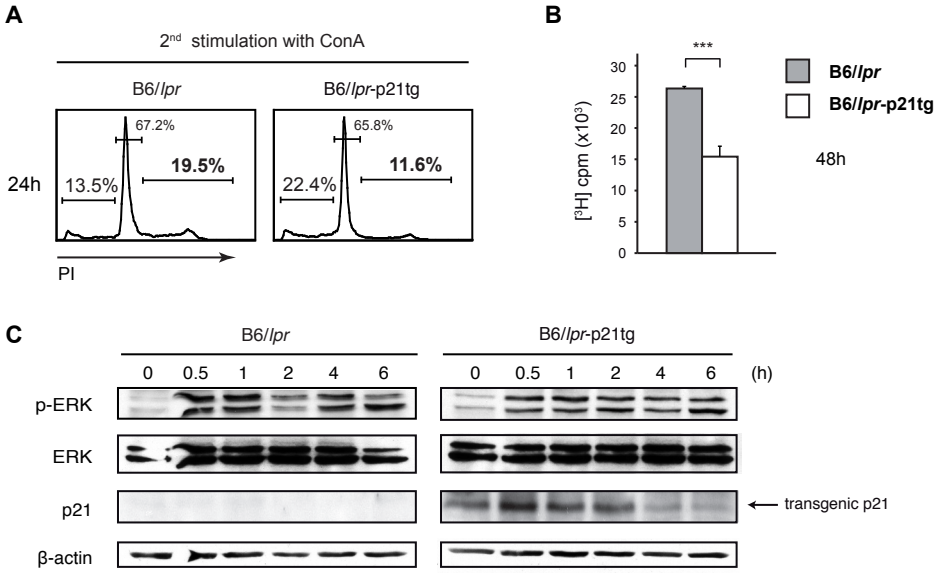

Figure 4.31. B6/*lpr* T cell activation and proliferation is reduced by p21 overexpression. A. Cell cycle analysis of B6/*lpr* and B6/*lpr*-p21tg effector/memory T cells at 24 h after secondary ConA stimulation. Representative histograms are shown (n = 2). **B.** [^{3}H] thymidine uptake of B6/*lpr* and B6/*lpr*-p21tg effector/memory T cells at 48 h after secondary TCR challenge with ConA. Values show mean ± SD (n = 2; p = 0.0003). **C.** Western blot shows variations in ERK1/2 phosphorylation in B6/lpr-p21tg effector/memory T cells in response to secondary ConA stimulation (n = 3).

4.4.4 Exogenous p21 expression controls CDK2 and NF-κB activation in B6/*lpr* memory-phenotype T cells

As we found that p21 overexpression reduced T cell hyperactivation and hyperproliferation *in vitro* and *in vivo*, and thus has an important regulatory role in B6/*lpr*-p21tg effector/memory T cells, we examined CDK2 activity in B6/*lpr* and B6/*lpr*-p21tg memory-phenotype T cells. At 24 h after restimulation, CDK2 activity was clearly reduced in B6/*lpr*-p21tg effector/memory T cells (*Fig. 4.32A*). This fact could explain the decrease in effector/memory T cell proliferation in the presence of overexpressed p21, as p21 is able to induce cell cycle arrest in a CDK2-dependent manner.

In previous experiments, we identified NF-κB as an effector molecule responsible for hyperactivation of B6/*lpr*-p21$^{-/-}$ effector/memory T cells (*Fig. 4.23B*). We thus tested NF-κB activation levels in B6/*lpr* and B6/*lpr*-p21tg effector/memory T cells in response to a secondary TCR challenge, to evaluate the effect of p21 overexpression on NF-κB activation. EMSA showed lower NF-κB activity in B6/*lpr*-p21tg effector/memory T cells at 4 h and 24 h post-restimulation

(*Fig. 4.32B*). The data indicated that exogenous p21 is able to control B6/*lpr* effector/memory T cell activation and proliferation via both CDK2 and NF-κB.

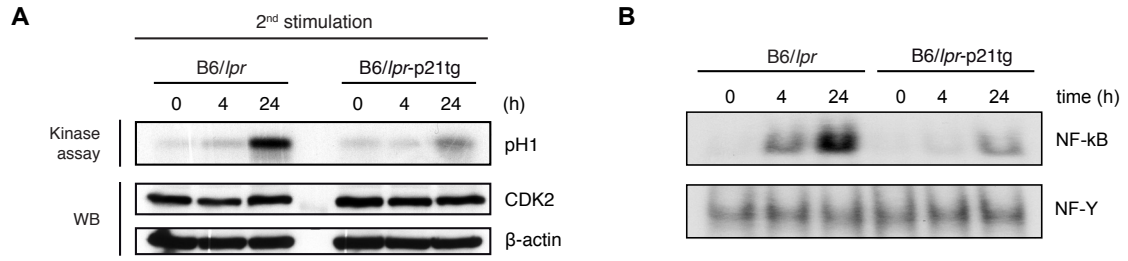

Figure 4.32. p21 overexpression inhibits both CDK2 and NF-κB activity in B6/*lpr* effector/memory T cells. A. CDK2 activity levels in B6/*lpr* and B6/*lpr*-p21tg effector/memory T cells at indicated times after secondary ConA stimulation, as determined by a CDK2-specific kinase assay. A representative experiment is shown (*n* = 2). **B.** NF-κB activation levels in B6/*lpr* and B6/*lpr*-p21tg effector/memory T cells after secondary stimulation as detected by EMSA. A representative experiment is shown (*n* = 2).

4.4.5 p21 overexpression reduces pro-inflammatory cytokine production of B6/*lpr* memory-phenotype T cells *in vitro*

In accordance with our finding that p21 overexpression reduced hyperactivation of B6/lpr effector/memory T cells *in vitro*, we detected notably decreased IFNγ production in response to secondary stimulation (*Fig. 4.33A*). To confirm that the reduction observed was due to p21 overexpression in B6/*lpr* T cells, we induced IFNγ production directly by secondary stimulation with IL-12 and IL-18. Together, IL-12 and IL-18 trigger IFNγ production in a TCR-independent manner[145,146], and in our system strongly induced IFNγ expression in B6/*lpr* effector/memory T cells (*Fig. 4.33B*, left). In B6/*lpr*-p21tg effector/memory T cells, IFNγ production was markedly reduced (*Fig. 4.33B*, right), which confirmed our hypothesis that p21 overexpression negatively controls IFNγ induction in effector/memory T cells.

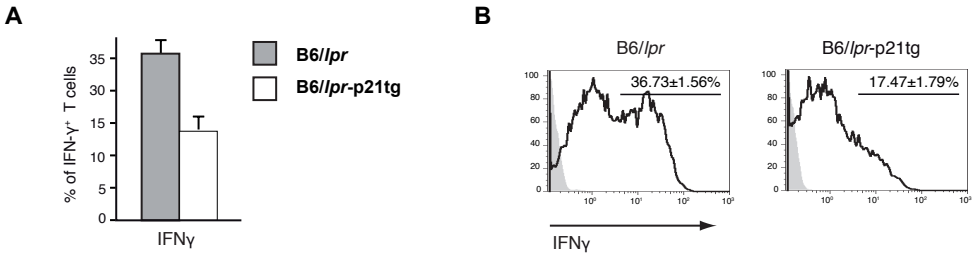

Figure 4.33. Enhanced p21 expression dampens IFNγ induction by IL-12 and IL-18. A. Percentages of IFNγ-producing B6/*lpr* and B6/*lpr*-p21tg effector/memory T cells at 24 h after secondary stimulation with (**A**) PMA and ionomycin or (**B**) IL-12 and IL-18 (10 µg/ml). Values show mean ± SD (**A:** n = 4 T cell preparations from distinct mice; $p < 10^{-2}$; **B:** n = 3, p = 0.0013).

p21 overexpression considerably reduced B6/*lpr* effector/memory T cell activation and pro-inflammatory cytokine production, pointing to an autoimmune-suppressing function of p21. Indeed, exogenous p21 expression ameliorated lupus development and notably reduced death rates (data not shown). p21 could possibly have a role in therapeutic approaches for autoimmune diseases.

5. DISCUSSION

5. DISCUSSION

5.1 p21 is involved in effector/memory T cell activation

A delicate balance between T cell activation, proliferation and death is responsible for establishing and maintaining T cell tolerance, a crucial characteristic of the immune system. In a work previously published, we found that lack of p21 leads to hyperactivation, and in consequence to hyperproliferation of effector/memory T cells and development of mild lupus-like disease[56]. The way how p21 influences T cell activation nonetheless remained elusive, as massive hyperproliferation of effector/memory T cells was not detectable in $p21^{-/-}$ mice *in vivo*. Here we used diverse experimental approaches to confirm a possible role of p21 in effector/memory T cell activation and to gain further insight into the regulatory function of p21 in this process.

5.1.1 Subcellular localization of p21 is crucial for differential regulation of T cell activation

The most prominent role of p21 is its well-known function as a cell cycle inhibitor in response to extracellular signals. Following DNA damage, p21 is translocated into the nucleus, where it suppresses CDK2 activity and thus blocks cell cycle progression[97]. After successful DNA repair, p21 is degraded and the cell cycle proceeds to S phase[147,148]. Depending on its subcellular localization, however, endogenous p21 exerts distinct functions within eucaryotic cells.

In the present study, we observed very low levels of nuclear p21 in effector/memory T cells in response to activation (*Fig. 4.9A*). This finding supports our hypothesis that p21 has a function in effector/memory T cells other than cell cycle regulation, as direct p21-CDK2 interaction would require nuclear presence of p21.

We also observed increasing p21 levels in cytoplasm after TCR stimulation (*Fig. 4.9*). The cytoplasmic location enables p21 interaction with various molecules involved in T cell activation pathways. TCR-specific and intracellular stimulation with the DAG analog PMA resulted in similar T cell responses (*Fig. 4.8*), excluding the possibility that p21 regulates early steps in T cell activation. PMA directly stimulates PKCθ, bypassing TCR proximal events; p21 might therefore act on PKCθ or in downstream pathways that lead to T cell activation.

5.1.2 Regulation of effector/memory T cell activation by p21 is not dependent on CDK2

Following TCR stimulation, a highly conserved regulatory apparatus coordinates cell cycle progression and links extracellular signals to cellular responses, inducing a complex series of events that leads to cell division. The G1-S phase transition is initiated by the assembly of cyclinD-CDK4/6 complexes and subsequent activation of cyclinE/A-CDK2, considered a key step for induction of DNA synthesis[149,150]. Cyclin/CDK complexes phosphorylate pRb molecules and trigger E2F2-mediated transcription of genes that promote cell cycle progression (*Fig. 1.6*). In its role as a cell cycle inhibitor, p21 regulates cyclinE/CDK2 complex activity and is able to induce cell cycle arrest at this point[85,88]. In agreement, we observed dysregulated CDK2 activity in naïve T cells that lacked p21; CDK2 was hyperactivated at 72 h due to the absence of p21 in $CD4^+$ T cells (*Fig. 4.1B*). In WT T cells, p21 expression was evident at 48 h after primary stimulation (*Fig. 4.1A*) and its presence efficiently controlled CDK2 activity (*Fig. 4.1B*). This observation suggests that p21 is a negative regulator of CDK2 activity following activation of naïve T cells. We nonetheless observed no growth alteration in p21-deficient naïve T cells up to 48 h post-TCR stimulation (*Fig. 4.3*). Longer exposure to stimulants leads to some hyperproliferation of $p21^{-/-}$ T cells[56], which could be associated to altered CDK2 activity or be driven by re-encounter with the same antigen. In this study, we provide evidence that activation of naïve and effector/memory T cells are differentially regulated, although controlling elements other than CDK2 remain to be identified.

Although p21 regulates proliferation in fibroblasts in a CDK2-independent manner[151], in $CD4^+$ effector/memory T cells, the scenario for cell cycle regulation appeared to be different. p21 expression was observed shortly after secondary TCR challenge (*Fig. 4.4B*), but CDK2 activity was not influenced by lack of p21 (*Fig. 4.7A,B*). This finding coincides with the observation of low p21 levels in the nucleus of effector/memory T cells, suggesting minor importance of the p21-CDK2 interaction for T cell activation in these cells. Significant hyperproliferation of $p21^{-/-}$ effector/memory T cells was nevertheless observed after TCR stimulation (*Fig. 4.6*), which implied CDK2-independent control of memory T cell expansion by p21. This observation is supported by other studies showing that CDK2 is not essential for cell cycle inhibition[152,153]. To confirm this finding, we treated naïve and effector/memory T cells with the CDK2-specific inhibitor CVT-313[124,125]. Proliferation of naïve T cells was greatly reduced (*Fig. 4.7E*), whereas the inhibitory effect of CVT-313 was less pronounced in effector/memory T cells (*Fig. 4.7D*).

p21-mediated inhibition of CDK2 activity is thus not an essential mechanism in activation control of specific cell types such as $CD4^+$ effector/memory T cells, and other regulatory mechanisms are likely to influence T cell activation and proliferation.

5.1.3 p21 negatively regulates activation of memory-like T cells after repeated stimulation

Interaction of the TCR with its antigen initiates a variety of signaling cascades, resulting in T cell activation and subsequent realization of its effector functions. After primary stimulation of naïve $CD4^+$ T cells, we observed comparable expression of CD69/CD25 activation markers (*Fig. 4.2A*), and intracellular activation indicators such as ERK1/2 phosphorylation did not show substantial differences in the absence of p21 (*Fig. 4.2B*). In accordance with this finding, we detected similar proliferation levels of naïve B6 and $p21^{-/-}$ $CD4^+$ T cells in response to ConA stimulation (*Fig. 4.3*). These results indicate that late p21 expression does not influence activation and subsequent proliferation of naïve $CD4^+$ T cells after primary TCR challenge.

More detailed analysis of $CD4^+$ T cells in $p21^{-/-}$ mice showed an elevated proportion of $CD4^+CD69^+$ memory T cells (*Fig. 4.5A*). The ERK1/2 phosphorylation pattern also appeared to be altered in the absence of p21, with a prolonged hyperphosphorylated state in $p21^{-/-}$ effector/memory T cells (*Fig. 4.5B*). ERK1/2 downstream effector molecules such as the transcription factor AP-1 reflected the hyperactivation of p21-deficient effector/memory T cells (*Fig. 4.5C*), which led to increased production of the pro-inflammatory cytokines IL-17, IL-2 (*Fig. 4.5D*) and IFNγ *in vitro* (*Fig. 4.5E*, top). High IFNγ levels were also detected in effector/memory T cells of 1-year-old $p21^{-/-}$ mice *in vivo* (*Fig. 4.5E*, bottom), which supports the physiological significance of this finding. The hyperactive state of p21-deficient effector/memory T cells was translated to extended proliferation of $p21^{-/-}$ effector/memory cells (*Fig. 4.6, 4.15B-D* and *4.18D,E*), and an increased proportion of $CD4^+CD44^{high}CD62L^{low}$ $p21^{/}$ T cells *in vitro* (*Fig. 4.15F*) compared to B6 effector/memory T cells in response to secondary antigen encounter.

To show that these results are not a peculiarity of the ConA system, we used a specific antigen for repeated *in vitro* stimulation. In this biologically relevant approach, we exposed T cells that presented a transgenic TCR to OVA-loaded dendritic cells (DC) (*see 3.2.6*). We found similar activation of OT-II and $p21^{-/-}$ OT-II cells after primary stimulation (*Fig. 4.14*); however, $p21^{-/-}$ OT-II effector/memory T cells were hyperactivated and proliferated at higher rates than their control counterparts in response to secondary TCR stimulation (*Fig. 4.15, 4.16*). *In vivo* challenge of adoptively transferred $CD4^+$ T cells with OVA-presenting DC and subsequent restimulation *ex vivo* led to similar results (*Fig. 4.17; see 3.3*). These data confirmed our hypothesis that p21 acts as a regulator of effector/memory T cell activation.

5.2 p21 controls ERK1/2 and NF-κB signaling pathways in effector/memory T cells

The absence of p21 leads to hyperactivation and thus to hyperproliferation of effector/memory T cells in response to a second antigen encounter. To better understand the regulatory role of p21 in intracellular processes initiated by TCR stimulation, we analyzed two major signaling pathways crucial for T cell activation, ERK1/2 and NF-κB.

5.2.1 p21 limits late ERK activation in effector/memory T cells

Following TCR stimulation, early activation events lead to calcium influx and initiation of distinct pathways such as the MAPK cascade. In accordance with our observations indicating that p21 is not involved in TCR proximate events (*Fig. 4.8*), we detected no differences in Ca^{2+} mobilization after TCR engagement in the absence of p21 (*Fig. 4.10*). Within the MAPK cascade, however, both ERK1/2 and its downstream effector AP-1 appeared to be hyperactivated in p21-deficient effector/memory T cells compared to controls (*Fig. 4.5B,C*), leading to elevated pro-inflammatory cytokine production (*Fig. 4.5D*). To show that ERK1/2 hyperphosphorylation in the absence of p21 is also responsible for the hyperproliferation observed in $p21^{-/-}$ effector/memory T cells, we used an inhibitor that selectively interrupts MAPK cascade signal transduction and thus inhibits ERK1/2 phosphorylation[122]. Inhibition of ERK1/2 phosphorylation led to a significant reduction in $p21^{-/-}$ effector/memory T cell hyperproliferation (*Fig. 4.11B-D*), which confirmed an important role for p21 in the control of MAPK activation. The precise way in which p21 regulates ERK1/2 phosphorylation requires further study, although preliminary data from our lab indicate the involvement of Traf6 and the PI3K subunit p85 in this process.

Other systems show similar Ca^{2+} influx levels, although with elevated ERK1/2 phosphorylation; this is the case for $DGK\zeta^{-/-}$ or $DGK\alpha^{-/-}$ mice[154,155]. These mice develop normally, but show hyperresponsiveness to TCR stimulation. DGK (diacylglycerol kinase) terminate DAG signaling by catalyzing its phosphorylation and, in consequence, influence PKCθ activity; it would thus be of interest in future studies to investigate the possible relation of p21 with this pathway.

Treatment of B6 and $p21^{-/-}$ memory T cells with the ERK1/2 inhibitor excluded the possibility that T cell activation is CDK2-dependent (*Fig. 4.11E*), which supports the hypothesis that p21 controls T cell activation via ERK1/2 rather than via CDK2. We observed that auto-reactive effector/memory T cells ($p21^{-/-}$) were more susceptible than controls to inhibition of ERK1/2 phosphorylation by the inhibitor concentrations used here (*Fig. 4.11B-D*), indicating an important p21 function in MAPK activation following secondary T cell stimulation.

As ERK1/2 activation after TCR-dependent stimulation advances in two main phases[136], we analyzed whether early ERK1/2 phosphorylation is sufficient to induce hyperproliferation in p21-deficient memory T cells or if later hyperactivation is required. Proliferation was reduced significantly only in p21-deficient T cells (not in B6 controls), and inhibitor addition after 6 h was sufficient to limit hyperproliferation of $p21^{-/-}$ effector/memory T cells (*Fig. 4.12B,C*). p21 thus controls the proliferative response of effector/memory T cells via late ERK1/2 activation, and ERK1/2 hyperphosphorylation in the absence of p21 promotes extensive T cell proliferation after TCR restimulation.

5.2.2 p21 controls T cell activation via the NF-κB activation pathway

One of the pathways commonly used to detect T cell activation is the nuclear translocation of the transcription factor NF-κB in response to TCR stimulation. NF-κB triggers expression of pro-inflammatory cytokines such as IL-2 and IFNγ, as well as transcription of crucial genes involved in T cell proliferation and survival. A previous study from our laboratory showed that p21 regulates NF-κB activation in macrophages[111].

In the absence of p21, we observed substantial hyperactivation of NF-κB in response to secondary TCR challenge with ConA or OVA (*Fig. 4.13A-C, 4.16B*). As early as 1 h after restimulation of effector/memory T cells, we detected elevated NF-κB activity levels that reached maximum at 48 h post-stimulation. To determine whether NF-κB hyperactivation affected the $p21^{-/-}$ effector/memory T cell hyperproliferation, we treated memory-like T cells with $BAY_{11\text{-}7082}$, a specific inhibitor of NF-κB activation. Prevention of NF-κB activation led to a significant reduction in proliferation by restimulated p21-deficient T cells (*Fig. 4.13D*), confirming that elevated NF-κB activity is associated with hyperproliferation of effector/memory T cells in the absence of p21. This inhibitory effect was even stronger when we inhibited NF-κB at a later time after initiation of secondary T cell stimulation (*Fig. 4.13E*); thus, in addition to ERK phosphorylation, the hyperactive state and the subsequent hyperproliferation of p21-deficient effector/memory T cells depends critically on late NF-κB hyperactivation.

Both ERK1/2 and NF-κB have crucial physiological functions in the immune system[37]; it is thus not surprising that several studies related hyperactivation of ERK1/2 or NF-κB with pathological manifestations in human autoimmune diseases such as ALPS, SLE or RA[81,156]. These autoimmune diseases are also linked to excessive lymphoproliferation.

The observation that inhibitors of ERK1/2 and NF-κB activity specifically reduced p21-deficient effector/memory T cell hyperproliferation suggests that, in specific conditions, potentially auto-reactive T cells are more susceptible to inhibitor treatment. Several murine

models of human autoimmune diseases confirmed the therapeutic potential of these inhibitors. Decreased hyperactivation of the MAPK cascade by treatment with Ras inhibitor leads to reduced lymphadenopathy and lower anti-DNA antibody levels in MRL/*lpr* mice[157], and specific inhibition of NF-κB has an important anti-inflammatory effect in several arthritis models[158,159]. In addition to NF-κB, we found higher AP-1 activity p21$^{-/-}$ effector/memory T cells (*Fig. 4.5C*). This observation was anticipated, as AP-1 is a direct effector of phosphorylated ERK1/2, which showed high activity levels in the absence of p21 (*Fig. 4.5B*).

Although both AP-1 and NF-κB were overactivated in the absence of p21, this observation does not represent a general characteristic of effector/memory T cells. NFAT, another transcription factor essential for T cell activation, was not hyperactivated immediately after TCR stimulation (*Fig. 4.10B*), and its later hyperactivation might be due to feedback mechanisms induced by other pathways hyperactivated due to lack of p21.

The constitutive hyperactivation of both ERK1/2 and NF-κB pathways in p21$^{-/-}$ effector/memory T cells led not only to increased proliferation, but also to elevated production of pro-inflammatory cytokines such as IFNγ and IL-2 (*Fig. 4.5D,E*). High IFNγ expression was closely linked to development of lupus-like disease[140]. Our data suggest a protective function of p21 in autoimmune disease development, as it controls effector/memory T cell activation via the ERK1/2 and NF-κB pathways.

5.2.3 Model for the differential regulation of tolerance establishment and maintenance by p21 in naïve and memory-phenotype T cells

In this study, we define distinct roles for p21 in the immune response of T cells after repeated TCR stimulation. As observed here, p21 is expressed relatively late (more than 48 h) after TCR stimulation, and subsequently controls cell cycle progression by interacting with CDK2, a known and extensively studied p21 function (*Fig. 5.1A*).

In effector/memory T cells, we identified a previously unreported function for p21 as an activation regulator. After TCR challenge, p21 is expressed within a few hours and controls effector/memory T cell activation by inhibiting main activation pathways. In contrast to its classical function, p21 limits effector/memory T cell activation in a CDK2-independent manner (*Fig. 5.1B*). In its role as a negative regulator of ERK1/2 and NF-κB activity, cytoplasmic p21 efficiently limits effector/memory T cell proliferation.

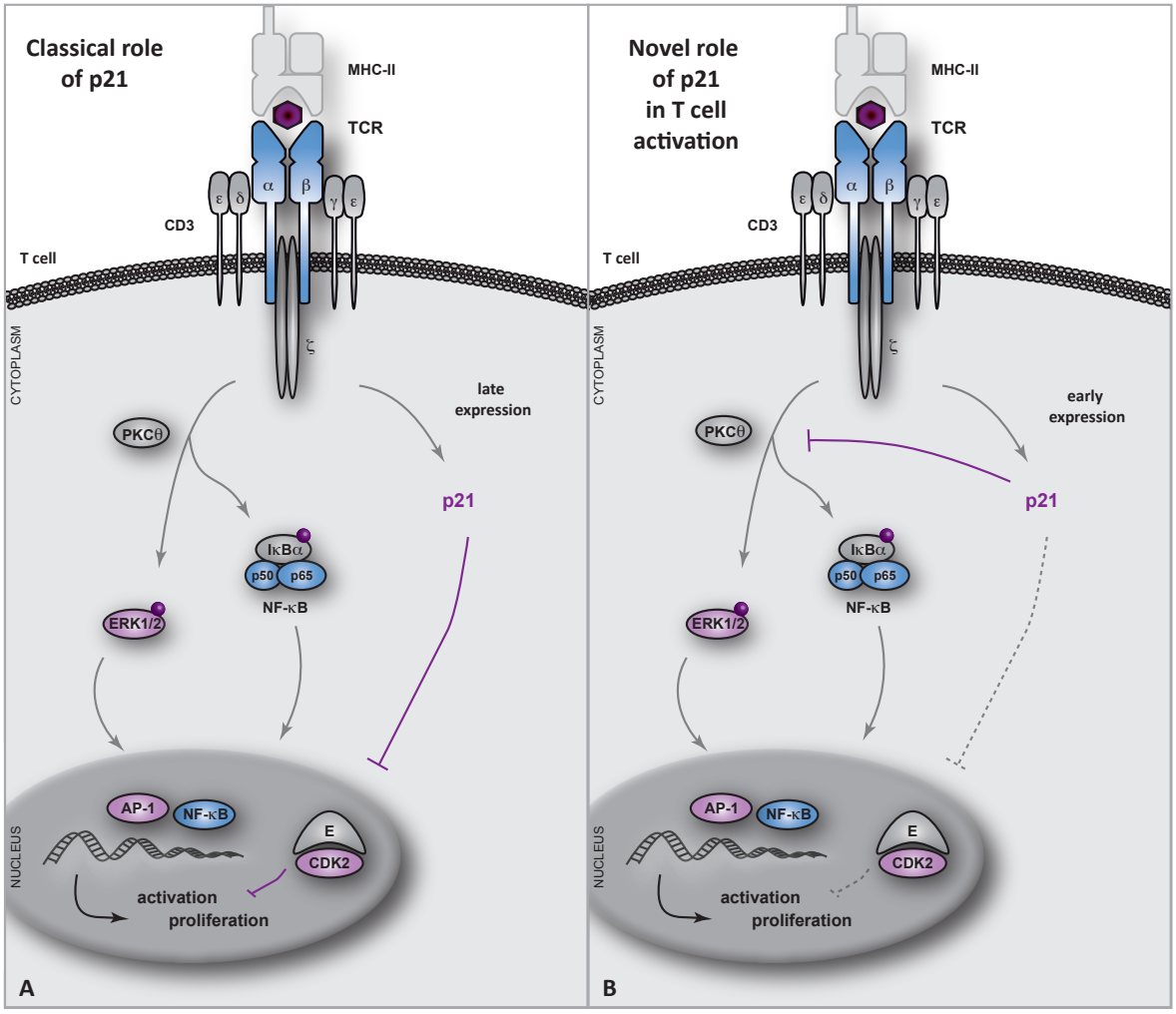

Figure 5.1. Differential regulation of T cell activation by p21. A. The classical role of p21, as currently accepted. **B.** A novel role for p21: In response to repeated stimulation, p21 negatively regulates effector/memory T cell activation and subsequent proliferation.

5.3 p21 influences the activation threshold of effector/memory T cells

During T cell development, potentially auto-reactive lymphocytes are inactivated or directly eliminated. Some auto-reactive T cells are able to escape negative selection in the thymus and originate autoimmune diseases; in peripheral tissues, autoimmune T cells might be activated by auto-antigens, which have low affinity for the TCR[139].

To examine whether p21 has a role in determining the activation threshold in effector/memory T cells, we analyzed the T cell response by presenting a transgenic TCR stimulated with antigens of high (PCC, representing exogenous antigens) or low affinity (A96I, representing endogenous antigens) for this TCRtg. During primary ConA stimulation, we detected no significant differences in

proliferation between naïve pcc.TCRtg and pcc.TCRtg-p21$^{-/-}$ T cells in response to primary stimulation with PCC (*Fig. 4.18B,C*). Following secondary TCR challenge with the same antigen, however, p21-deficient pcc.TCRtg memory-phenotype T cells showed considerable hyperproliferation and high levels of apoptosis were induced (*Fig. 4.18D,E*), indicating a strong stimulating effect of PCC. When stimulated with PCC and restimulated with a low affinity antigen (A96I), pcc.TCRtg-p21$^{-/-}$ effector/memory T cells clearly hyperproliferated in response to A96I (*Fig. 4.19A*); the proliferation difference between pcc.TCRtg and pcc.TCRtg-p21$^{-/-}$ memory T cells was even greater than after restimulation with PCC. These findings define a model in which p21 modulates the activation threshold of effector/memory T cells, as its absence leads to a reduction in this threshold and enables T cell responses to low affinity peptides. As a result, these overactivated effector/memory T cells lose tolerance, leading to development of autoimmunity. p21 expression prevents immune responses to auto-antigens with low TCR affinity and could thus have an important function in the establishment of T cell tolerance and in autoimmune suppression.

5.4 Lack of p21 exacerbates the autoimmune phenotype in B6/*lpr* mice

Fas-deficient mice develop lupus-like autoimmune disease due to defective apoptosis signaling. One of the most common manifestations is glomerulonephritis, caused by chronic inflammation and immune complex accumulation (*see 1.1.2*). In B6/*lpr* mice, a mild course of disease is generally observed. To establish the biological significance of the p21 function in T cell activation *in vivo*, we generated B6/*lpr*-p21$^{-/-}$ mice in our laboratory and found higher disease incidence in these mice.

In vitro analysis of B6/*lpr*-p21$^{-/-}$ memory-like T cells revealed a hyperactive state after secondary stimulation; both ERK1/2 and NF-κB were hyperactivated (*Fig. 4.23A,B*). Production of pro-inflammatory cytokines by B6/*lpr*-p21$^{-/-}$ effector/memory T cells was thus notably increased compared to B6/*lpr* controls (*Fig. 4.23D*). We also observed significant B6/*lpr*-p21$^{-/-}$ effector/memory T cell hyperproliferation in response to repeated TCR challenge (*Fig. 4.24*); Fas and p21 showed an additive effect in the control of effector/memory T cell proliferation in response to secondary TCR challenge (*Fig. 4.25*). The *in vitro* findings were similar to the characteristics observed in B6 and p21$^{-/-}$ mice, but more severe. This suggests p21 involvement in processes that lead to autoimmune disease development.

To study the effect of p21 deficiency on autoimmune manifestations *in vivo*, we analyzed several T cell populations in B6/*lpr* and B6/*lpr*-p21$^{-/-}$ mice and their implication in disease development. Lack of p21 led to clear hyperactivation of CD4^{+} effector/memory T cells in 1-year-

old B6/*lpr*-p21$^{-/-}$ mice (*Fig. 4.22B*) and thus to CD44^{high}CD62L^{low} T cell accumulation in secondary lymphoid organs (*Fig. 4.22A*), an autoimmune characteristic typical of several models of lupus-like disease[56,60,160]. In addition, we found higher expression of the pro-inflammatory cytokines IFNγ, IL-17 and IL-2 in CD4^{+}CD44^{high}CD62L^{high} and CD4^{+}CD44^{high}CD62L^{low} memory T cells from p21-deficient B6/*lpr* mice (*Fig. 4.27, 4.28*). In accordance with these findings, B6/*lpr*-p21$^{-/-}$ mice developed severe glomerulonephritis (*Fig. 4.20A*) and pronounced proteinuria (*Fig. 4.20B*). The lack of p21 did not alter DN T cell proliferation or accumulation in B6/*lpr* mice (*Fig. 4.21B*), and lymphadenopathy manifestations remained unchanged (data not shown). This observation raises the possibility that hyperactivated B6/*lpr*-p21$^{-/-}$ effector/memory T cells are involved in development of autoimmunity. p21 deletion had a strong effect on B6/*lpr* mice and caused serious aggravation of pathological manifestations, including increased B6/*lpr* effector/memory T cell activation, elevated IFNγ production, severe glomerulonephritis and lethal disease development. This animal model confirmed the biological relevance of our findings, suggesting an autoimmune suppressor function for p21.

5.5 Overexpression of p21 reduces hyperactivation of B6/*lpr* effector/memory T cells and ameliorates autoimmune manifestations

To provide the final demonstration of p21 involvement in the regulation of memory T cell activation and to show its therapeutic potential, we used a mouse model characterized by expression of transgenic human p21 in a T cell-specific manner[106]. In a recently published article by our group, we report that T cell-directed exogenous expression of p21 leads to reduced production of pro-inflammatory cytokines, less immune complex deposition in kidneys and decreased anti-DNA autoantibody production in MRL/*lpr*-p21tg mice[161]. As a result, the usually severe outcome of the autoimmune disease in MRL/*lpr* mice was clearly improved and early mortality (due to the autoimmunity-prone MRL background) was restricted in the MRL/*lpr*-p21tg mice[161].

An important characteristic of lupus-like diseases is the development of anti-DNA autoantibodies, which is closely linked to high IFNγ levels[55,162]. We showed that reduced IFNγ production by B6/*lpr*-p21tg T cells leads to a notable reduction in auto-antibody levels[161], indicating that p21 overexpression is able to ameliorate the outcome of autoimmune disease. p21 overexpression did not alter activation of B6-p21tg effector/memory T cells or their IFNγ expression (*Fig.4.28, 4.29*), which indicates that endogenous p21 expression is sufficient to control the immune response of B6 effector/memory T cells. In contrast, higher p21 levels are necessary to control activation of B6/*lpr*-p21tg effector/memory T cells after stimulation, which suggests a specific role

for p21 in negative regulation of activation events and immune responses of auto-reactive T cells.

In B6/*lpr* effector/memory T cells, expression of exogenous p21 efficiently reduced *in vitro* hyperactivation, as reflected by ERK1/2 phosphorylation (*Fig. 4.31C*) and NF-κB activity levels (*Fig. 4.32B*). In addition, hyperproliferation of B6/*lpr* effector/memory T cells notably decreased in response to secondary TCR challenge, due to transgenic p21 expression (*Fig. 4.31A,B*). This can be attributed, at least in part, to the reduced CDK2 activity in B6/*lpr*-p21tg effector/memory T cells (*Fig. 4.32A*). We detected no differences in B6-p21tg effector/memory T cell activation and expansion (*Fig. 4.30*), however; p21 thus does not act as a negative regulator of B6 T cell proliferation via CDK2. In accordance with their less activated phenotype, B6/*lpr*-p21tg effector/memory T cells produced lower amounts of IFNγ than B6/*lpr* memory T cells (*Fig. 4.33A*). p21 overexpression notably inhibited IFNγ induction after IL-12 and IL-18 stimulation (*Fig. 4.33B*).

p21 expression is also an important factor in human autoimmune disease. A study of SLE patients showed low p21 and p27 expression in hyperproliferating T cells of some patients; however, treatment with FasL induced p21 expression, which ameliorated disease manifestations[163]. p21 is thus an essential factor in the control of hyperactivation in autoimmune-prone but not in normal effector/memory T cells, and could be a suitable target for the design of new treatment strategies to reduce lymphoproliferation in autoimmune diseases.

5.6 Concluding remarks

Imbalanced tolerance of the immune system generates auto-reactive T cells and thus presents a threat to health. A variety of mechanisms during T cell development prevent the appearance of T cells able to respond to self-antigens, and several intrinsic mechanisms ensure adequate T cell function.

Here we describe an unreported function for p21, and show its implication in the regulation of memory-phenotype T cell activation; its absence leads to hyperactivation and therefore to hyperproliferation of $p21^{-/-}$ memory T cells. We showed that p21 targets intracellular activation pathways such as ERK1/2 and NF-κB, whereas its interaction with CDK2 appeared to be of minor importance. In addition, overactivated $p21^{-/-}$ effector/memory T cells responded to autoantigen-mimicking molecules with low affinity for the TCR, indicating a p21 function in modulation of the TCR activation threshold.

The biological relevance of these findings was demonstrated in several mouse models (summarized in *Fig. 5.2*). In B6/*lpr* mice, which typically present mild autoimmune manifestations,

lack of p21 led to development of severe autoimmunity and high death rates. B6/*lpr*-p21$^{-/-}$ T cells were hyperactivated and produced large amounts of IFNγ; these factors are known to promote loss of tolerance and autoimmunity development. Both Fas and p21 thus appear to have autoimmune suppressive functions, although they do not play an essential role in normal immune responses.

T cell-specific overexpression provided direct evidence for p21 as negative regulator of autoimmunity. B6/*lpr*-p21tg effector/memory T cells showed notably decreased activation as well as reduced IFNγ expression. As a consequence, autoimmunity in B6/*lpr* mice was ameliorated considerably due to enhanced p21 expression in T cells. p21 overexpression nonetheless had little or no effect on T cell activation in B6 mice, pointing to a specific role for p21 in autoimmune, but not normal immune responses.

In general, p21 might not be a strong inhibitor of T cell activation, but it appears to control specifically the activity of autoreactive effector/memory T cells. Low p21 expression[164,165] and elevated levels of pro-inflammatory cytokines such as IFNγ[166,167] are important characteristics of several autoimmune diseases, including human SLE. Based on our findings, IFNγ production by hyperactivated T cells is negatively controlled by p21, which is thus an optimal target for therapeutic strategies directed to autoimmune cells.

As design of therapies based on molecules with an essential role in T cell activation has failed to be of benefit in autoimmune disease treatment, perhaps less potent molecules that appear to be specific for autoimmune T cell function will constitute a more efficient therapeutic target for autoimmune disease[15-18,54].

autoimmune manifestations	B6-p21$^{-/-}$	B6	B6-p21tg	B6/*lpr*-p21$^{-/-}$	B6/*lpr*	B6/*lpr*-p21tg
memory T cell hyperactivation	+	–	–	++	+	–
elevated IFNγ levels	+	–	–	+++	++	+
anti-DNA antibodies	+	–	–	+++	++	+
glomerulonephritis grade	II	0	NA	IV	III	NA
lymphadenopathy	–	–	–	+++	++	+

Figure 5.2. Overview of phenotypes observed in the mouse models used in this study. Glomerulonephritis grades were determined according to the scale defined by Weening *et al.*[132] (NA = not assessed).

6. CONCLUSIONS

6. CONCLUSIONS

1. p21 controls activation of memory-phenotype T cells after repeated TCR stimulation in a CDK2-independent manner, but has no effect on naïve T cells. Stimulation of TCRtg T cells with a specific antigen (OVA) confirmed the hypothesis that p21 is involved in activation of effector/memory T cells in an *in vivo* setting.

2. p21 is unrelated to TCR proximate events, but might act on PKCθ or on downstream activation pathways, as it is located in the cytoplasm of $CD4^+$ effector/memory T cells.

3. p21 negatively regulates the proliferative response of effector/memory T cells via ERK1/2 and NF-κB activation pathways. In the absence of p21, memory-phenotype T cells show hyperactivation of both ERK1/2 and NF-κB, which leads to increased proliferation and pro-inflammatory cytokine production (IFNγ, IL-2).

4. p21-deficient pcc.TCRtg effector/memory T cells are more susceptible to activation by antigens with low TCR affinity that mimic auto-antigens, which suggests that p21 regulates the activation threshold and thus maintains tolerance and suppresses autoimmunity.

5. B6/*lpr*-$p21^{-/-}$ mice confirmed the *in vivo* biological relevance of our findings. Absence of p21 caused increased activation of memory T cells and elevated production of pro-inflammatory cytokine such as IFNγ, leading to notable aggravation of lupus-like disease manifestations and death in B6/*lpr* mice.

6. Constitutive p21 overexpression by T cells efficiently reduced pathological manifestations in B6/*lpr*-p21tg mice. Lower IFNγ levels represent a critical feature of the reduced activation, since they control loss of tolerance and lupus development.

7. p21 is an autoimmunity suppressor that acts by inhibiting T cell activation and reducing pro-inflammatory cytokine production by auto-reactive, but not by normal T cells after repeated antigen encounter, and thus might have therapeutic relevance.

7. CONCLUSIONES

7. CONCLUSIONES

1. p21 controla la activación de células T de memoria/efectoras de manera independiente a CDK2 después de una estimulación repetida del TCR, sin influir la activación de las células T naïve. La estimulación de células con un TCR transgénico con el antígeno específico OVA *in vivo* confirma el papel p21 en la activación de células T de memoria/efectoras.

2. p21 está localizado en el citoplasma de las células T de memoria/efectoras y no está involucrado en la cascada de activación próxima al TCR, ya que actúa a nivel de la PKCθ o en las vías de activación reguladas por esta quinasa.

3. p21 controla de manera negativa la respuesta proliferativa de las células T de memoria/efectoras regulando las vías de activación de ERK1/2 y NF-κB. La ausencia de p21 en las células de memoria causa la sobreactivación de ERK1/2 y NF-κB de estas células y, en consecuencia, su hiperproliferación y una mayor producción de citoquinas pro-inflamatorias (IFNγ, IL-2).

4. Las células T de memoria/efectoras deficientes en p21 con un TCR transgénico (pcc.TCRtg-p21$^{-/-}$) tienen una alta susceptibilidad a activarse frente a antígenos de baja afinidad, sugiriendo que p21 juega un papel en el control del umbral de activación de las células T de memoria/efectoras. De ésta manera, p21 ayuda a mantener la tolerancia frente a antígenos propios y a suprimir el desarrollo de autoinmunidad.

5. Los ratones B6/*lpr* deficientes en p21 (B6/*lpr*-p21$^{-/-}$) confirman la relevancia biológica de nuestros resultados: en ausencia de p21, las células T de memoria/efectoras están hiperactivadas y producen elevadas cantidades de citoquinas pro-inflamatorias como IFNγ. Como consecuencia, se produce un aumento en las manifestaciones de la enfermedad autoinmune en los ratones B6/*lpr* que finalmente causa su muerte.

6. En ratones B6/*lpr*-p21tg, la sobre-expresión constitutiva de p21 de manera específica en las células T reduce las manifestaciones patológicas de los ratones deficientes en FAS de forma eficaz. La disminución en los niveles de IFNγ es un elemento crítico en la reducción de la activación de las células T, ya que esta citoquina controla la pérdida de tolerancia y el desarrollo de la enfermedad autoinmune.

7. p21 es un potente supresor de autoinmunidad y ejerce su función inhibiendo la activación y la producción de citoquinas pro-inflamatorias de las células T potencialmente auto-reactivas en respuesta a una estimulación repetida, sin afectar a células T normales. Por lo tanto, p21 podría ser relevante para el diseño de nuevas terapias en el tratamiento de enfermedades autoinmunes.

9. REFERENCES

8. REFERENCES

1. Medzhitov, R. Recognition of microorganisms and activation of the immune response. *Nature* **449,** 819–826 (2007). DOI 10.1038/nature06246
2. Chaplin, D. D. Overview of the immune response. *J. Allergy Clin. Immunol.* **125,** S3–23 (2010). DOI 10.1016/j.jaci.2009.12.980
3. Boehm, T. Design principles of adaptive immune systems. *Nat. Rev. Immunol.* **11,** 307–317 (2011). DOI 10.1038/nri2944
4. Goodnow, C. C., Sprent, J., Fazekas de St Groth, B. & Vinuesa, C. G. Cellular and genetic mechanisms of self tolerance and autoimmunity. *Nature* **435,** 590–597 (2005). DOI 10.1038/nature03724
5. Carpenter, A. C. & Bosselut, R. Decision checkpoints in the thymus. *Nat. Immunol.* **11,** 666–673 (2010). DOI 10.1038/ni.1887
6. Ciofani, M. & Zúñiga-Pflücker, J. C. Determining γδ versus αß T cell development. *Nat. Rev. Immunol.* **10,** 657–663 (2010). DOI 10.1038/nri2820
7. Yamasaki, S. & Saito, T. Molecular basis for pre-TCR-mediated autonomous signaling. *Trends in Immunology* **28,** 39–43 (2007). DOI 10.1016/j.it.2006.11.006
8. Starr, T. K., Jameson, S. C. & Hogquist, K. A. Positive and negative selection of T cells. *Annu. Rev. Immunol.* **21,** 139–76 (2003). DOI 10.1146/annurev.immunol.21.120601.141107
9. Xing, Y. & Hogquist, K. A. T-cell tolerance: central and peripheral. *Cold Spring Harb. Perspect. Biol.* **4,** (2012). DOI 10.1101/cshperspect.a006957
10. Metzger, T. C. & Anderson, M. S. Control of central and peripheral tolerance by Aire. *Immunol. Rev.* **241,** 89–103 (2011). DOI 10.1111/j.1600-065X.2011.01008.x
11. Benoist, C. & Mathis, D. Treg cells, life history, and diversity. *Cold Spring Harbor perspectives in biology* **4,** (2012). DOI 10.1101/cshperspect.a007021
12. Romagnani, S. Immunological tolerance and autoimmunity. *Intern. Emerg. Med.* **1,** 187–196 (2006). DOI 10.1007/BF02934736
13. Appleman, L. J. & Boussiotis, V. A. T cell anergy and costimulation. *Immunol. Rev.* **192,** 161–180 (2003). DOI 10.1034/j.1600-065X.2003.00009.x
14. Ise, W., Kohyama, M., Nutsch, K. M., Lee, H. M., Suri, A., Unanue, E. R., Murphy, T. L. & Murphy, K. M. CTLA-4 suppresses the pathogenicity of self antigen-specific T cells by cell-intrinsic and cell-extrinsic mechanisms. *Nat. Immunol.* **11,** 129–135 (2010). DOI 10.1038/ni.1835
15. Fife, B. T., Pauken, K. E., Eagar, T. N., Obu, T., Wu, J., Tang, Q., Azuma, M., Krummel, M. F. & Bluestone, J. A. Interactions between PD-1 and PD-L1 promote tolerance by blocking the TCR-induced stop signal. *Nat. Immunol.* **10,** 1185–1192 (2009). DOI 10.1038/ni.1790
16. Okazaki, T. & Honjo, T. The PD-1-PD-L pathway in immunological tolerance. *Trends in Immunology* **27,** 195–201 (2006). DOI 10.1016/j.it.2006.02.001
17. Jury, E. C., Flores-Borja, F., Kalsi, H. S., Lazarus, M., Isenberg, D. A., Mauri, C. & Ehrenstein, M. R. Abnormal CTLA-4 function in T cells from patients with systemic lupus erythematosus. *Eur. J. Immunol.* **40,** 569–578 (2010). DOI 10.1002/eji.200939781
18. Tivol, E. A., Borriello, F., Schweitzer, A. N., Lynch, W. P., Bluestone, J. A. & Sharpe, A. H. Loss of CTLA-4 leads to massive lymphoproliferation and fatal multiorgan tissue destruction, revealing a critical negative regulatory role of CTLA-4. *Immunity* **3,** 541–547 (1995). DOI 10.1016/1074-7613(95)90125-6

19. Nishimura, H., Nose, M., Hiai, H., Minato, N. & Honjo, T. Development of lupus-like autoimmune diseases by disruption of the PD-1 gene encoding an ITIM motif-carrying immunoreceptor. *Immunity* **11,** 141–151 (1999). DOI 10.1016/S1074-7613(00)80089-8

20. Bluestone, J. A. & Abbas, A. K. Natural versus adaptive regulatory T cells. *Nat. Rev. Immunol.* **3,** 253–257 (2003). DOI 10.1038/nri1032

21. Strasser, A. & Pellegrini, M. T-lymphocyte death during shutdown of an immune response. *Trends in Immunology* **25,** 610–615 (2004). DOI 10.1016/j.it.2004.08.012

22. Green, D. R., Droin, N. & Pinkoski, M. Activation-induced cell death in T cells. *Immunol. Rev.* **193,** 70–81 (2003). DOI 10.1034/j.1600-065X.2003.00051.x

23. Weiss, A & Littman, D. R. Signal transduction by lymphocyte antigen receptors. *Cell* **76,** 263–74 (1994).

24. Rudolph, M. G., Stanfield, R. L. & Wilson, I. A. How TCRs bind MHCs, peptides, and coreceptors. *Annu. Rev. Immunol.* **24,** 419–466 (2006). DOI 10.1146/annurev.immunol.23.021704.115658

25. Salmond, R. J., Filby, A., Qureshi, I., Caserta, S. & Zamoyska, R. T-cell receptor proximal signaling via the Src-family kinases, Lck and Fyn, influences T-cell activation, differentiation, and tolerance. *Immunol. Rev.* **228,** 9–22 (2009). DOI 10.1111/j.1600-065X.2008.00745.x

26. Smith-Garvin, J. E., Koretzky, G. a & Jordan, M. S. T cell activation. *Annu. Rev. Immunol.* **27,** 591–619 (2009). DOI 10.1146/annurev.immunol.021908.132706

27. Sedwick, C. E. & Altman, A. Perspectives on PKCtheta in T cell activation. *Mol. Immunol.* **41,** 675–86 (2004). DOI 10.1016/j.molimm.2004.01.007

28. Gwack, Y., Feske, S., Srikanth, S., Hogan, P. G. & Rao, A. Signalling to transcription: store-operated Ca2+ entry and NFAT activation in lymphocytes. *Cell Calcium* **42,** 145–56 (2007). DOI 10.1016/j.ceca.2007.03.007

29. Feske, S. Calcium signalling in lymphocyte activation and disease. *Nat. Rev. Immunol.* **7,** 690–702 (2007). DOI 10.1038/nri2152

30. Díaz-Flores, E., Siliceo, M., Martínez-A, C. & Mérida, I. Membrane translocation of protein kinase Ctheta during T lymphocyte activation requires phospholipase C-gamma-generated diacylglycerol. *J. Biol. Chem.* **278,** 29208–29215 (2003). DOI 10.1074/jbc.M303165200

31. Lorenzo, P. S., Beheshti, M., Pettit, G. R., Stone, J. C. & Blumberg, P. M. The guanine nucleotide exchange factor RasGRP is a high -affinity target for diacylglycerol and phorbol esters. *Mol. Pharmacol.* **57,** 840–846 (2000).

32. Zhang, Y. L. & Dong, C. MAP kinases in immune responses. *Cell. Mol. Immunol.* **2,** 20–27 (2005).

33. Karin, M., Liu, Z. G. & Zandi, E. AP-1 function and regulation. *Current Opinion in Cell Biology* **9,** 240–246 (1997). DOI 10.1016/S0955-0674(97)80068-3

34. Oh, H. & Ghosh, S. NF-κB: roles and regulation in different CD4(+) T-cell subsets. *Immunol. Rev.* **252,** 41–51 (2013). DOI 10.1111/imr.12033

35. Ruland, J. & Mak, T. W. Transducing signals from antigen receptors to nuclear factor kappaB. *Immunol. Rev.* **193,** 93–100 (2003). DOI 10.1034/j.1600-065X.2003.00049.x

36. Lin, X. & Wang, D. The roles of CARMA1, Bcl10, and MALT1 in antigen receptor signaling. *Semin. Immunol.* **16,** 429–35 (2004). DOI 10.1016/j.smim.2004.08.022

37. Li, Q. & Verma, I. M. NF-κB regulation in the immune system. *Nature Reviews Immunology* **2,** 725–734 (2002). DOI 10.1038/nri910

38. Shambharkar, P. B., Blonska, M., Pappu, B. P., Li, H., You, Y., Sakurai, H., Darnay, B. G., Hara, H., Penninger, J. & Lin, X. Phosphorylation and ubiquitination of the IkappaB kinase complex by two distinct signaling pathways. *EMBO J.* **26,** 1794–1805 (2007). DOI 10.1038/sj.emboj.7601622

39. Cheng, J., Montecalvo, A. & Kane, L. P. Regulation of NF-κB induction by TCR/CD28. *Immunol. Res.* **50,** 113–7 (2011). DOI 10.1007/s12026-011-8216-z

40. Zhu, J., Yamane, H. & Paul, W. E. Differentiation of effector CD4 T cell populations (*). *Annu. Rev. Immunol.* **28,** 445–489 (2010). DOI 10.1146/annurev-immunol-030409-101212

41. Wan, Y. Y. & Flavell, R. A. How diverse-CD4 effector T cells and their functions. *Journal of Molecular Cell Biology* **1,** 20–36 (2009). DOI 10.1093/jmcb/mjp001

42. Takahashi, S., Fossati, L., Iwamoto, M., Merino, R., Motta, R., Kobayakawa, T. & Izui, S. Imbalance towards Th1 predominance is associated with acceleration of lupus-like autoimmune syndrome in MRL mice. *J. Clin. Invest.* **97,** 1597–1604 (1996). DOI 10.1172/JCI118584

43. Zhu, J. & Paul, W. E. CD4 T cells: Fates, functions, and faults. *Blood* **112,** 1557–1569 (2008). DOI 10.1182/blood-2008-05-078154

44. Lee, Y. K., Mukasa, R., Hatton, R. D. & Weaver, C. T. Developmental plasticity of Th17 and Treg cells. *Current Opinion in Immunology* **21,** 274–280 (2009). DOI 10.1016/j.coi.2009.05.021

45. Apostolidis, S. A., Crispín, J. C. & Tsokos, G. C. IL-17-producing T cells in lupus nephritis. *Lupus* **20,** 120–124 (2011). DOI 10.1177/0961203310389100

46. Hemdan, N. Y. A., Birkenmeier, G., Wichmann, G., Abu El-Saad, A. M., Krieger, T., Conrad, K. & Sack, U. Interleukin-17-producing T helper cells in autoimmunity. *Autoimmunity Reviews* **9,** 785–792 (2010). DOI 10.1016/j.autrev.2010.07.003

47. Wing, K. & Sakaguchi, S. Regulatory T cells exert checks and balances on self tolerance and autoimmunity. *Nat. Immunol.* **11,** 7–13 (2010). DOI 10.1038/ni.1818

48. Kannan, A., Huang, W., Huang, F. & August, A. Signal transduction via the T cell antigen receptor in naïve and effector/memory T cells. *Int. J. Biochem. Cell Biol.* **44,** 2129–34 (2012). DOI 10.1016/j.biocel.2012.08.023

49. Sprent, J. & Surh, C. D. Normal T cell homeostasis: the conversion of naive cells into memory-phenotype cells. *Nat. Immunol.* **131,** 478–484 (2011). DOI 10.1038/ni.2018

50. Boyman, O., Létourneau, S., Krieg, C. & Sprent, J. Homeostatic proliferation and survival of naïve and memory T cells. *Eur. J. Immunol.* **39,** 2088–94 (2009). DOI 10.1002/eji.200939444

51. Zehn, D., King, C., Bevan, M. J. & Palmer, E. TCR signaling requirements for activating T cells and for generating memory. *Cell. Mol. Life Sci.* **69,** 1565–75 (2012). DOI 10.1007/s00018-012-0965-x

52. McKinstry, K. K., Strutt, T. M. & Swain, S. L. The potential of CD4 T-cell memory. *Immunology* **130,** 1–9 (2010). DOI 10.1111/j.1365-2567.2010.03259.x IMM3259 [pii]

53. Sharpe, A. H., Wherry, E. J., Ahmed, R. & Freeman, G. J. The function of programmed cell death 1 and its ligands in regulating autoimmunity and infection. *Nat. Immunol.* **8,** 239–245 (2007). DOI 10.1038/ni1443

54. Bertsias, G. K., Nakou, M., Choulaki, C., Raptopoulou, A., Papadimitraki, E., Goulielmos, G., Kritikos, H., Sidiropoulos, P., Tzardi, M., Kardassis, D., Mamalaki, C. & Boumpas, D. T. Genetic, immunologic, and immunohistochemical analysis of the programmed death 1/programmed death ligand 1 pathway in human systemic lupus erythematosus. *Arthritis Rheum.* **60,** 207–218 (2009). DOI 10.1002/art.24227

55. Balomenos, D., Rumold, R. & Theofilopoulos, A. N. Interferon-gamma is required for lupus-like disease and lymphoaccumulation in MRL-lpr mice. *J. Clin. Invest.* **101,** 364–371 (1998). DOI 10.1172/JCI750

56. Arias, C. F., Ballesteros-Tato, A., García, M. I., Martín-Caballero, J., Flores, J. M., Martínez-A, C. & Balomenos, D. p21CIP1/WAF1 controls proliferation of activated/memory T cells and affects homeostasis and memory T cell responses. *J. Immunol.* **178,** 2296–2306 (2007). DOI 178/4/2296 [pii]

57. Balomenos, D., Martín-Caballero, J., García, M. I., Prieto, I., Flores, J. M., Serrano, M. & Martínez-A, C. The cell cycle inhibitor p21 controls T-cell proliferation and sex-linked lupus development. *Nat. Med.* **6,** 171–176 (2000). DOI 10.1038/72272

58. Salvador, J. M., Hollander, M. C., Nguyen, A. T., Kopp, J. B., Barisoni, L., Moore, J. K., Ashwell, J. D. & Fornace Jr., A. J. Mice lacking the p53-effector gene Gadd45a develop a lupus-like syndrome. *Immunity* **16,** 499–508 (2002). DOI S1074761302003023 [pii]

59. Liu, L., Tran, E., Zhao, Y., Huang, Y., Flavell, R. & Lu, B. Gadd45 beta and Gadd45 gamma are critical for regulating autoimmunity. *J. Exp. Med.* **202,** 1341–1347 (2005). DOI 10.1084/jem.20051359

60. Murga, M., Fernández-Capetillo, O., Field, S. J., Moreno, B., R.-Borlado, L., Fujiwara, Y., Balomenos, D., Vicario, A., Carrera, A. C., Orkin, S. H., Greenberg, M. E. & Zubiaga, A. M. Mutation of E2F2 in mice causes enhanced T lymphocyte proliferation, leading to the development of autoimmunity. *Immunity* **15,** 959–970 (2001). DOI 10.1016/S1074-7613(01)00254-0

61. Crispín, J. C., Oukka, M., Bayliss, G., Cohen, R. A., Van Beek, C. A., Stillman, I. E., Kyttaris, V. C., Juang, Y.-T. & Tsokos, G. C. Expanded double negative T cells in patients with systemic lupus erythematosus produce IL-17 and infiltrate the kidneys. *J. Immunol.* **181,** 8761–8766 (2008). DOI 10.4049/jimmunol.181.12.8761

62. Rajagopalan, S., Zordan, T., Tsokos, G. C. & Datta, S. K. Pathogenic anti-DNA autoantibody-inducing T helper cell lines from patients with active lupus nephritis: isolation of CD4-8- T helper cell lines that express the gamma delta T-cell antigen receptor. *Proc. Natl. Acad. Sci. U. S. A.* **87,** 7020–7024 (1990). DOI 10.1073/pnas.87.18.7020

63. Nagata, S. & Golstein, P. The Fas death factor. *Science* **267,** 1449–1456 (1995). DOI 10.1126/science.7533326

64. Wang, J. & Lenardo, M. J. Molecules involved in cell death and peripheral tolerance. *Curr. Opin. Immunol.* **9,** 818–825 (1997).

65. Strasser, A., Whittingham, S., Vaux, D. L., Bath, M. L., Adams, J. M., Cory, S. & Harris, A. W. Enforced BCL2 expression in B-lymphoid cells prolongs antibody responses and elicits autoimmune disease. *Proc. Natl. Acad. Sci. U. S. A.* **88,** 8661–8665 (1991). DOI 10.1073/pnas.88.19.8661

66. Li-Weber, M. & Krammer, P. H. Function and regulation of the CD95 (APO-1/Fas) ligand in the immune system. *Seminars in Immunology* **15,** 145–157 (2003). DOI 10.1016/S1044-5323(03)00030-7

67. Brunner, T., Mogil, R. J., LaFace, D., Yoo, N. J., Mahboubi, A., Echeverri, F., Martin, S. J., Force, W. R., Lynch, D. H. & Ware, C. F. Cell-autonomous Fas (CD95)/Fas-ligand interaction mediates activation-induced apoptosis in T-cell hybridomas. *Nature* **373,** 441–444 (1995). DOI 10.1038/373441a0

68. Krueger, A., Fas, S. C., Baumann, S. & Krammer, P. H. The role of CD95 in the regulation of peripheral T-cell apoptosis. *Immunol. Rev.* **193,** 58–69 (2003). DOI 10.1034/j.1600-065X.2003.00047.x

69. Lavrik, I. N. & Krammer, P. H. Regulation of CD95/Fas signaling at the DISC. *Cell Death and Differentiation* **19,** 36–41 (2012). DOI 10.1038/cdd.2011.155

70. Boatright, K. M., Renatus, M., Scott, F. L., Sperandio, S., Shin, H., Pedersen, I. M., Ricci, J. E., Edris, W. A., Sutherlin, D. P., Green, D. R. & Salvesen, G. S. A unified model for apical caspase activation. *Mol. Cell* **11,** 529–541 (2003). DOI 10.1016/S1097-2765(03)00051-0

71. Watanabe-Fukunaga, R., Brannan, C. I., Copeland, N. G., Jenkins, N. A. & Nagata, S. Lymphoproliferation disorder in mice explained by defects in Fas antigen that mediates apoptosis. *Nature* **356,** 314–317 (1992). DOI 10.1038/356314a0

72. Walker, L. S. K. & Abbas, A. K. The enemy within: keeping self-reactive T cells at bay in the periphery. *Nat. Rev. Immunol.* **2,** 11–19 (2002). DOI 10.1038/nri701

73. Singer, G. G., Carrera, A. C., Marshak-Rothstein, A., Martinez, C. & Abbas, A. K. Apoptosis, Fas and systemic autoimmunity: the MRL-lpr/lpr model. *Curr Opin Immunol* **6,** 913–920 (1994).

74. Vidal, S., Kono, D. H. & Theofilopoulos, A. N. Loci predisposing to autoimmunity in MRL-Fas(lpr) and C57BL/6-Fas(lpr) mice. *J. Clin. Invest.* **101,** 696–702 (1998). DOI 10.1172/JCI1817

75. Newton, K., Kurts, C., Harris, A. W. & Strasser, A. Effects of a dominant interfering mutant of FADD on signal transduction in activated T cells. *Curr. Biol.* **11,** 273–276 (2001). DOI 10.1016/S0960-9822-(01)00067-7

76. Salmena, L., Lemmers, B., Hakem, A., Matysiak-Zablocki, E., Murakami, K., Billie Au, P. Y., Berry, D. M., Tamblyn, L., Shehabeldin, A., Migon, E., Wakeham, A., Bouchard, D., Yeh, W. C., McGlade, J. C., Ohashi, P. S. & Hakem, R. Essential role for caspase 8 in T-cell homeostasis and T-cell-mediated immunity. *Genes Dev.* **17,** 883–895 (2003). DOI 10.1101/gad.1063703

77. Balomenos, D., Rumold, R. & Theofilopoulos, A. N. The proliferative in vivo activities of lpr double-negative T cells and the primary role of p59fyn in their activation and expansion. *J. Immunol.* **159,** 2265–2273 (1997).

78. Fortner, K. A. & Budd, R. C. The death receptor Fas (CD95/APO-1) mediates the deletion of T lymphocytes undergoing homeostatic proliferation. *J. Immunol.* **175,** 4374–4382 (2005). DOI 175/7/4374 [pii]

79. Nagata, S. Human autoimmune lymphoproliferative syndrome, a defect in the apoptosis-inducing Fas receptor: A lesson from the mouse model. *Journal of Human Genetics* **43,** 2–8 (1998). DOI 10.1007/s100380050029

80. Straus, S. E., Jaffe, E. S., Puck, J. M., Dale, J. K., Elkon, K. B., Rösen-Wolff, A., Peters, A. M. J., Sneller, M. C., Hallahan, C. W., Wang, J., Fischer, R. E., Jackson, C. M., Lin, A. Y., Bäumler, C., Siegert, E., Marx, A., Vaishnaw, A. K., Grodzicky, T., Fleisher, T. A., Lenardo, M. J. The development of lymphomas in families with autoimmune lymphoproliferative syndrome with germline Fas mutations and defective lymphocyte apoptosis. *Blood* **98,** 194–200 (2001). DOI 10.1182/blood.V98.1.194

81. Oliveira, J. B., Bidère, N., Niemela, J. E., Zheng, L., Sakai, K., Nix, C. P., Danner, R. L., Barb, J., Munson, P. J., Puck, J. M., Dale, J., Straus, S. E., Fleisher, T. A. & Lenardo, M. J. NRAS mutation causes a human autoimmune lymphoproliferative syndrome. *Proc. Natl. Acad. Sci. U. S. A.* **104,** 8953–8958 (2007). DOI 10.1073/pnas.0702975104

82. Teachey, D. T., Seif, A. E. & Grupp, S. A. Advances in the management and understanding of autoimmune lymphoproliferative syndrome (ALPS). *British Journal of Haematology* **148,** 205–216 (2010). DOI 10.1111/j.1365-2141.2009.07991.x

83. Teachey, D. T. New advances in the diagnosis and treatment of autoimmune lymphoproliferative syndrome. *Current Opinion in Pediatrics* **24,** 1–8 (2012). DOI 10.1097/MOP.0b013e32834ea739

84. Malumbres, M., Harlow, E., Hunt, T., Hunter, T., Lahti, J. M., Manning, G., Morgan, D. O., Tsai, L.-H. & Wolgemuth, D. J. Cyclin-dependent kinases: a family portrait. *Nature cell biology* **11,** 1275–1276 (2009). DOI 10.1038/ncb1109-1275

85. Malumbres, M. & Barbacid, M. Cell cycle kinases in cancer. *Current Opinion in Genetics and Development* **17,** 60–65 (2007). DOI 10.1016/j.gde.2006.12.008

86. Vidal, A. & Koff, A. Cell-cycle inhibitors: Three families united by a common cause. *Gene* **247,** 1–15 (2000). DOI 10.1016/S0378-1119(00)00092-5

87. Hara, E., Smith, R., Parry, D., Tahara, H., Stone, S. & Peters, G. Regulation of p16CDKN2 expression and its implications for cell immortalization and senescence. *Mol. Cell. Biol.* **16,** 859–867 (1996).

88. Brugarolas, J., Moberg, K., Boyd, S. D., Taya, Y., Jacks, T. & Lees, J. A. Inhibition of cyclin-dependent kinase 2 by p21 is necessary for retinoblastoma protein-mediated G1 arrest after gamma-irradiation. *Proc. Natl. Acad. Sci. U. S. A.* **96,** 1002–1007 (1999). DOI 10.1073/pnas.96.3.1002

89. Bianchi, T., Rufer, N., MacDonald, H. R. & Migliaccio, M. The tumor suppressor p16Ink4a regulates T lymphocyte survival. *Oncogene* **25,** 4110–4115 (2006). DOI 10.1038/sj.onc.1209437

90. Li, L., Iwamoto, Y., Berezovskaya, A. & Boussiotis, V. a. A pathway regulated by cell cycle inhibitor p27Kip1 and checkpoint inhibitor Smad3 is involved in the induction of T cell tolerance. *Nat. Immunol.* **7,** 1157–65 (2006). DOI 10.1038/ni1398

91. Rowell, E. A., Wang, L., Hancock, W. W. & Wells, A. D. The cyclin-dependent kinase inhibitor p27kip1 is required for transplantation tolerance induced by costimulatory blockade. *J. Immunol.* **177,** 5169–5176 (2006). DOI 10.4049/jimmunol.177.8.5169

92. Harper, J. W., Adami, G. R., Wei, N., Keyomarsi, K. & Elledge, S. J. The p21 Cdk-interacting protein Cip1 is a potent inhibitor of G1 cyclin-dependent kinases. *Cell* **75,** 805–816 (1993). DOI 10.1016/0092-8674(93)90499-G

93. El-Deiry, W. S., Tokino, T., Velculescu, V. E., Levy, D. B., Parsons, R., Trent, J. M., Lin, D., Mercer, W. E., Kinzler, K. W. & Vogelstein, B. WAF1, a potential mediator of p53 tumor suppression. *Cell* **75,** 817–825 (1993). DOI 10.1016/0092-8674(93)90500-P

94. Waldman, T., Kinzler, K. W. & Vogelstein, B. p21 is necessary for the p53-mediated G1 arrest in human cancer cells. *Cancer Res* **55,** 5187–90. (1995).

95. Goubin, F. & Ducommun, B. Identification of binding domains on the p21Cip1 cyclin-dependent kinase inhibitor. *Oncogene* **10,** 2281–2287 (1995).

96. Fotedar, R., Fitzgerald, P., Rousselle, T., Cannella, D., Dorée, M., Messier, H. & Fotedar, A. p21 contains independent binding sites for cyclin and cdk2: both sites are required to inhibit cdk2 kinase activity. *Oncogene* **12,** 2155–2164 (1996).

97. Dotto, G. P. p21(WAF1/Cip1): more than a break to the cell cycle? *Biochim. Biophys. Acta* **1471,** M43–56 (2000).

98. Cazzalini, O., Scovassi, a I., Savio, M., Stivala, L. a & Prosperi, E. Multiple roles of the cell cycle inhibitor p21(CDKN1A) in the DNA damage response. *Mutat. Res.* **704,** 12–20 (2010). DOI 10.1016/j.mrrev.2010.01.009

99. El-Deiry, W. S., Harper, J. W., O'Connor, P. M., Velculescu, V. E., Canman, C. E., Jackman, J., Pietenpol, J. A., Burrell, M., Hill, D. E., Wang, Y., Wiman, K. G., Mercer, W. E., Kastan, M. B., Kohn, K. W., Elledge, S. J., Kinzler, K. W. & Vogelstein, B. WAF1/CIP1 is induced in p53-mediated G1 arrest and apoptosis. *Cancer Res.* **54,** 1169–1174 (1994).

100. Cazzalini, O., Perucca, P., Riva, F., Stivala, L. A., Bianchi, L., Vannini, V., Ducommun, B. & Prosperi, E. p21CDKN1A does not interfere with loading of PCNA at DNA replication sites, but inhibits subsequent binding of DNA polymerase delta at the G1/S phase transition. *Cell Cycle* **2,** 596–603 (2003). DOI 10.4161/cc.2.6.502

101. Kraljevic Pavelic, S., Cacev, T. & Kralj, M. A dual role of p21waf1/cip1 gene in apoptosis of HEp-2 treated with cisplatin or methotrexate. *Cancer Gene Ther.* **15,** 576–590 (2008). DOI 10.1038/cgt.2008.28

102. Lee, E.-W., Lee, M.-S., Camus, S., Ghim, J., Yang, M.-R., Oh, W., Ha, N.-C., Lane, D. P. & Song, J. Differential regulation of p53 and p21 by MKRN1 E3 ligase controls cell cycle arrest and apoptosis. *EMBO J.* **28,** 2100–2113 (2009). DOI 10.1038/emboj.2009.164

103. Suzuki, A., Tsutomi, Y., Miura, M. & Akahane, K. Caspase 3 inactivation to suppress Fas-mediated apoptosis: identification of binding domain with p21 and ILP and inactivation machinery by p21. *Oncogene* **18,** 1239–1244 (1999). DOI 10.1038/sj.onc.1202409

104. Besson, A., Dowdy, S. F. & Roberts, J. M. CDK Inhibitors: Cell Cycle Regulators and Beyond. *Developmental Cell* **14,** 159–169 (2008). DOI 10.1016/j.devcel.2008.01.013

105. Coqueret, O. New roles for p21 and p27 cell-cycle inhibitors: A function for each cell compartment? *Trends in Cell Biology* **13,** 65–70 (2003). DOI 10.1016/S0962-8924(02)00043-0

106. Fotedar, R., Brickner, H., Saadatmandi, N., Rousselle, T., Diederich, L., Munshi, A., Jung, B., Reed, J. C. & Fotedar, A. Effect of p21waf1/cip1 transgene on radiation induced apoptosis in T cells. *Oncogene* **18,** 3652–3658 (1999). DOI 10.1038/sj.onc.1202693

107. Liu, S., Bishop, W. R. & Liu, M. Differential effects of cell cycle regulatory protein p21WAF1/Cip1 on apoptosis and sensitivity to cancer chemotherapy. *Drug Resist. Updat.* **6,** 183–195 (2003). DOI 10.1016/S1368-7646(03)00044-X

108. Gartel, A. L. & Radhakrishnan, S. K. Lost in transcription: p21 repression, mechanisms, and consequences. *Cancer Res.* **65,** 3980–5 (2005). DOI 10.1158/0008-5472.CAN-04-3995

109. Abbas, T. & Dutta, A. P21 in Cancer: Intricate Networks and Multiple Activities. *Nat. Rev. Cancer* **9,** 400–14 (2009). DOI 10.1038/nrc2657

110. Deng, C., Zhang, P., Harper, J. W., Elledge, S. J. & Leder, P. Mice lacking p21CIP1/WAF1 undergo normal development, but are defective in G1 checkpoint control. *Cell* **82,** 675–684 (1995). DOI 10.1016/0092-8674(95)90039-X

111. Trakala, M., Arias, C. F., García, M. I., Moreno-Ortiz, M. C., Tsilingiri, K., Fernández, P. J., Mellado, M., Díaz-Meco, M. T., Moscat, J., Serrano, M., Martínez-A, C. & Balomenos, D. Regulation of macrophage activation and septic shock susceptibility via p21(WAF1/CIP1). *Eur. J. Immunol.* **39,** 810–9 (2009). DOI

10.1002/eji.200838676

112. Shiohara, M., el-Deiry, W. S., Wada, M., Nakamaki, T., Takeuchi, S., Yang, R., Chen, D. L., Vogelstein, B. & Koeffler, H. P. Absence of WAF1 mutations in a variety of human malignancies. *Blood* **84,** 3781–3784 (1994).

113. Kim, K., Sung, Y.-K., Kang, C. P., Choi, C.-B., Kang, C. & Bae, S.-C. A regulatory SNP at position -899 in CDKN1A is associated with systemic lupus erythematosus and lupus nephritis. *Genes Immun.* **10,** 482–486 (2009). DOI 10.1038/gene.2009.5

114. Martens, H. A., Nolte, I. M., van der Steege, G., Schipper, M., Kallenberg, C. G. M., Te Meerman, G. J. & Bijl, M. An extensive screen of the HLA region reveals an independent association of HLA class I and class II with susceptibility for systemic lupus erythematosus. *Scand. J. Rheumatol.* **38,** 256–262 (2009). DOI 10.1080/03009740802552469

115. Yang, W., Ng, P., Zhao, M., Hirankarn, N., Lau, C. S., Mok, C. C., Chan, T. M., Wong, R. W. S., Lee, K. W., Mok, M. Y., Wong, S. N., Avihingsanon, Y., Lee, T. L., Ho, M. H. K., Lee, P. P. W., Wong, W. H. S. & Lau, Y. L. Population differences in SLE susceptibility genes: STAT4 and BLK, but not PXK, are associated with systemic lupus erythematosus in Hong Kong Chinese. *Genes Immun.* **10,** 219–226 (2009). DOI 10.1038/gene.2009.1

116. Tsokos, G. C. Systemic lupus erythematosus. *N. Engl. J. Med.* **365,** 2110–2121 (2011). DOI 10.1056/NEJMra1100359

117. Kong, P. L., Odegard, J. M., Bouzahzah, F., Choi, J.-Y., Eardley, L. D., Zielinski, C. E. & Craft, J. E. Intrinsic T cell defects in systemic autoimmunity. *Ann. N. Y. Acad. Sci.* **987,** 60–67 (2003).

118. Kaye, J., Hsu, M. L., Sauron, M. E., Jameson, S. C., Gascoigne, N. R. & Hedrick, S. M. Selective development of CD4+ T cells in transgenic mice expressing a class II MHC-restricted antigen receptor. *Nature* **341,** 746–749 (1989). DOI 10.1038/341746a0

119. Barnden, M. J., Allison, J., Heath, W. R. & Carbone, F. R. Defective TCR expression in transgenic mice constructed using cDNA-based alpha- and beta-chain genes under the control of heterologous regulatory elements. *Immunol. Cell Biol.* **76,** 34–40 (1998). DOI 10.1046/j.1440-1711.1998.00709.x

120. Robertson, J. M., Jensen, P. E. & Evavold, B. D. DO11.10 and OT-II T cells recognize a C-terminal ovalbumin 323-339 epitope. *J. Immunol.* **164,** 4706–4712 (2000). DOI 10.4049/jimmunol.164.9.4706

121. Slee, E. A., Zhu, H., Chow, S. C., MacFarlane, M., Nicholson, D. W. & Cohen, G. M. Benzyloxycarbonyl-Val-Ala-Asp (OMe) fluoromethylketone (Z-VAD.FMK) inhibits apoptosis by blocking the processing of CPP32. *Biochem. J.* **315 (Pt 1,** 21–24 (1996).

122. Favata, M. F., Horiuchi, K. Y., Manos, E. J., Daulerio, A. J., Stradley, D. A., Feeser, W. S., Van Dyk, D. E., Pitts, W. J., Earl, R. A., Hobbs, F., Copeland, R. A., Magolda, R. L., Scherle, P. A. & Trzaskos, J. M. Identification of a novel inhibitor of mitogen-activated protein kinase kinase. *J. Biol. Chem.* **273,** 18623–18632 (1998). DOI 10.1074/jbc.273.29.18623

123. Hernandez, A., Burger, M., Blomberg, B. B., Ross, W. A., Gaynor, J. J., Lindner, I., Cirocco, R., Mathew, J. M., Carreno, M., Jin, Y., Lee, K. P., Esquenazi, V. & Miller, J. Inhibition of NF-kappa B during human dendritic cell differentiation generates anergy and regulatory T-cell activity for one but not two human leukocyte antigen DR mismatches. *Hum. Immunol.* **68,** 715–729 (2007). DOI 10.1016/j.humimm.2007.05.010

124. Campaner, S., Doni, M., Hydbring, P., Verrecchia, A., Bianchi, L., Sardella, D., Schleker, T., Perna, D., Tronnersjö, S., Murga, M., Fernandez-Capetillo, O., Barbacid, M., Larsson, L.-G. & Amati, B. Cdk2 suppresses cellular senescence induced by the c-myc oncogene. *Nat. Cell Biol.* **12,** 54–9; sup pp 1–14 (2010). DOI 10.1038/ncb2004

125. Brooks, E. E., Gray, N. S., Joly, A., Kerwar, S. S., Lum, R., Mackman, R. L., Norman, T. C., Rosete, J., Rowe, M., Schow, S. R., Schultz, P. G., Wang, X., Wick, M. M. & Shiffman, D. CVT-313, a specific and potent inhibitor of CDK2 that prevents neointimal proliferation. *J. Biol. Chem.* **272,** 29207–29211 (1997). DOI 10.1074/jbc.272.46.29207

126. Page, D. M., Alexander, J., Snoke, K., Appella, E., Sette, A., Hedrick, S. M. & Grey, H. M. Negative selection of CD4+ CD8+ thymocytes by T-cell receptor peptide antagonists. *Proc. Natl. Acad. Sci. U. S. A.* **91,** 4057–4061 (1994). DOI 10.1073/pnas.91.9.4057

127. Vratsanos, G. S., Jung, S., Park, Y.-M. & Craft, J. Cd4+ T Cells from Lupus-Prone Mice Are Hyperresponsive to T Cell Receptor Engagement with Low and High Affinity Peptide Antigens. *J. Exp. Med.* **193,** 329–338 (2001).

128. Sprent, J. & Surh, C. D. T cell memory. *Annu. Rev. Immunol.* **20,** 551–579 (2002). DOI 10.1146/annurev.immunol.20.100101.151926

129. Hintzen, G., Ohl, L., del Rio, M.-L., Rodriguez-Barbosa, J.-I., Pabst, O., Kocks, J. R., Krege, J., Hardtke, S. & Förster, R. Induction of tolerance to innocuous inhaled antigen relies on a CCR7-dependent dendritic cell-mediated antigen transport to the bronchial lymph node. *J. Immunol.* **177,** 7346–7354 (2006).

130. Quah, B. J. C., Warren, H. S. & Parish, C. R. Monitoring lymphocyte proliferation in vitro and in vivo with the intracellular fluorescent dye carboxyfluorescein diacetate succinimidyl ester. *Nat. Protoc.* **2,** 2049–2056 (2007). DOI 10.1038/nprot.2007.296

131. Tough, D. F. & Sprent, J. Turnover of naive- and memory-phenotype T cells. *J. Exp. Med.* **179,** 1127–1135 (1994). DOI 10.1084/jem.179.4.1127

132. Weening, J. J., D'Agati, V. D., Schwartz, M. M., Seshan, S. V., Alpers, C. E., Appel, G. B., Balow, J. E., Bruijn, J. A., Cook, T., Ferrario, F., Fogo, A. B., Ginzler, E. M., Hebert, L., Hill, G., Hill, P., Jennette, J. C., Kong, N. C., Lesavre, P., Lockshin, M. *et al.* The classification of glomerulonephritis in systemic lupus erythematosus revisited. *Kidney Int.* **65,** 521–530 (2004). DOI 10.1111/j.1523-1755.2004.00443.x

133. Castagna, M., Takai, Y., Kaibuchi, K., Sano, K., Kikkawa, U. & Nishizuka, Y. Direct activation of calcium-activated, phospholipid-dependent protein kinase by tumor-promoting phorbol esters. *J. Biol. Chem.* **257,** 7847–7851 (1982).

134. Lindquist, J. A. & Schraven, B. Systems biology of T cell activation. *Ernst Scher. Found Symp Proc* 43–61 (2007).

135. Macián, F., López-Rodríguez, C. & Rao, a. Partners in transcription: NFAT and AP-1. *Oncogene* **20,** 2476–89 (2001). DOI 10.1038/sj.onc.1204386

136. Koike, T., Yamagishi, H., Hatanaka, Y., Fukushima, A., Chang, J., Xia, Y., Fields, M., Chandler, P. & Iwashima, M. A novel ERK-dependent signaling process that regulates interleukin-2 expression in a late phase of T cell activation. *J. Biol. Chem.* **278,** 15685–92 (2003). DOI 10.1074/jbc.M210829200

137. Pape, K. A., Kearney, E. R., Khoruts, A., Mondino, A., Merica, R., Chen, Z.-M., Ingulli, E., White, J., Johnson, J. G. & Jenkins, M. K. Use of adoptive transfer of T-cell antigen-receptor-transgenic T cells for the study of T-cell activation in vivo. *Immunol. Rev.* **156,** 67–78 (1997). DOI 10.1111/j.1600-065X.1997.tb00959.x

138. Jenkins, M. K., Khoruts, A., Ingulli, E., Mueller, D. L., McSorley, S. J., Reinhardt, R. L., Itano, A. & Pape, K. A. In vivo activation of antigen-specific CD4 T cells. *Annu. Rev. Immunol.* **19,** 23–45 (2001). DOI 10.1146/annurev.immunol.19.1.23

139. Choi, J.-Y. & Craft, J. Activation of naive CD4+ T cells in vivo by a self-peptide mimic: mechanism of tolerance maintenance and preservation of immunity. *J. Immunol.* **172,** 7399–7407 (2004). DOI 172/12/7399 [pii]

140. Hayashi, T. Therapeutic strategies for SLE involving cytokines: Mechanism-oriented therapies especially IFN-gamma targeting gene therapy. *Journal of Biomedicine and Biotechnology* **2010,** (2010). DOI 10.1155/2010/461641

141. Altman, A., Theofilopoulos, A. N., Weiner, R., Katz, D. H. & Dixon, F. J. Analysis of T cell function in autoimmune murine strains. Defects in production and responsiveness to interleukin 2. *J. Exp. Med.* **154,** 791–808 (1981). DOI 10.1084/jem.154.3.791

142. Theofilopoulos, A. N., Koundouris, S., Kono, D. H. & Lawson, B. R. The role of IFN-gamma in systemic lupus erythematosus: a challenge to the Th1/Th2 paradigm in autoimmunity. *Arthritis Res.* **3,** 136–141 (2001). DOI 10.1186/ar290

143. Schoenberger, S. P. CD69 guides CD4+ T cells to the seat of memory. *Proc Natl Acad Sci U S A* **109,** 8358–8359 (2012). DOI 10.1073/pnas.1204616109

144. Peng, S. L., Moslehi, J. & Craft, J. Roles of interferon-gamma and interleukin-4 in murine lupus. *J Clin Invest* **99,** 1936–1946 (1997). DOI 10.1172/JCI119361

145. Perez, V. L., Lederer, J. A., Carniel, E., Lichtman, A. & Abbas, A. K. The role of IL12 in helper T-cell differentiation. *Res. Immunol.* **146,** 477–80 (1995).

146. Robinson, D., Shibuya, K., Mui, A., Zonin, F., Murphy, E., Sana, T., Hartley, S. B., Menon, S., Kastelein, R., Bazan, F. & Garra, A. O. IGIF Does Not Drive Th1 Development but Synergizes with IL-12 for Interferon- Production and Activates IRAK and NF B. *Immunity* **7,** 571–581 (1997).

147. Bornstein, G., Bloom, J., Sitry-Shevah, D., Nakayama, K., Pagano, M. & Hershko, A. Role of the SCFSkp2 ubiquitin ligase in the degradation of p21Cip1 in S phase. *J. Biol. Chem.* **278,** 25752–25757 (2003). DOI 10.1074/jbc.M301774200

148. Gottifredi, V., McKinney, K., Poyurovsky, M. V. & Prives, C. Decreased p21 Levels Are Required for Efficient Restart of DNA Synthesis after S Phase Block. *J. Biol. Chem.* **279,** 5802–5810 (2004). DOI 10.1074/jbc.M310373200

149. Sherr, C. J. & Roberts, J. M. Living with or without cyclins and cyclin-dependent kinases. *Genes and Development* **18,** 2699–2711 (2004). DOI 10.1101/gad.1256504

150. Ortega, S., Malumbres, M. & Barbacid, M. Cyclin D-dependent kinases, INK4 inhibitors and cancer. *Biochimica et Biophysica Acta - Reviews on Cancer* **1602,** 73–87 (2002). DOI 10.1016/S0304-419-X(02)00037-9

151. Satyanarayana, A., Hilton, M. B. & Kaldis, P. p21 Inhibits Cdk1 in the absence of Cdk2 to maintain the G1/S phase DNA damage checkpoint. *Mol. Biol. Cell* **19,** 65–77 (2008). DOI 10.1091/mbc.E07-06-0525

152. Martín, A., Odajima, J., Hunt, S. L., Dubus, P., Ortega, S., Malumbres, M. & Barbacid, M. Cdk2 is dispensable for cell cycle inhibition and tumor suppression mediated by p27(Kip1) and p21(Cip1). *Cancer Cell* **7,** 591–8 (2005). DOI 10.1016/j.ccr.2005.05.006

153. Barrière, C., Santamaría, D., Cerqueira, A., Galán, J., Martín, A., Ortega, S., Malumbres, M., Dubus, P. & Barbacid, M. Mice thrive without Cdk4 and Cdk2. *Mol. Oncol.* **1,** 72–83 (2007). DOI 10.1016/j.molonc.2007.03.001

154. Zhong, X.-P., Hainey, E. a, Olenchock, B. a, Jordan, M. S., Maltzman, J. S., Nichols, K. E., Shen, H. & Koretzky, G. a. Enhanced T cell responses due to diacylglycerol kinase zeta deficiency. *Nat. Immunol.* **4,** 882–90 (2003). DOI 10.1038/ni958

155. Rincón, E., Gharbi, S. I., Santos-Mendoza, T. & Mérida, I. Diacylglycerol kinase ζ: at the crossroads of lipid signaling and protein complex organization. *Prog. Lipid Res.* **51,** 1–10 (2012). DOI 10.1016/j.plipres.2011.10.001

156. Mor, A., Philips, M. R. & Pillinger, M. H. The role of Ras signaling in lupus T lymphocytes: Biology and pathogenesis. *Clinical Immunology* **125,** 215–223 (2007). DOI 10.1016/j.clim.2007.08.008

157. Katzav, A., Kloog, Y., Korczyn, A. D., Niv, H., Karussis, D. M., Wang, N., Rabinowitz, R., Blank, M., Shoenfeld, Y. & Chapman, J. Treatment of MRL/lpr mice, a genetic autoimmune model, with the ras inhibitor, farnesylthiosalicylate (FTS). *Clin. Exp. Immunol.* **126,** 570–577 (2001). DOI 10.1046/j.1365-2249.2001.01674.x

158. Pierce, J. W., Schoenleber, R., Jesmok, G., Best, J., Moore, S. A., Collins, T. & Gerritsen, M. E. Novel inhibitors of cytokine-induced IkappaBalpha phosphorylation and endothelial cell adhesion molecule expression show anti-inflammatory effects in vivo. *J. Biol. Chem.* **272,** 21096–21103 (1997).

159. Kubota, T., Hoshino, M., Aoki, K., Ohya, K., Komano, Y., Nanki, T., Miyasaka, N. & Umezawa, K. NF-kappaB inhibitor dehydroxymethylepoxyquinomicin suppresses osteoclastogenesis and expression of NFATc1 in mouse arthritis without affecting expression of RANKL, osteoprotegerin or macrophage colony-stimulating factor. *Arthritis Res. Ther.* **9,** R97 (2007). DOI 10.1186/ar2298

160. Gupta, V. A., Hermiston, M. L., Cassafer, G., Daikh, D. I. & Weiss, A. B cells drive lymphocyte activation and expansion in mice with the CD45 wedge mutation and Fas deficiency. *J. Exp. Med.* **205,** 2755–2761 (2008). DOI 10.1084/jem.20081204

161. Daszkiewicz, L., Vázquez-Mateo, C., Rackov, G., Ballesteros-Tato, A., Weber, K., Madrigal-Avilés, A., Di Pilato, M., Fotedar, A., Fotedar, R., Flores, J. M., Esteban, M., Martínez-A, C. & Balomenos, D. Distinct p21 requirements for regulating normal and self-reactive T cells through IFN-γ production. *Sci. Rep.* **5,** 7691 (2015). DOI 10.1038/srep07691

162. Carvalho-Pinto, C. E., García, M. I., Mellado, M., Rodríguez-Frade, J. M., Martín-Caballero, J., Flores, J., Martínez-A, C. & Balomenos, D. Autocrine production of IFN-gamma by macrophages controls their recruitment to kidney and the development of glomerulonephritis in MRL/lpr mice. *J. Immunol.* **169,** 1058–1067 (2002).

163. Bosque, A., Aguiló, J. I., del Rey, M., Paz-Artal, E., Allende, L. M., Naval, J. & Anel, A. Cell cycle regulation by FasL and Apo2L/TRAIL in human T-cell blasts. Implications for autoimmune lymphoproliferative syndromes. *J. Leukoc. Biol.* **84,** 488–498 (2008). DOI 10.1189/jlb.0108043

164. Crispin, J. C., Kyttaris, V. C., Juang, Y. T. & Tsokos, G. C. How signaling and gene transcription aberrations dictate the systemic lupus erythematosus T cell phenotype. *Trends Immunol* **29,** 110–115 (2008). DOI 10.1016/j.it.2007.12.003

165. Tang, H., Tan, G., Guo, Q., Pang, R. & Zeng, F. Abnormal activation of the Akt-GSK3beta signaling pathway in peripheral blood T cells from patients with systemic lupus erythematosus. *Cell Cycle* **8,** 2789–2793 (2009).

166. Higgs, B. W., Liu, Z., White, B., Zhu, W., White, W. I., Morehouse, C., Brohawn, P., Kiener, P. A., Richman, L., Fiorentino, D., Greenberg, S. A., Jallal, B. & Yao, Y. Patients with systemic lupus erythematosus, myositis, rheumatoid arthritis and scleroderma share activation of a common type I interferon pathway. *Ann Rheum Dis* **70,** 2029–2036 (2011). DOI 10.1136/ard.2011.150326

167. Ronnblom, L. & Eloranta, M. L. The interferon signature in autoimmune diseases. *Curr Opin Rheumatol* **25,** 248–253 (2013). DOI 10.1097/BOR.0b013e32835c7e32

10. ACKNOWLEDGEMENTS

After several years of work, I still can´t believe that my time as PhD student at the CNB is now coming to an end. The realization of this thesis would not have been possible without the contribution of a lot of people, and I would like to take the chance to express my acknowledgements.

First of all, I would like to thank my supervisor Dr. Dimitrios Balomenos for the opportunity to work on this interesting project, the scientific discussions and his patient guidance to complete this thesis. I appreciate the things I learned in your lab and I am sure they will be of great value in the future. Also, I thank my co-director Dr. Carlos Martínez-A. for the provided confidence and his cooperation to obtain the resources required for the realization of this work, as well as my tutor Dr. Cristina Murga for her effort and encouraging words in particular moments.

Of course I thank all the past and present members of the laboratory 412, especially Kris, Lidia, Gorjana, Adri, María L., Marisa, Rahman, Jorge and Ana, for all your help, advices and the great atmosphere in- and outside the lab.

From the first day on, I had a special connection with you, Kris, and apart from teaching me a lot, you became one of my closest friends. Thank you for being with me in good and bad times, near or far, and the million favors you did for me! I never thought I could actually enjoy teaching students, but the time I spent together with you, Adri, was so much fun – thank you for your invincible good humor and your constant encouragement.

As another person that accompanied me from the first day on, I would like to give special thanks to María (411), for helping me out in every imaginable way, for all the “relaxing cafés con leche” we had together and for the great friendship we share! Of course I won´t forget to thank Martina (116), for her contagious good mood and for always lending me an ear.

In general, I would like to thank all members of the DIO, it was a real pleasure to work in this department and I appreciate the support I experienced from you. I would like to mention Antonio, Coral and the kitchen, you facilitated my day-to-day routine in many ways and Cathy for proofreading my manuscript at record speed.

As mice present an important element of this work, tight cooperation with the CNB´s animal facility was essential. Special thanks go to Raquel, Javier, Antonio, Iván, Lucio and the whole team, for all your help, last-minute-jobs and injections as well as the incredible amount of tails and blood samples processed. In particular, working with you, Raquel, was a real pleasure, you lent me a hand wherever you could, and I will always remember the moments shared with you in- and outside the S90.

Another place where I spent innumerable hours is our FACS facility, and sometimes it would have been really difficult without its friendly and helpful staff. A big “thank you” especially to Mari-Carmen and Sara, your professional help and advices were priceless and the laughter (and tears) we shared will remain unforgettable. With you, Sara, I also had the pleasure to spend lots of hours in our free time – thank you and your family for being such good friends and for always cheering me up with your good spirits.

During my stay in Spain, I met a lot of wonderful people and made friendships of inestimable value: Kris, Carlitos, María, Sergio, Darío, Maitane, Mario, Bea, Ángel, Pili, Michele, Dani, Tere, Franzi, Oskar, los llaneros con sus novias and all the others – thank you for all the great moments we had together, the time here would not have been the same without you.

Also, big thanks to my “homies” for staying in touch all those years and for being there for me at any time: Judith, Ali, Tanja, Max, Eri, Corni, Anja, Alban, Damaris, Coco, Stefan, Heike, Till, Michi, Chrissie, Eugen, Fabi H., Amparo, Nina, Fabi K., Ines, Julia (alias Keule), Martina, Markus, David, Toni (and many others) – you never forget about me and you always warm my heart.

Some moments would have been difficult without my family close by. Therefore, I am particularly grateful to Marina as well as Nagore and Iñigo with their families, for giving me second home and for always taking care of me.

Without any doubt, this work would not have been possible without the unconditional support of my loving family, especially my parents. I know, sometimes it was not easy for you knowing me far away, but you always believed in me and encouraged me to give my best. Thank you for everything! Danke für Alles!

Finally, special thanks to Koldo, for his love and moral support, for always standing by me during this work, in good and bad times. You (and Bali, of course!) light up my day, and I´m looking forward to spend more adventures together – let´s see what comes next?!

11. SUPPLEMENTARY INFORMATION